THE MULTI-REFERENCE CORRELATION CONSISTENT COMPOSITE APPROACH: A NEW VISTA IN QUANTITATIVE PREDICTION OF THERMOCHEMICAL AND SPECTROSCOPIC PROPERTIES

Gbenga A. Oyedepo, B.S.

Dissertation Prepared for the Degree of

DOCTOR OF PHILOSOPHY

UNIVERSITY OF NORTH TEXAS

December 2011

APPROVED:

Angela K. Wilson, Major Professor
Weston T. Borden, Committee Member
Thomas R. Cundari, Committee Member
Martin Schwartz, Committee Member
William E. Acree, Jr., Chair of the Department of Chemistry
James D. Meernik, Acting Dean of the Toulouse Graduate School

Oyedepo, Gbenga A. The Multi-reference Correlation Consistent Composite Approach: A New Vista in Quantitative Prediction of Thermochemical and Spectroscopic Properties. Doctor of Philosophy (Chemistry - Physical Chemistry), December 2011, 156 pp., 32 tables, 18 illustrations, references, 381 titles.

The multi-reference correlation consistent composite approach (MR-ccCA) was designed to reproduce the accuracy of more computationally intensive ab initio quantum mechanical methods like MR-ACPF-DK/aug-cc-pCV∞Z-DK, albeit at a significantly reduced cost. In this dissertation, the development and applications of the MR-ccCA method and a variant of its single reference equivalent (the relativistic pseudopotential ccCA method) are reported. MR-ccCA is shown to predict the energetic properties of reactive intermediates, excited states species and transition states to within chemical accuracy (i.e. ±1.0 kcal mol^{-1}) of reliable experimental values. The accuracy and versatility of MR-ccCA are also demonstrated in the prediction of the thermochemical and spectroscopic properties (such as atomization energies, enthalpies of formation and adiabatic transition energies of spin-forbidden excited states) of a series of silicon-containing compounds.

The thermodynamic and kinetic feasibilities of the oxidative addition of an archetypal arylglycerol β-aryl ether (β-O-4 linkage) substructure of lignin to Ni, Cu, Pd and Pt transition metal atoms using the efficient relativistic pseudopotential correlation consistent composite approach within an ONIOM framework (rp-ccCA-ONIOM), a multi-level multi-layer QM/QM method formulated to enhance the quantitative predictions of the chemical properties of heavy element-containing systems larger than hitherto attainable, are also reported.

ACKNOWLEDGEMENTS

I would first like to exalt the name of the lord my God who has been the bedrock of my hope and confidence. I also wish to express my profound gratitude to my mentor and academic advisor, Professor Angela K. Wilson, for her invaluable guidance, encouragement and patience throughout the period of this work. Her constructive criticisms and suggestions over the years have enriched my growth as a scientist.

The support and motivation of my colleagues in the Wilson's research group are greatly appreciated. I am particularly grateful to Dr. Wanyi Jiang, Dr. Nathan DeYonker, Dr. Michael Drummond, Dr. Scott Yockel, Dr. Ben Mintz, Dr. Brian Prascher, Dr. Gavin Williams, Dr. Sammer Tekarli, Dr. John Determan, Dr. Brent Wilson, Kameron Jorgensen, Marie Majkut, Charlie Peterson, Cong Liu, Josh Gibson, Amanda Riojas, Andrew Mahler, Rebecca Weber and Jiaqi Wang for their helpful comments and general assistance throughout the studies. Special thanks to Prof. W. T. Borden for his feedback on this dissertation.

I am especially grateful to Prof. Raifu Durodoye and Ayodele Bello for their financial and moral supports.

Finally, this dissertation would not have been possible without the prayers and support of my immediate family members who have been my greatest source of inspiration and strength. No word can capture the depth of my gratitude to my parents, Jolaade Oyedepo and Adewuyi Oyedepo, and my wife, Oluwasayo Oyedepo. I will forever remain in their debts.

TABLE OF CONTENTS

Page

LIST OF TABLES

Page

LIST OF ILLUSTRATIONS

Page

CHAPTER 1

INTRODUCTION

The evolution of quantum chemistry into a veritable quantitative tool has been made possible due to several important technological and methodological advances over the last few decades. Computational chemistry has especially benefitted from the increased availability and affordability of high-performance computational hardware such as multi-core multiprocessor systems and computer clusters which have motivated the development of faster parallelized algorithms for solving quantum mechanical equations. However, to better exploit the burgeoning computer technologies, there is a need to develop versatile but highly accurate quantum mechanical methodologies whose applications in many areas of chemistry and molecular physics can provide quantitative data in the prediction, confirmation or rejection of experimental observations and measurements.

While reliable quantitative studies of molecular systems can in principle be done using a sophisticated but computationally intensive *ab initio* theoretical method such as the coupled cluster approach in combination with a very large basis set, a more efficient yet similarly accurate route involves performing a series of less expensive calculations and then combining them using various additivity schemes. These additivity schemes are generally referred to as composite approaches. Many of the existing composite methods have been successfully applied to study varieties of chemical properties that are intimately connected with the assumption that a single reference determinant (usually modeled as Hartree-Fock theory) represents a very good approximation of the overall wavefunction of the system. However, for many chemical phenomena such as bond dissociation processes, reaction paths for symmetry-forbidden

chemical reactions, excited electronic states and many other cases where several configurations become degenerate or nearly-degenerate, the Hartree-Fock model breaks down.

A simple example of a nearly degenerate system can be found in a distorted ethylene molecule where one methylene group is rotated relative to the other. The reference wavefunction of the $\widetilde{X}^1A$ state, when the C-C torsion angle is 85° and the π-bond is effectively broken (D_2 symmetry), can be represented as follows:

$$\begin{aligned}\left|\widetilde{X}^1A\right\rangle \approx\ & 0.77\left|1a^2 1b_1^2 2a^2 2b_1^2 1b_2^2 3a^2 1b_3^2 2b_3^2\right\rangle \\ & -0.58\left|1a^2 1b_1^2 2a^2 2b_1^2 1b_2^2 3a^2 1b_3^2 2b_2^2\right\rangle\end{aligned} \tag{1.1}$$

The observation that the coefficients of the two leading configurations are very large and of nearly equal magnitude (0.77 and 0.58) indicates that both are similarly probable and thus quasi-degenerate. At the Hartree-Fock level, only one of these configurations will be arbitrarily selected which will result in a qualitatively wrong wavefunction. The only reasonable alternative is to select both configurations using a multi-configurational method.

The most obvious approach to constructing qualitatively reasonable wavefunction for quasi-degenerate systems is the generalization of the Hartree-Fock method to give the multi-configurational Hartree-Fock (MCHF) method which historically is often referred to as the multi-configuration self-consistent field (MCSCF) method (see section 2.5). The energy difference between the MCSCF and Hartree-Fock theory is called non-dynamical correlation since MCSCF, like its single configuration counterpart, does not truly account for instantaneous motion of electrons (also known as dynamic correlation). Theoretical methods like CASPT2,[1,2] MRCISD(+Q),[3] MR-ACPF[4] and many others have been developed to account for dynamic correlation effects based on the MCSCF wavefunction. However, in order to achieve a

chemically accurate result (within ±1.0 kcal mol^{-1} of reliable experiment) for an energetic property like enthalpy of formation, a computationally expensive post-MCSCF method like MR-ACPF will need to be combined with a very large basis set. The theme of this dissertation is thus the development and applications of a versatile, efficient yet qualitatively and quantitatively accurate quantum methodology called the multi-reference correlation consistent composite approach (MR-ccCA).

In Chapter 2, the theoretical foundations underpinning the varieties of quantum mechanical methods used in this dissertation are reviewed. The basic assumptions and approximations underlying the working equations in each method are summarily discussed.

Since the crux of this dissertation is the development and applications of composite methodologies, Chapter 3 illustrates the success of the single reference correlation consistent composite approach (ccCA) in the determination of the enthalpies of formation for forty highly energetic nitrogen-containing compounds. The results obtained with ccCA were also compared to that of two other *ab initio* composite methods and available experimental values. Based on its demonstrated accuracy, the ccCA method was subsequently utilized to predict the enthalpies of formation of five energetic but highly endothermic tetrazine-containing compounds with potential applications in insensitive high explosives.

The routine predictions of energetic properties for moderate to large-sized chemical systems (particularly for transition metal compounds) to within ±1.0 kcal mol^{-1} of experimental values have been a problem for theoretical chemists due to the attendant high computational cost. For instance, while it is well known that such accuracies can, in principle, be achieved using coupled cluster methods (i.e., CCSD(T)), this is only generally practical for systems

containing less than 15 non-hydrogen atoms. Chapter 4 thus describes a multi-level multi-layer QM/QM approach that can be used to achieve chemical accuracy at a fraction of the computational costs of coupled cluster methods. The QM/QM method described is a hybrid of the single reference relativistic pseudopotential correlation consistent composite approach (rp-ccCA) and density functional theory within an ONIOM framework aptly referred to as rp-ccCA-ONIOM method. The oxidative addition reactions of the C_α-C_β bond in an archetypal β-O-4 substructure of lignin to transition metals are thus reported using rp-ccCA-ONIOM method.

The primary focus of Chapters 5 and 6 is the development and applications of the MR-ccCA method. In Chapter 5, the utility of MR-ccCA in the quantitative predictions of the thermochemistry and spectroscopy of a set of diradical species and unsaturated compounds is demonstrated. Chapter 6 consequently details the applications of MR-ccCA to the accurate studies of the energetic properties of many silicon compounds.

CHAPTER 2

AN OVERVIEW OF QUANTUM MECHANICAL METHODOLOGIES

2.1 The Molecular Problem

A major objective of quantum chemical calculations is finding solutions to the time-independent non-relativistic Schrödinger equation[5-8]

$$\widehat{H}\Psi = E\Psi \tag{2.1}$$

where $\widehat{H}$ is the Hamiltonian operator, Ψ is the wavefunction which contains all the information on the system described and E is the total energy of the system. For a molecule consisting of *N* electrons and *M* nuclei, the full Hamiltonian operator can be written in atomic mass units (i.e. $e = \hbar = \frac{h}{2\pi} = m_e = 1;$ where ϵ is the charge of an electron, h is Planck's constant and m_e is the rest mass of an electron) as

$$\widehat{H} = -\sum_{i=1}^{N}\frac{1}{2}\nabla_i^2 - \sum_{A=1}^{M}\frac{1}{2M_A}\nabla_A^2 - \sum_{i=1}^{N}\sum_{A=1}^{M}\frac{Z_A}{r_{iA}} + \sum_{i=1}^{N}\sum_{j>i}^{N}\frac{1}{r_{ij}} + \sum_{A=1}^{M}\sum_{A>B}^{M}\frac{Z_A Z_B}{R_{AB}} \tag{2.2}$$

where M_A is the nuclear mass of atom A in units of electron mass, Z_A is the charge on nucleus A, r_{iA} is the distance of electron *i* from nucleus A, r_{ij} is the distance between electrons *i* and *j*, and R_{AB} is the distance between nuclei A and B. The first term in equation 2.2 is the kinetic energy of the electrons, where ∇^2 is the Laplacian operator; the second term is the kinetic energy of the nuclei; the third term is the electron-nuclear attraction operator; the fourth is the electron-electron electrostatic repulsion term; and the fifth is the nuclear-nuclear repulsion term.

The Hamiltonian in equation 2.2 is usually simplified using the Born-Oppenheimer (BO) approximation[9] based on the observation that nuclei are much heavier than electrons, and consequently move much more slowly than electrons move. The BO approximation affords the uncoupling of the motion of the nuclei in a system from the motion of the electrons. Thus the nuclei can be viewed as stationary with respect to the motion of the electrons. The resultant electronic Hamiltonian $\widehat{H_{el}}$ is given by

$$\widehat{H_{el}} = -\sum_{i=1}^{N}\frac{1}{2}\nabla_i^2 - \sum_{i=1}^{N}\sum_{A=1}^{M}\frac{Z_A}{r_{iA}} + \sum_{i=1}^{N}\sum_{j>i}^{N}\frac{1}{r_{ij}} \tag{2.3}$$

The nuclear repulsion energy (the fifth term in equation 2.2) will be constant for a fixed geometry and can be evaluated separately. Equation 2.1 can therefore be re-written as

$$\widehat{H_{el}}\Psi = E\Psi \tag{2.4}$$

where E is the pure electronic energy plus the constant nuclear repulsion energy. In most systems, the error introduced by the BO approximation is negligible for energetically well-separated electronic states. However, this approximation fails when two electronic states approach each other e.g. near conical intersections, avoided crossings.[10] In the rest of this dissertation, the Hamiltonian operator refers to the electronic Hamiltonian, unless otherwise stated. As such, the subscript "el" in the Hamiltonian will hereafter be dropped.

Despite the BO approximation, equation 2.4 is still a high dimensional, non-linear differential equation that cannot be solved analytically for two or more electrons. The standard approach to solving differential equations such as equation 2.4 is to discretize them using one-electron wavefunctions also called basis functions.[11] The electronic wavefunction Ψ can thus be expanded as a product of finite one-electron functions ψ_i called spin-orbitals

$$\Psi = \prod_{i=1}^{N} \psi_i \tag{2.5}$$

The molecular spin-orbitals ψ_i are composed of spatial functions ϕ_i (which describe the position r_i of electron i) and spin components ω_i (described by one of the orthogonal pair of functions α and β). In practice, each molecular orbital ϕ_i is expanded as linear combination of atomic orbitals χ_μ (basis functions)

$$\phi_i = \sum_{\mu} C_{\mu i} \chi_\mu \tag{2.6}$$

However, the wavefunction obtained from equation 2.5 (the Hartree product)[12-14] does not follow the Pauli exclusion principle[15,16] which requires that a wavefunction be antisymmetric upon the exchange of any two electrons. A convenient mathematical method of constructing such an antisymmetric wavefunction is to use a Slater determinant[17,18]

$$\Psi = \frac{1}{\sqrt{N!}} \begin{vmatrix} \psi_1(1) & \psi_2(1) & \cdots & \psi_N(1) \\ \psi_1(2) & \psi_2(2) & \cdots & \psi_N(2) \\ \vdots & \vdots & \ddots & \vdots \\ \psi_1(N) & \psi_2(N) & \cdots & \psi_N(N) \end{vmatrix} \tag{2.7}$$

where the prefactor $(\sqrt{N!})^{-1}$ is the normalization factor. Equation 2.7 can be written in a more compact form as

$$\Psi = \left| \psi_1(1) \psi_2(2) \cdots \psi_N(N) \right\rangle \tag{2.8}$$

where only the diagonal elements of the Slater determinant are explicitly shown. For mathematical convenience, the one-electron spin-orbitals are required to be orthonormal (i.e. mutually orthogonal and normalized)

$$\langle \psi_i | \psi_j \rangle = \delta_{ij}, \quad i,j = 1, 2, \ldots, N \tag{2.9}$$

where the Kronecker delta symbol δ_{ij} is equal to 1 if i=j and zero if otherwise. The energy expectation value of Ψ is thus given by

$$E = \frac{\langle \Psi | \hat{H} | \Psi \rangle}{\langle \Psi | \Psi \rangle} \tag{2.10}$$

Several approximations need to be introduced to facilitate the solutions of equation 2.10 using numerical calculations. The simplest approach upon which most of the other quantum mechanical methods are based is the Hartree-Fock approximation.[18,19]

2.2 The Hartree-Fock Approximation

The Hartree-Fock (HF) approximation is a mean-field theory where each electron in a system experiences the average field of all the other electrons. The HF approximation is a variational method in that the energy obtained is guaranteed to be higher than the exact energy of the system which implies that the wavefunction obtained can be improved in a systematic way. In the simplest case of a closed-shell system, the HF method can be used to find the optimized sets of one-electron molecular orbitals that minimize the energy expectation value in equation 2.10.

To find the optimized sets of one-electron functions, the electronic Hamiltonian of equation 2.3 can be recast as a new one-electron Fock operator[20]

$$\hat{f}_i = \hat{h}_i + \upsilon_i^{HF}\{j\} \tag{2.11}$$

where

$$h_i = -\frac{1}{2}\nabla_i^2 - \sum_{i=1}^{N}\sum_{A=1}^{M}\frac{Z_A}{r_{iA}} \tag{2.12}$$

and $\upsilon_i^{HF}\{j\}$ is an effective single-particle potential operator defined such that an electron i interacts with an average field of all the other electrons in orbitals {j}

$$\upsilon_i^{HF} = \sum_j (2\widehat{J}_j - \widehat{K}_j) \tag{2.13}$$

The one-particle Coulomb and exchange operators $\widehat{J}_i$ and $\widehat{K}_i$ are respectively defined by their actions on an arbitrary function $\varphi(x)$ as follows:

$$\widehat{J}_i\varphi_j(x_1) = [\int \frac{\varphi_i^*(x_2)\varphi_i(x_2)}{r_{12}}dx_2]\varphi_j(x_1) \tag{2.14}$$

$$\widehat{K}_i\varphi_j(x_1) = [\int \frac{\varphi_i^*(x_2)\varphi_j(x_2)}{r_{12}}dx_2]\varphi_i(x_1) \tag{2.15}$$

Substituting into equation 2.10, the HF electronic energy is given by

$$E = 2\sum_{i=1}^{N} h_i + \sum_{i=1}^{N}\sum_{j=1}^{N}(2J_{ij} - K_{ij}) \tag{2.16}$$

The Hartree-Fock equations can thus be written in the eigenvalue form as

$$\widehat{f}_i|\phi_i\rangle = \varepsilon_i|\phi_i\rangle \tag{2.17}$$

where ε_i are the orbital energies. To solve the HF equations, ϕ_j is left projected onto equation 2.17 and then substitute equation 2.6

$$\sum_i\sum_j C_{\mu i}C_{\mu j}\langle\chi_j|\widehat{f}_i|\chi_i\rangle = \sum_i\sum_j C_{\mu i}C_{\mu j}\varepsilon_i\langle\chi_j|\chi_i\rangle \tag{2.18}$$

which leads to a matrix eigenvalue form referred to as Roothaan-Hall equations[21,22]

$$\mathbf{FC} = \mathbf{SC\varepsilon} \tag{2.19}$$

where $\mathbf{F}$ is the notation for the Fock integral $\left\langle \chi_j \middle| \hat{f}_i \middle| \chi_i \right\rangle$, $\mathbf{C}$ is the matrix of the expansion coefficients arranged in columns, $\mathbf{S}$ is the overlap integral $\left\langle \chi_i \middle| \chi_j \right\rangle$ and $\boldsymbol{\varepsilon}$ is the diagonal matrix of eigenvalues. The iterative procedure utilized in solving equation 2.19 is also called the self-consistent field (SCF) method.

A number of chemically important properties can be obtained from a converged SCF wavefunction and energy. The total electronic energy can be used to determine the relative conformational energies of different geometries of a molecule, while the individual orbital energies are usually good approximations of the ionization potential of electrons occupying the orbitals (Koopman's theorem).[23] The electron density can be calculated from the squared norm of the converged wavefunction. Properties like atomic charges and multipole moments of a molecule can be estimated from the electron density.

2.3 Post Hartree-Fock Methods

The HF ansatz described above can account for up to 99% of the total exact electronic energy of a system;[24] however, it is usually the residual energy that provides quantitative (in some severe cases, even qualitative such as for the dissociation of N_2)[25] information about most chemical reactions. The difference between the HF energy and the exact solution of the non-relativistic Schrödinger equation is the electron correlation energy. There are two types of electron correlation energy: static (non-dynamic) and dynamic.[26] Static correlation is a long-range effect that is related to degenerate or quasi-degenerate states, the wavefunctions of which cannot be properly described by a single electronic configuration like the SCF method. Static correlation becomes important at the dissociation limit of a molecule. Dynamic

correlation is a short-range effect that is related to the instantaneous adjustment of an electron to the position of each of the other electrons to avoid collisions. This is an improvement on the treatment of each electron relative to the spatially averaged position of all the other electrons obtained at the HF level of theory. The conceptually simplest post Hartree-Fock approach to include dynamic correlation is the configuration interaction method.[18,19]

2.3.1 Configuration Interaction Method

Configuration interaction (CI) theory describes the interaction of other possible determinants, formed from the HF reference wavefunction by excitations of electrons from occupied to virtual (unoccupied) molecular spin orbitals, with the ground state wavefunction.[18] Thus a CI wavefunction may be expressed as a linear combination of reference and excited Slater determinants as

$$\left|\Psi_{CI}\right\rangle = c_o\left|\Psi_o\right\rangle + \sum_{i}^{occ}\sum_{r}^{virt} c_i^r \left|\Psi_i^r\right\rangle + \sum_{ij}^{occ}\sum_{rs}^{virt} c_{ij}^{rs}\left|\Psi_{ij}^{rs}\right\rangle + \sum_{ijk}^{occ}\sum_{rst}^{virt} c_{ijk}^{rst}\left|\Psi_{ijk}^{rst}\right\rangle + \cdots \tag{2.20}$$

where $\left|\Psi_o\right\rangle$ is the HF or reference determinant, $\left|\Psi_i^r\right\rangle$, $\left|\Psi_{ij}^{rs}\right\rangle$ and $\left|\Psi_{ijk}^{rst}\right\rangle$ correspond respectively to the single-, double-, and triple-electron excitations from the HF spin-orbitals to the virtual orbitals, C_o, C_i^r and C_{ij}^{rs} are the CI coefficients of the determinants that are typically determined variationally and the occupied molecular orbitals are labeled by the indices i, j, k, …, while virtual molecular orbitals by r, s, t, ….

If all the possible $\binom{2K}{N}$ configurations (where K is the number of one-electron basis functions and N is the number of electrons) are allowed in the expansion of equation 2.20 (i.e.

full configuration interaction (FCI)), the energy obtained from the resultant wavefunction (E_{FCI}) is the best possible approximation to the exact solution of the electronic energy in a given basis set. In practice, however, the expansion is truncated after the double- (CISD) or triple-excitation (CISDT) to maintain computational feasibility. The truncation of CI space results in a particularly undesirable result; the truncated CI method will not be size consistent or size extensive. A method is considered to be size consistent if the sum of the total energies of two non-interacting subsystems A and B that are separated by a large distance are equal to the sum of their individually calculated total energies. A size extensive method, on the other hand, scales linearly with the size of the particles. Thus truncated CI methods can give large errors when used to compute properties like atomization energies and enthalpies of formation due to their lack of size consistency.

2.3.2 Møller-Plesset Perturbation Theory

The idea behind many body perturbation theory[18,19,27] is the partitioning of the electronic Hamiltonian $\hat{H}$ into an unperturbed Hamiltonian $\hat{H}_o$ and a perturbation operator $\hat{V}$. The extent of the perturbation can be represented by a scaling parameter λ, with $\lambda = 0$ corresponding to the unperturbed system

$$\hat{H}=\hat{H}_o+\lambda\hat{V} \tag{2.21}$$

The Schrödinger equation for the system can thus be written as

$$(\hat{H}_o+\lambda\hat{V})\left|\Psi\right\rangle = E\Psi \tag{2.22}$$

In the Møller-Plesset ansatz[28] for second-order perturbation (known as MP2 method), $\widehat{H}_o$ is chosen to be the sum of Fock operators over the occupied molecular orbitals while the difference between the electronic Hamiltonian $\widehat{H}$ and HF operator $\hat{f}_i$ is the perturbation or fluctuation potential

$$\hat{V} = \sum_{i>j} \frac{1}{r_{ij}} - \sum_i \upsilon_i^{HF} \tag{2.23}$$

Since the extent of perturbation can be increased from zero to other integer values, the wavefunction and the energy can also be expressed as a Taylor expansion of λ such that

$$\Psi = \lambda^0 E_0 + \lambda^1 E_1 + \lambda^2 E_2 + \cdots \tag{2.24}$$

and

$$E = \lambda^0 \Psi_0 + \lambda^1 \Psi_1 + \lambda^2 \Psi_2 + \cdots \tag{2.25}$$

where E_n and Ψ_n are the *n*-th order energy and wavefunction, respectively, while Ψ_0 is the optimized single determinant HF reference wavefunction. Unlike the HF and truncated CI methods, there is no guarantee that the electronic energy obtained within perturbation theory framework is an upper-bound to the exact energy i.e. perturbation theory is not variational.

2.3.3 Coupled Cluster Theory

The central idea behind coupled cluster (CC) theory[19,27,29,30] is that the FCI wavefunction can be described as an expansion of the exponential cluster operator on HF reference wavefunction

$$\Psi_{CC} = e^{\hat{T}} \left| \Psi_{HF} \right\rangle \tag{2.26}$$

where

$$e^{\hat{T}} = 1 + \hat{T}_1 + (\hat{T}_2 + \frac{1}{2!}\hat{T}_1^2) + (\hat{T}_3 + \hat{T}_1\hat{T}_2 + \frac{1}{3!}\hat{T}_1^3) + (\hat{T}_4 + \hat{T}_3\hat{T}_1 + \frac{1}{2!}\hat{T}_2^2 + \frac{1}{2!}\hat{T}_1^2\hat{T}_2 + \frac{1}{4!}\hat{T}_1^4) + \ldots \quad (2.27)$$

while the connected $\hat{T}_i$ operators acting on the HF reference wavefunction generate all *i*th excited Slater determinants

$$\hat{T}_1 \left| \Psi_{HF} \right\rangle = \sum_{i,r} t_i^r \left| \Psi_i^r \right\rangle \quad (2.27)$$

$$\hat{T}_2 \left| \Psi_{HF} \right\rangle = \sum_{i>j,r>s} t_{ij}^{rs} \left| \Psi_{ij}^{rs} \right\rangle \quad (2.28)$$

$$\hat{T}_3 \left| \Psi_{HF} \right\rangle = \sum_{i>j>k,r>s>t} t_{ijk}^{rst} \left| \Psi_{ijk}^{rst} \right\rangle \quad \ldots \quad (2.29)$$

The CC amplitude t is the expansion coefficient of each cluster expansion. By virtue of the non-linear terms in the exponential expansion, there exist disconnected components of the cluster operator

$$\frac{1}{2}\hat{T}_1^2 \left| \Psi_{HF} \right\rangle = \sum_{\substack{i,r \\ j,s}} t_i^r t_j^s \left| \Psi_i^r \right\rangle \quad (2.30)$$

$$\frac{1}{2}\hat{T}_2^2 \left| \Psi_{HF} \right\rangle = \sum_{\substack{i>j,r>s \\ k>l,t>u}} t_{ij}^{rs} t_{kl}^{tu} \left| \Psi_{ijkl}^{rstu} \right\rangle \quad (2.31)$$

$$\hat{T}_1\hat{T}_2 \left| \Psi_{HF} \right\rangle = \sum_{\substack{\mathrm{i,r} \\ j>k,s>t}} t_i^r t_{jk}^{st} \left| \Psi_{ijk}^{rst} \right\rangle \quad \ldots \quad (2.32)$$

Physically, a connected cluster operator such as $\hat{T}_3$ corresponds to the simultaneous excitation of three electrons from occupied to virtual orbitals, while a disconnected term like $\hat{T}_1\hat{T}_2$ corresponds to the product of two different, non-interacting excitations; a single and then a double. It should be noted that the existence of the disconnected terms in the

exponential ansatz of CC theory has indirectly introduced some effects of higher-order excitations in the wavefunction, even if Equation 2.27 is truncated at a given excitation level. For instance, as discussed above, $\hat{T}_1\hat{T}_2$ would introduce triple excitations into the CC wavefunction, even when the cluster expansion is truncated at the double excitations. The presence of these disconnected terms in CC theory ensures its size consistency and extensitivity. However, like perturbation theory, CC theory is also not variational.[31]

As with the CI method, the inclusion of all possible excitations within Equation 2.26 is required to obtain the FCI wavefunction, which is impractical. Therefore, Equation 2.27 is usually truncated at a given excitation level to give several CC methods like CCSD (coupled cluster method including all single and double excitations), CCSDT (coupled cluster method including all single, double, and triple excitations), etc. The combination of perturbation and CC theories by Raghavachari et al.[32] results in the derivation of non-iterative approximations like CCSD(T) where the triple excitations have been perturbatively included to the CCSD method. For quantitatively accurate calculations, it is usually advantageous to use CCSD(T) due to its considerable computational savings (relative to CCSDT) without significant loss in accuracy.[33]

2.4 Basis Sets

In computational quantum chemistry, a basis set is a collection of fixed functions used to approximate an electronic wavefunction. It is known[34] that the exact solution to the Schrödinger equation for the hydrogen atom is separable into a product of radial $[R_{n,l}(r)]$ and angular (also known as a spherical harmonic function) $[Y_{l,m_l}(\theta,\phi)]$ components as

$$\Psi_{n,l,m_l}(r,\theta,\phi) = R_{n,l}(r).Y_{l,m_l}(\theta,\phi) \tag{2.33}$$

where n, l and m_l are the principal, angular and magnetic quantum numbers, respectively, while r is a distance from the nucleus. Therefore, it is reasonable that the discretization of an electronic wavefunction should be done using functions constructed from hydrogen-like wavefunctions. Thus, molecular orbitals are usually constructed as a linear combination of the atomic basis functions. There are two primary functional types of basis functions used in quantum chemistry: Slater-type functions or orbitals (STOs)[35] and Gaussian-type functions or orbitals (GTOs).[36] STOs have the hydrogenic form

$$\chi^{STO}_{\zeta,n,l,m_l}(r,\theta,\phi) = NY_{l,m_l}(\theta,\phi)r^{n-1}e^{-\zeta r} \tag{2.34}$$

where N is a normalization factor and ζ is a parameter that denotes the radial extent of the function. STOs satisfy two important requirements for an atomic wavefunction: (1) exponential decay of the function at large distance from the nucleus (2) correct description of the non-zero derivative or "cusp" of the function at the nucleus. However, for computational convenience and efficiency of finding analytic rather than numerical solutions of complex integrals in many-electron systems, GTOs are used in practice. The GTOs can be written as

$$\chi^{STO}_{\zeta,n,l,m_l}(r,\theta,\phi) = NY_{l,m_l}(\theta,\phi)r^{2n-2-l}e^{-\zeta r^2} \tag{2.35}$$

GTOs, unlike STOs, do not satisfy the two requirements mentioned above for an atomic wavefunction: at short range, they do not describe the cusp condition and at long range, they decay too rapidly due to the r^2 dependence of the exponential. Though GTOs lack the ability to provide qualitative descriptions, they compensate for this in the ease of multi-centric integrations.[18] The qualitative description of the GTOs can be improved by using a linear

combination of the GTOs to approximate the atomic wavefunction as described above in Equation 2.6. This is the technique mostly utilized in molecular calculations.

2.4.1 Correlation Consistent Basis Sets

It is well known that the one-particle basis set is an important component of wavefunction based *ab initio* calculation on molecules. Moreover, since the advent of coupled cluster theory, the many-particle problem can be considered to a large extent as solved – from a theoretical standpoint, leaving the one-particle basis set as the major factor that determines the quality of an electronic structure calculation. The correlation consistent basis sets (denoted as cc-pVnZ, where n=D, T, Q, 5 etc.), introduced by Dunning in 1989,[37] were developed to systematically recover electron correlation energy in correlated *ab initio* calculations following the discovery by Almlöf and Taylor[38,39] that basis sets constructed from atomic natural orbitals (ANOs) provide accurate solutions of the molecular Schrödinger equation. While both ANOs and correlation consistent basis sets can provide a balanced description of electron distribution in atoms and molecules, the latter has become more popular due to its compactness in terms of the number of uncontracted Gaussian functions (primitive functions) utilized.[40]

The correlation consistent basis sets are built on a core set of atomic Hartree-Fock primitive functions by systematically adding shells of additional primitive Gaussian functions that describe polarization and valence correlation. The core orbitals are usually described by a single contracted GTO while the valence orbitals are described by multiple functions. For instance, for the first (H-He) and second row (Li-Ne) atoms, the smallest basis set (the cc-pVDZ set), is formed from the core atomic HF orbitals (1*s*, 2*s* and 2*p*) plus single *s*, *p*, and *d* primitive

functions optimized using the CISD method. This gives a [3*s*2*p*1*d*] set. The next hierarchical basis set (cc-pVTZ) adds *s*, *p*, *d*, *f* functions to the cc-pVDZ to give [4*s*3*p*2*d*1*f*] set and so on. Thus for main group elements, the cc-pVDZ set contains two functions per valence orbital (double-ζ), cc-pVTZ has three functions for each valence orbital (triple-ζ), etc. Since the wavefunction for anions and weakly interacting molecules are substantially more diffuse than those for the corresponding neutral atoms, extra functions (i.e. diffuse or small exponent *s*-, *p*-, and *d*-function to cc-pVDZ set, etc.) must be added to form the so-called augmented correlation consistent basis sets (aug-cc-pVnZ, n = D, T, Q etc.). However, to properly recover the core-core and core-valence correlation effects, large (tight) exponent functions must be added to the cc-pVnZ set to produce the cc-pCVnZ basis sets.[41] For the inclusion of scalar relativistic effects in an electronic calculation, the cc-pVnZ sets have been recontracted using the spin-free Douglas-Kroll-Hess Hamiltonian, to give the cc-pVnZ-DK sets.[42] One of the major advantages of using these basis sets is that the correlation energies calculated by a given method converge smoothly and systematically to the complete basis set (CBS) limit,[43] a limit at which the errors due to the use of finite one-particle basis set would be effectively removed.

2.5 Multireference Approaches

Reliable qualitative descriptions of processes where a single configuration is inadequate for accurate representation of the reference state (e.g. transition states, excited states) can be achieved using a multi-configurational self-consistent field (MCSCF)[44-49] method. The most successful MCSCF variant is the complete active space self consistent field (CASSCF)[50] method, also known as the fully optimized reaction space (FORS)[45] method. Its success can be attributed

to the partitioning of the electrons and orbitals into spectator and active sets. The spectator orbitals are usually the core orbitals of a chemical species that are assumed to be uninvolved in the chemistry of interest. As a result, the spectator orbitals are usually doubly occupied and are optimized at the SCF level of theory. The active electrons are those associated with the orbitals that undergo significant changes during the process of interest. These orbitals are optimized at the full configuration interaction (full CI) level of theory, where all possible configurations within a given orbital basis or space are taken into consideration. The general form[51] of a MCSCF wavefunction can be represented as

$$\Psi_{MCSCF} = \sum_{I} P_I \Phi_I \tag{2.36}$$

$$\Phi_I = Q \prod_{k \subset I} \varphi_k \tag{2.37}$$

$$\varphi_k = \sum_{\mu} C_{\mu k} \chi_\mu \tag{2.38}$$

where Φ_I are configuration state functions and I runs over all contributing configurations, φ_k are molecular orbitals expanded in the basis of atomic basis functions χ_μ and Q is a normalization constant.

The MCSCF wavefunction, Ψ_{MCSCF}, is written as a linear combination of many-electron functions (Slater determinants or configuration state functions which differ in how electrons are arranged in their constituting molecular orbitals ϕ_k) and can be obtained by simultaneously optimizing the configuration mixing coefficients P_I and molecular orbital coefficient $C_{\mu k}$ in a variational fashion. This approach allows the method both to include relevant near-degenerate configurations in the electronic states under study and to provide a foundation for more sophisticated theories that would bring the computed properties closer to the exact solution of the Schrödinger equation. Additional electronic correlation effects can then be accounted for

using methods such as multireference second-order perturbation theory (e.g CASPT2),[1,2] multireference configuration interaction with single and double excitations (quadruple and higher excitations may be included *a posteriori* via Langhoff-Davidson correction[3], commonly referred to as Davidson correction denoted as MRCISD(+Q)), and multireference coupled cluster (MRCC) methods.

The major shortcoming of CASSCF calculations is that the method scales with the system size and can get very expensive due to the factorial dependence of the active electrons and orbitals on the number of possible configurations since the active set is treated within the full CI level of theory, which can be described in terms of the number of Slater determinants using the formula:

$$n_{Slater} = \begin{pmatrix} m \\ N_\alpha \end{pmatrix} \begin{pmatrix} m \\ N_\beta \end{pmatrix} \tag{2.39}$$

where m is the number of active orbitals and N_α and N_β are the numbers of active electrons with α- and β- spins, respectively. If configuration state functions (CSFs), which are spin-adapted linear combination of Slater determinants, are used instead of Slater determinants, the number of configurations is given by the Weyl-Robinson Formula:[52]

$$n_{CSFs} = \frac{2S+1}{m+1} \begin{pmatrix} m+1 \\ m-0.5N-S \end{pmatrix} \begin{pmatrix} m+1 \\ 0.5N-S \end{pmatrix} \tag{2.40}$$

where S is the total spin, and N is total number of active electrons. Therefore, a singlet wavefunction for a full valence active space calculation on ethylene (C_2H_4) with 12 electrons distributed in 12 orbitals will consist of 853,776 and 226,512 Slater determinants and CSFs, respectively.

Despite the vast number of successes of single reference coupled cluster methods, most notably CCSD(T) which is often referred to as the "gold standard" of computational chemistry,[53-56] the multireference equivalents of coupled cluster methods have yet to become standard computational methods, as they are not available in commonly used quantum mechanical programs. Meanwhile, the accuracy of the readily available and relatively less computationally costly CASPT2 method may be improved by using a more rigorous and costly correlation method like MRCISD which is variational, but not size consistent, due to truncation of the CI expansion to include only singles and doubles excitations. The simplest correction for the lack of size consistency in MRCISD, as suggested by Bruna, Peyerimhoff and Buenker,[57] is to use Davidson-type correction, $E_{\text{D. Corr.}}$,[3]

$$E_{D.Corr} = \left(1 - \sum_{i \in \text{Ref}} c_i^2\right)(E_{MRCISD} - E_o) \tag{2.41}$$

where c_i are the coefficients of contributing configurations in the CASSCF wavefunction E_0 and E_{MRCISD} are the energies of CASSCF and MRCISD wavefunctions, respectively. $E_{\text{D.Corr}}$ is an estimate of quadruple excitations to the electronic energy. The size consistency and extensitivity properties of MRCISD may also be improved by using methods like multireference averaged coupled pair functional (MR-ACPF)[4] and multireference averaged quadratic coupled cluster (MR-AQCC)[58] methods where such corrections are embedded into the MRCI equations, *a priori*, as energy functionals.

2.6 Density Functional Theory

A different approach used to solve the Schrödinger equation 2.1, instead of the

wavefunction-based methods described above, is to use density functional theory (DFT). DFT is based on the theorems of Hohenberg and Kohn (1964)[59] which prove the existence of the ground state energy of a molecular system as a unique functional of its electron density and that this energy functional must be a minimum when the exact ground state density is used. Thus every observable quantity of a quantum system defined by an external potential V_{ext} can be calculated from the ground state density of the system. However, Hohenberg and Kohn did not prescribe any method for finding the functional of the electron density that would variationally yield the exact ground state energy of an atom or molecule.

Kohn and Sham (1965)[60] subsequently devised a formulation that results in a practical way to express the electronic density in terms of one-electron orbitals φ_i (known as Kohn-Sham orbitals) which can be constructed from basis sets of Slater or Gaussian functions

$$\rho = \sum_i |\varphi_i|^2 \tag{2.42}$$

In analogy to the Hartree-Fock method, the expression for the DFT energy functional can thus be written as

$$E_{DFT}[\rho] = T_S[\rho] + V_{ext}[\rho] + J[\rho] + E_{XC}[\rho] \tag{2.43}$$

where T_S is the kinetic energy of a system of fictitious non-interacting electrons constructed in such a way that its density is the same as that of the real interacting electrons, V_{ext} is the electron-nuclei attraction potential (also called external potential), J is the classical Coulomb interaction, while E_{xc} (called the exchange-correlation term) accounts for the quantum electron exchange and all electron correlation, including that from the kinetic energy.

DFT has been a powerful and computationally efficient approach used by chemists and physicists because it affords the inclusion of electron correlation effects in calculation with nearly the same computational cost as a HF calculation. The major challenges to DFT are that the exact form of the exchange-correlation functional $E_{xc}[\rho]$ is currently unknown and also there is no clear way to systematically improve the accuracy of computed chemical properties. Thus the development of the theory relies more on intuition and comparison of its results to experimental values and those of more computationally expensive but reliable methods like coupled cluster.

As the exact expression for $E_{xc}[\rho]$ is yet unknown, numerous formulations of DFT have been proposed based on different ways of approximating the functional. Some examples of existing DFT methods include: B3LYP,[61-63] PBE0,[64] M06,[65] B2PLYP[66].

CHAPTER 3

HIGHLY ENERGETIC NITROGEN SPECIES: RELIABLE ENERGETICS VIA THE CORRELATION CONSISTENT COMPOSITE APPROACH[†]

3.1 Introduction

One of the most complicated tasks that confronted the major powers during the World Wars was the development of explosives, propellants and projectiles.[67] Of the many energetic compounds developed around the time, RDX (1,3,5-trinitro-1,3,5-triazacyclohexane) has proven to be of high brisance (shattering power) but is also known to be extremely sensitive to shock, impact and friction.[68] Although RDX is still widely used for military and non-military purposes, for instance in Composition H-6 and Cyclotol explosives, it is prone to premature deflagration and detonation when employed in delayed-action payload dropped from high altitude.[69] The risks of catastrophic explosions during manufacture, storage, destruction, demilitarization and disposal of many common sensitive explosives have prompted continuing research on the discovery and synthesis of insensitive high explosives for military and commercial uses (such as fireworks, demolition, excavation, and mining).[67] Such compounds are characterized by the swiftness with which their decomposition, detonation or explosion occur supersonically but are surprisingly insensitive to triggering stimuli such as impact, friction and electrostatic discharge. Potential alternatives to the existing shock and friction-sensitive energetic compounds include caged polynitropolycycloalkanes, polynitramines and many N-heterocycles due to their high nitrogen content. These compounds exhibit high endothermicity, a property that is suggestive of their incredible insensitivity, and high densities, i.e. large amount of energy can be liberated

[†] This chapter is presented in its entirety from K. R. Jorgensen, G. A. Oyedepo, and A.K. Wilson, "Highly energetic nitrogen species: Reliable energetics via the correlation consistent Composite Approach (ccCA)." *J. Hazard. Mater.* **2011**, *186*, 583 with permission from Elsevier.

from a small quantity of the material. These critical properties are important to explosive performance.[70]

Energetic species containing nitrogen-substituted benzene rings derive their high energies from the increased carbon-nitrogen and nitrogen-nitrogen bonds, in contrast to carbon-based non-substituted explosives which draw their energies mostly from the oxidation of the carbon and hydrogen atoms.[71] The oxidation of a carbon-based explosive leads to an incomplete combustion reaction, resulting in toxic gases such as carbon monoxide and nitrogen oxides. The oxygen balance (a measurement of the ability of an explosive compound to become oxidized) of nitrogen-substituted compounds is usually close to zero, indicating a more complete combustion reaction than for carbon-based explosives. Optimal sensitivity, power, and brisance of an explosive tend to be attained as the oxygen balance approaches zero.

While highly endothermic compounds are the most sought after to ensure high insensitivity and complete decomposition,[72] energetics for these mostly nitrogen-rich compounds have been observed to be directly related to explosive properties examined in propellant development. Properties derived from $\Delta H_f^{o}{}_{(g)}$ include: enthalpy of explosion (ΔH_e) which is used in computing the temperature of explosion (T_e), work potential (nRT), and velocity of detonation (VOD) which is used in the prediction of detonation pressure (P_d).[73] For example, ΔH_e is calculated:

$$\Delta H_e = \Sigma \Delta H_{f,(product)} - \Sigma \Delta H_{f,(explosive)} \quad (3.1)$$

The prediction of thermochemical properties to within “chemical accuracy” (usually defined as theoretical values with mean absolute deviation (MAD) within 1.0 kcal mol^{-1} from experimental data for main group species) using computational chemistry ensures that

experimental efforts are focused on promising compounds exhibiting required enhanced performance. Since the development, manufacture, testing and fielding of a new energetic material is costly in terms of time and money, using accurate energetics to eliminate poor candidates lacking required sensitivity or having performance problems through theoretical predictions at the early stages of development is highly desirable. Computational chemistry provides an effective means for the prediction of gas phase $\Delta H_f^{o}{}_{(g)}$ for energetic species. Any chosen methods, however, must first demonstrate utility, reliability, and accuracy for the prediction of energetic properties before being utilized in the prediction of the energetic behavior of species not yet fully characterized experimentally.

In a study by Rice et al.,[74] the $\Delta H_f^{o}{}_{(g)}$ of energetic materials including nitroaliphatics, nitroaromatics, nitroamines, nitrotriazoles, nitrofuroxans, nitrate esters, nitrites, azidoaliphatics, azidoaromatic, and C-nitroso species were predicted. An objective of the study was to determine the impact of methodological choice on the $\Delta H_f^{o}{}_{(g)}$, with the goal of identifying a suitable strategy of studying CHNO systems. The methodology used by the authors comprised a semi-empirical approach to obtaining $\Delta H_f^{o}{}_{(g)}$ from quantum mechanical energies using a training set for the parameterization of the method. However, cautions must be exercised in utilizing this method on compounds that are not contained in the training set due to this parameterization. B3LYP/6-31G* was used for geometry optimization in the method while an increase in basis set size from 6-31G* to 6-311++G(2*df*,2*p*) was used for single point energy calculations to give slightly improved $\Delta H_f^{o}{}_{(g)}$. The root mean squared (RMS) deviation improved from 3.1 to 2.9 kcal mol^{-1} (using a so-called group-equivalent method) with respect to experimental $\Delta H_f^{o}{}_{(g)}$. The dependence of the training set on the methods was also investigated

with the conclusion that molecules not included in the training set (compounds containing tetrazole rings, doubly bonded NH groups, and nitrogen linked bridges) tend to result in an increased RMS deviation by as much as one order of magnitude when compared with experimental $\Delta H_f^{o}{}_{(g)}$. The authors' semi-empirical atom- and group-equivalent methods are only viable for CHNO molecules which display properties related to those in the training set, eliminating large classes of energetic compounds such as highly nitrogen-rich compounds.

Identifying computationally feasible methodology to quantitatively predict $\Delta H_f^{o}{}_{(g)}$ has continued to be of much interest. The Rice et al. study[74] shows that increasing basis set size and introducing a group equivalence approach, which concomitantly includes reliance on empirically optimized parameters, could lead to a decrease in MAD from experimental values. However, to consistently obtain chemical accuracy for $\Delta H_f^{o}{}_{(g)}$, a high level electron correlation method such as coupled cluster with singles, doubles and quasi-perturbative triples excitations [CCSD(T)] should be used in conjunction with a very large basis set.[75] Alternatively, a series of single point CCSD(T) energies can be computed and extrapolated to the asymptotic complete basis set (CBS) limit, the point at which errors arising from basis set incompleteness have been removed leaving only the intrinsic error in the method utilized. But using CCSD(T) with a large basis set quickly becomes too costly as molecule size increases, and an alternative strategy is to use *ab initio* composite methods.

Composite methods use less sophisticated theories in conjunction with a series of basis sets to approximate results that would be obtained with higher levels of theory but at significantly reduced computational costs (i.e. reduced CPU time, memory, and disk space requirements). A few representative *ab initio* composite methods include the Weizmann-*n*

(W*n*), High Accuracy Extrapolated *ab initio* Thermochemistry (HEAT), and the Gaussian-*n* (G*n*) methods. The W*n* method of Martin and co-workers[76-79] and the HEAT method of Stanton and coworkers[80,81] use a series of coupled cluster calculations with an objective of achieving accuracy comparable to full configuration interaction (FCI)/CBS limit (within 0.1 kJ mol^{-1} of reliable experimental values). The drawback of the W*n* and HEAT methods is their exorbitant computational costs, rendering these methods impractical or unfeasible for molecules with more than a couple of non-hydrogen atoms. The G*n* methods of Pople, Curtiss, Redfern, Raghavachari, and co-workers[82-88] are based on the less expensive Møller-Plesset perturbation theory (second or fourth order) reference energy. The G*n* methods have been shown to be accurate within 1-2 kcal mol^{-1} of experimental values for energetic properties, such as enthalpies of formation, ionization potentials, electron and proton affinities. The G*n* methodologies however make use of empirical high-level corrections (HLC). For most G*n* approaches, the HLC are parameters fit to decrease the MAD for a set of energetic properties (G2/97 test set for the G2, G3 methods and a subset of G5/03 for the G4 method) from corresponding experimental values. Subsequently, the HLC has been shown to account mostly for basis set incompleteness error in the composite method.[89] A possible consequence of fitting HLC to experimental values for a specific set of molecules is uncertain performance when the G*n* methods are applied to novel molecules that appreciably differ from the test set. There is thus a need for composite methodology based only on first principle solution of the Schrödinger equation.

Our group has developed an *ab initio* composite method free from empirical parameters called the correlation consistent composite approach (ccCA).[89-92] The method has been

successful in the prediction of energetic properties, even where other composite approaches have had difficulties (e.g., s-block[93]) or may be undeveloped or in their infancy (e.g., for transition metal species [91,94]). The ccCA utilizes the correlation consistent basis sets [95,96] which are extrapolated to the complete basis set (CBS) limit and MP2 calculations to obtain a reference energy upon which the composite method is based. An example of the success of the ccCA methodology is for the G3/99 test set,[90] which included 222 enthalpies of formation, where ccCA resulted in a MAD of 0.96 kcal mol^{-1} (ccCA-P) and 0.97 kcal mol^{-1} (ccCA-S4), an improvement in comparison to the G3 method with a MAD of 1.16 kcal mol^{-1}.

Recently Kiselev and Gritsan[97] computed $\Delta H_f^o{}_{(g)}$ for nitroalkanes, their isomers and radical forms using the G2[85], G3[85,98], and G2M(CC5)[99] composite methods. B3LYP/6-31+G(*d,p*), B3LYP/6-311G(*d,p*), MPW1B95/6-31+G(*d,p*),[100] and MPWB1K/6-31+G(d,p)[101] density functional theory methods were also utilized. Though their molecule set included fourteen neutral and four radical compounds that contain one or more NO_2 or ONO groups, experimental values are only available for eight of these species. More recent experimental $\Delta H_f^o{}_{(g)}$ for two of these molecules, dinitromethane (-9.2±0.3 kcal mol^{-1}) and trinitromethane (5.7±0.3 kcal mol^{-1}), have been determined by Miroshnichenko et al.[102] Of the eight molecules with available experimental values, (including the updated experimental values for dinitromethane and trinitromethane), the G3 method resulted in a MAD of 1.0 kcal mol^{-1}, which is within the desired threshold of 1.0 kcal mol^{-1}. The B3LYP/6-311G(*d,p*) method, on the other hand, resulted in a MAD of 5.7 kcal mol^{-1} while MPWB1K/6-31+G(*d,p*) method lead to an outrageously high MAD of 32.2 kcal mol^{-1} for the same species.

In this study, 40 R-NO_X and 5 heterocyclic tetrazine-containing species were examined using the ccCA, G3(MP2) and G3 methods. The R-NO_X compounds contain 3 – 15 non-hydrogen atoms and include several well-known explosive compounds like RDX, 1-methyl-4-nitrobenzene (PNT), and *N*-methyl-*N*-nitromethanamine (DMNO). 25 of the R-NO_x species in the Rice et al. study[74] are in this set of 40 species. As well, the $\Delta H_f^o{}_{(g)}$ for 5 heterocyclic tetrazine-containing species, for which there are limited experimental studies, have been predicted.

Tetrazine compounds are of high nitrogen content and produce nitrogen gas as the main combustion product rather than carbon monoxide and other toxic gases and are thus more "environmentally friendly" explosives. In addition to their military and commercial uses, they are also used in the pyrotechnics of smokeless and more vibrant fireworks due to their almost carbon-free combustion.[103] Tetrazine explosives are known to be highly endothermic (for instance, $\Delta H_f^o{}_{(g)}$ = +211.0 kcal mol^{-1} for 3,6-bis(1H-1,2,3,4-tetrazole-5-ylamino)-s-tetrazine) and usually exhibit high insensitivity towards increased temperature, impact, and friction.[70,100,104] An example is furazano-1,2,3,4-tetrazine-1,3-dioxide (FTDO) that has been considered[105] as a promising high energy additive candidate for increasing the momentum of propellants and as a component of energetic plasticizers. Teselkin[105] has studied the sensitivity of FTDO and has compared its critical initial pressure with those of well-known secondary high explosives like cyclotetramethylene-tetranitramine (also known as HMX) and pentaerythritol tetranitrate (PETN). The study revealed that FTDO has a relatively high sensitivity, similar to that of lead azide, a known sensitive compound used in detonators to initiate secondary explosives. Thus, this suggests that studies may discover better insensitive tetrazine compounds. There have been a number of studies[106-109] on the synthesis and characterization

of novel tetrazine compounds. However, additional insight would be gained by a computational study of these species. Thus, in this study, the $\Delta H_{f\,(g)}^{o}$ are predicted for several tetrazine compounds (Figure 3.1)[70,104,105,109-113]: ditetrazinetetroxide (DTTO), iso-ditetrazinetetroxide (isoDTTO), furazano-1,2,3,4-tetrazine-1,3-dioxide (FTDO), pyrido[2,3-e]-1,2,3,4-tetrazine-1,3-dioxide (PTDO), and benzotetrazine-1,3-dioxide (BTDO) that may have potential use as highly energetic species.

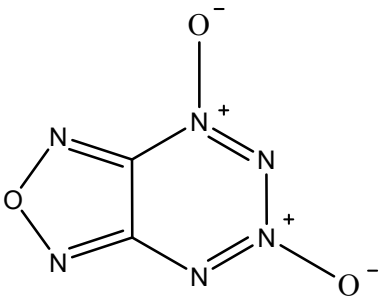

FTDO

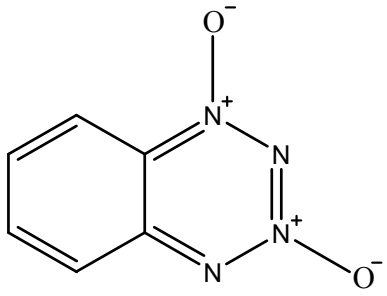

BTDO

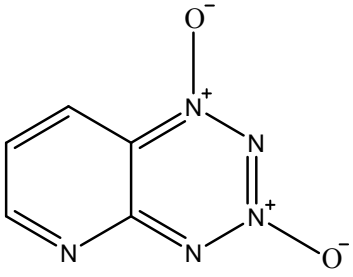

PTDO

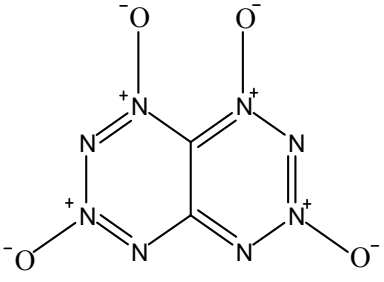

DTTO

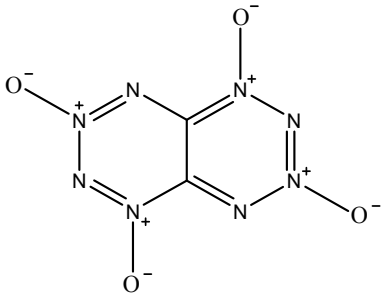

isoDTTO

Figure 3.1 Heterocyclic tetrazine-containing compounds

3.2 Computational Methods

Geometry optimizations and frequency calculations were performed for all of the molecules using B3LYP in combination with the cc-pVTZ basis sets. The zero-point vibrational energies and enthalpy corrections were scaled by a factor of 0.9890,[92] to account for deficiencies in the harmonic approximation. Single-point calculations were carried out at the B3LYP/cc-pVTZ optimized geometries for each of the ccCA steps,[92] which include a series of MP2/aug-cc-pVnZ (where n=D,T,Q) calculations for which the SCF and MP2 energies were then extrapolated to the CBS limit. A two point exponential extrapolation scheme developed by Feller[114,115] was used for the SCF extrapolation:

$$E(n) = E_{HF-CBS} + B\exp(-1.63n) \tag{3.2}$$

Two extrapolation schemes that resulted in the lowest MAD for the G3/99 test set[90] in an earlier study were considered for the extrapolation of the MP2 energies. The first was a mixed exponential/Gaussian formula (ccCA-P),[116] also known as the Peterson extrapolation:

$$E(n) = E_{CBS} + B\exp[-(n-1)] + C\exp\left[-(n-1)^2\right] \tag{3.3}$$

The second was an extrapolation based on the cubic inverse power of the highest angular momentum in the basis set (ccCA-S3)[79,117]

$$E(l_{\max}) = E_{CBS} + \frac{B}{(l_{\max})^3} \tag{3.4}$$

A mixed scheme was also used which was the arithmetic mean of the Schwartz-3 (ccCA-S3) and Peterson (ccCA-P) schemes, hereafter referred to as the ccCA-PS3 scheme, and has been shown in recent studies to be successful at reproducing experimental results.[92] The ccCA-PS3 scheme

has proven useful as the Peterson extrapolation tends to overestimate while the Schwartz-3 extrapolation tends to underestimate the CBS limit.[92] In the ccCA-P formula (Eq. 3.3), *n* = D,T,Q, corresponding to the ζ-level of the aug-cc-pV*n*Z basis set (for the extrapolation of the reference SCF, *n*=T,Q) and in the ccCA-S3 formula (Eq. 3.4) the $l_{\max}$variable represents the highest angular momentum in the basis set functions.

The Gaussian 03 program package[118] has been used for all calculations. To provide comparison to ccCA results, G3[98] and G3(MP2)[86] calculations have been performed. The $\Delta H_f^o{}_{(g)}$ have been calculated using an atomization energy approach. The atomic enthalpy of formation ΔH_f^o(0K) of elemental carbon, hydrogen, oxygen and nitrogen utilized are 170.11,[119] 51.63, 58.99 and 112.53 kcal mol^{-1} respectively.[120] The mean absolute deviations have been used as an assessment of chemical accuracy for the methods in this study.

3.3 Results and Discussion

The $\Delta H_f^o{}_{(g)}$ of the molecules in our test set have been reported in three tables: R-NO_2 (Table 3.1), R-ONO (Table 3.2), and R-ONO_2 (Table 3.3). Table 3.4 includes the MADs for all molecules in this study, including these three families of molecules. The MAD for each of the extrapolation schemes using the ccCA method is also shown in Table 3.4. The ccCA-PS3 variant has proven to be the most effective for the highly energetic nitrogen-containing species; hence, the MAD reported for the ccCA method in the remainder of this paper will be the PS3 scheme.

The overall MAD for the nitro-molecules (Table 3.1) is 1.2 kcal mol^{-1} using the ccCA method, 1.8 kcal mol^{-1} for the G3(MP2) approach, and 1.3 kcal mol^{-1} with the G3 method when compared to the experimental gas phase $\Delta H_f^o{}_{(g)}$. Since ccCA is MP2-based, its performance is

best compared with that of G3(MP2), another MP2 based method, rather than with the MP4 based G3 method. The maximum absolute deviation for ccCA is 4.1 kcal mol^{-1} and for G3(MP2) is 5.9 kcal mol^{-1}; both corresponding to the tetranitromethane compound. The G3 approach shows a deviation of only 0.9 kcal mol^{-1} for the same compound, suggesting that a higher level reference correlation method than MP2 is needed for this molecule. Interestingly, the G3 HLC is -38.1 kcal mol^{-1} while the HLC for G3(MP2) is -46.6 kcal mol^{-1}, indicating the significant reliance (but success of G3 for this molecule) on experimental parameterization. However, for the study of energetic properties of compounds without reliable experimental data, which is a major objective of this study, ccCA provides a useful approach, as it does not rely upon empirical parameters such as HLC's. The ccCA method is shown to be more accurate than G3(MP2), the more comparable method. If tetranitromethane is removed from the set of molecules, ccCA would result in a MAD, for the ensuing subset, of 1.1 kcal mol^{-1}, G3 would remain at 1.3 kcal mol^{-1}, and G3(MP2) would have a MAD of 1.6 kcal mol^{-1}. The ccCA method also results in a deviation of 4.2 kcal mol^{-1} for *m*-nitrotoluene for which the G3 method is in disagreement by 2.8 kcal mol^{-1} relative to the experimental value. The apparent consistency of the theoretical methods leads to the suggestion that experimental values could have been underestimated. For RDX, a well-known and studied explosive, ccCA is shown to deviate by 0.5 kcal mol^{-1} from the experimental value. G3 differs from the experiment by 3.1 kcal mol^{-1} while G3(MP2) has the highest absolute deviation of 4.0 kcal mol^{-1}. Overall, for the R-NO_2 compounds, the ccCA and G3 methods are quantitatively satisfactory for the study of nitro-containing energetic molecules.

Table 3.2 contains the results for the R-ONO compounds of the test set. The results show that the ccCA method leads to a MAD of 0.7 kcal mol^{-1} from the experimental values, the

G3 method results in a MAD of 0.9 kcal mol^{-1} while the MAD for G3(MP2) method is 1.8 kcal mol^{-1}. The ccCA method is within the threshold of chemical accuracy for the eight nitrite molecules considered. The maximum absolute deviation is 3.4 kcal mol^{-1} for G3(MP2) while G3 and ccCA exhibit maximum absolute deviations of 3.0 and 1.9 kcal mol^{-1} respectively, all corresponding to the molecule ethyl nitrite.

In Table 3.3, results for the R-ONO_2 molecules are presented. The ccCA method yields a MAD of 0.7 kcal mol^{-1}, G3 leads to a MAD of 0.6 kcal mol^{-1}, while the G3(MP2) method achieves a MAD of 1.8 kcal mol^{-1}. The ccCA and G3 methods show a maximum absolute deviation of 1.0 kcal mol^{-1} for *n*-propylnitrate, while G3(MP2) maximum deviation from experimental results is 2.3 kcal mol^{-1} for nitric acid. Overall, the performances of the ccCA and G3 methods are within the desired chemical accuracy when compared to experiment.

Table 3.4 contains the summary of the MAD for $\Delta H_f^{o}{}_{(g)}$ for the 40 compounds studied. The G3 approach, which is MP4 based, leads to a MAD of 1.2 kcal mol^{-1}. The ccCA method exhibits a MAD of 1.1 kcal mol^{-1}, indicating that it is a reliable method to predict and validate $\Delta H_f^{o}{}_{(g)}$ for highly energetic nitrogen-containing compounds. The G3(MP2) method results in a MAD of 1.8 kcal mol^{-1} for the entire test set, which is greater than the MAD obtained with the ccCA method even though both are based on MP2 method. The experimental $\Delta H_f^{o}{}_{(g)}$ plotted against the ccCA computed values (Figure 3.2) shows a linear regression coefficient (R^2) value of 0.996. The similarities observed in the MAD of the ccCA method compared to the G3 method, coupled with the aforementioned advantages of ccCA over G3, encourage our recommendation of ccCA for the prediction of highly energetic nitrogen containing compounds.

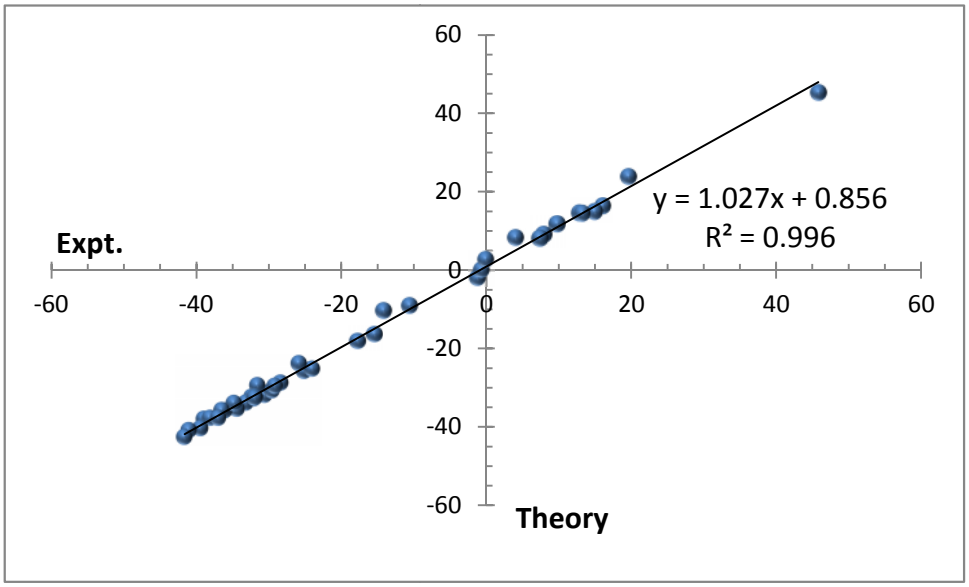

Figure 3.2 Experimental vs. theoretical ΔH_f^o (kcal mol^{-1}) calculated using ccCA-PS.

The ccCA and G3 methods have also been utilized in the determination of the $\Delta H_{f(g)}^o$ for five novel tetrazine compounds. The optimal synthetic methods for these compounds are currently under studies.[70,104,105,109-113] The results for the five potential insensitive heterocyclic explosives are shown in Table 3.5. The enthalpies of formation for furazano-1,2,3,4-tetrazine-1,3-dioxide (FTDO), pyrido-1,2,3,4-tetrazine-1,3-dioxide (PTDO), benzo-1,2,3,4-tetrazine-1,3-dioxide (BTDO) and isomeric 1,2,3,4,5,6,7,8-octazanaphthalene tetroxides (DTTO and isoDTTO) (Figure 3.1) have been computed using the G3 and ccCA methods due to their low MAD as found in this study. The predicted $\Delta H_{f(g)}^o$ (298K) for FTDO using the ccCA approach is 176.5 kcal mol^{-1}, in good agreement with 178.3 kcal mol^{-1} of the G3 method, but at variance with 171.7 and 168.8 kcal mol^{-1} of G2 and CBS-QB3 methods, respectively, as reported by Kiselev et al.[110] The ccCA method predicts the $\Delta H_{f(g)}^o$ for PTDO, BTDO, DTTO and isoDTTO as 137.6, 122.0,

232.2, and 231.1 kcal mol^{-1} while the results obtained using the G3 method for these compounds are 137.3, 121.5, 233.0, and 232.1 kcal mol^{-1} respectively.

3.4 Conclusions

Accurate prediction of the enthalpy of formation of potential energetic compounds will assist in the discovery of materials with low sensitivity to reduce disastrous premature explosions. Formulation of high explosives with enhanced performances can be improved by using chemically accurate $\Delta H_f^{o}{}_{(g)}$ in the calculation of explosive properties like VOD, T_e, ΔH_e and P_d. Three composite methods have been utilized in this study, the G3, G3(MP2), and ccCA methods, to determine an effective method able to accurately predict the gas phase ΔH_f^{o} at 298 K for highly energetic nitrogen containing compounds.

A test set of 40 nitrogen containing molecules was divided into three subsets in order to assess the energetic differences between the different types of nitrogen-containing groups (nitro, nitrate, and nitrite) in the study. The gas phase $\Delta H_f^{o}{}_{(g)}$ have also been predicted for five heterocycle-tetrazine compounds which have no experimental energetic data available. Due to their comparable accuracies and low MAD, the ccCA and G3 methods have been used to predict the $\Delta H_f^{o}{}_{(g)}$ for five tetrazine-based heterocyclic compounds with high-nitrogen content and desirable endothermic properties. The ccCA method predicts the $\Delta H_f^{o}{}_{(g)}$ for FTDO, PTDO, BTDO, DTTO and isoDTTO as 176.5, 137.6, 122.0, 232.2 and 231.1 kcal mol^{-1} respectively, while the G3 method results in 178.3, 137.3, 121.5, 233.0, and 232.1 kcal mol^{-1}, respectively indicating very good agreement between the two methods. The ccCA method, the only composite method in this study that does not depend on empirically derived parameterization, has been shown to produce highly accurate $\Delta H_f^{o}{}_{(g)}$ for highly energetic nitrogen-rich compounds. We recommend

the use of ccCA in future studies of highly energetic nitrogen-rich species. Additionally, based solely on their very high positive $\Delta H_{f\,(g)}^{o}$, DTTO and isoDTTO are good candidates for further consideration as insensitive high explosives.

Table 3.1 The enthalpies of formation (kcal mol^{-1}) of nitro compounds calculated by G3, G3(MP2) and variants of ccCA method.

Molecule	ccCA-P	ccCA-S3	ccCA-PS3	G3	G3(MP2)	Expt.[a]
Nitrogendioxide	9.3	8.5	8.9	8.1	9.1	8.1±0.2[b]
Nitroamine	0.8	-0.6	0.1	1.9	3.8	-0.7[c]
DMNO	-0.8	-3.1	-1.9	-1.4	1.1	-1.2±0.3[d]
Nitromethane	-17.4	-18.8	-18.1	-17.7	-16.0	-17.8±0.2[e]
Dinitromethane	-9.2	-11.4	-10.3	-11.2	-8.1	-9.2±0.3[e]
Trinitromethane	4.2	1.2	2.7	0.6	5.4	5.7±0.3[e]
Tetranitromethane	25.6	22.0	23.8	18.8	25.6	19.7±0.4[e]
Nitroethane	-24.5	-26.3	-25.4	-25.5	-24.1	-24.4±1.0[f]
n-Nitropropane	-29.6	-31.9	-30.8	-30.6	-28.8	-29.6±0.2[g]
Isonitropropane	-32.7	-35.0	-33.9	-33.8	-31.9	-33.2±0.2[g]
1,3-Dinitropropane	-30.9	-34.0	-32.5	-32.5	-29.3	-32.4±0.4
2,2-Dinitropropane	-31.4	-34.4	-32.9	-34.7	-31.0	-32.1±0.5
n-Nitrobutane	-34.1	-36.9	-35.5	-35.0	-33.2	-34.4±0.4[g]
1,4-Dinitrobutane	-36.2	-39.8	-38.0	-39.1	-35.9	-38.9±0.7
n-Nitropentane	-38.8	-42.0	-40.4	-40.3	-38.5	-39.4±0.5
Nitrocyclohexane	-36.1	-39.6	-37.8	-38.2	-36.4	-38.1±0.2[h]
n-Nitropiperidine	-7.4	-10.9	-9.1	-9.1	-6.7	-10.6±0.6[i]
RDX	47.8	42.8	45.3	42.7	49.8	45.8[j]
Nitrobenzene	17.7	14.6	16.2	15.2	15.2	16.1±0.1[i]
m-Dinitrobenzene	16.4	12.5	14.5	12.3	14.1	12.9±0.4[k]
p-Dinitrobenzene	16.3	12.5	14.4	12.5	14.3	13.3±0.2[h]
o-nitroaniline	16.5	13.0	14.8	14.7	15.5	15.0±1.0[l]
m-Nitrotoluene	10.1	6.5	8.3	6.9	7.1	4.1[m]
p-Nitrotoluene (PNT)	9.8	6.3	8.0	6.7	7.0	7.4±1.0[n]
2,6-Dinitrotoluene	13.6	9.3	11.5	7.9	10.3	9.6[c]
o-nitrophenol	-27.8	-31.2	-29.5	-30.4	-29.5	-31.6±0.3[i]
m-Nitrophenol	-24.3	-27.6	-25.9	-27.0	-26.4	-25.2±0.4[i]
2,4-Dinitrophenol	-29.9	-34.0	-32.0	-34.1	-31.4	-30.6±1.2

[a]Ref. 367; [b]Ref. 368; [c]Ref. 369; [d]Ref. 370; [e]Ref. 102; [f]Ref. 371; [g]Ref. 372; [h]Ref. 373; [i]Ref. 374 ; [j]Ref. 375; [k]Ref. 376; [l]Ref. 377; [m]Ref. 378; [n]Ref. 379

Table 3.2 The enthalpies of formation (kcal mol^{-1}) of nitrite compounds calculated by G3, G3(MP2) and variants of ccCA methods compared with experimental values.

Molecule	ccCA-P	ccCA-S3	ccCA-PS3	G3	G3(MP2)	Expt.[a]
Methylnitrite	-15.7	-17.1	-16.4	-15.5	-14.6	-15.6±0.2
Ethylnitrite	-23.1	-24.9	-24.0	-23.2	-22.2	-25.9
n-Propylnitrite	-27.8	-30.1	-28.9	-28.1	-27.1	-28.4±1.0
Isopropylnitrite	-31.3	-33.6	-32.5	-32.2	-31.6	-31.9±1.0
n-Butylnitrite	-32.6	-35.3	-34.0	-33.0	-32.0	-34.8±1.0
Isobutylnitrite	-34.5	-37.2	-35.9	-35.2	-34.1	-36.1±1.0
sec-Butylnitrite	-34.4	-37.1	-35.8	-35.5	-34.2	-36.5±1.0
t-butylnitrite	-39.5	-42.3	-40.9	-41.1	-39.7	-41.0±1.0

[a]*Ref. 367*

Table 3.3 The enthalpies of formation (kcal mol^{-1}) of nitrate compounds calculated by G3, G3(MP2) and variants of ccCA methods compared with experimental values.

Molecules	ccCA-P	ccCA-S3	ccCA-PS3	G3	G3(MP2)	Expt.[a]
Nitric acid	-32.1	-33.3	-32.7	-31.7	-29.8	-32.1±0.1
Methylnitrate	-28.8	-30.5	-29.7	-29.6	-27.3	-29.2±0.3
Ethylnitrate	-36.7	-38.8	-37.8	-37.8	-35.5	-37.0±0.8
n-Propylnitrate	-41.3	-43.9	-42.6	-42.6	-40.3	-41.6±0.3[b]

[a]*Ref. 367;* [b]*Ref. 374*

Table 3.4 The calculated MAD (kcal mol^{-1}) of the enthalpies of formation for all 40 molecules compared to experimental values.

	ccCA-P	ccCA-S3	ccCA-PS3	G3	G3(MP2)
Nitro	1.9	1.7	1.2	1.3	1.8
Nitrite	1.4	1.2	0.7	0.9	1.8
nitrate	0.3	1.7	0.7	0.6	1.8
Overall	1.6	1.6	1.1	1.2	1.8

Table 3.5 The predicted enthalpies (kcal mol^{-1}) of formation of tetrazine-containing compounds using G3 and variants of ccCA methods.

Molecule	ccCA-P	ccCA-S3	ccCA-PS3	G3
FTDO	178.2	174.7	176.5	178.3
PTDO	139.6	135.6	137.6	137.3
BTDO	124.1	120.0	122.0	121.5
DTTO	234.4	230.0	232.2	233.0
isoDTTO	233.3	228.8	231.1	232.1

CHAPTER 4

OXIDATIVE ADDITION OF THE C_α-C_β BOND IN β-O-4 LINKAGE OF LIGNIN TO TRANSITION METALS USING RELATIVISTIC PSEUDOPOTENTIAL CCCA-ONIOM METHOD[†]

4.1 Introduction

One of the major challenges, but least studied problems, in the development of integrated lignocellulosic biorefineries for the optimal co-production of transportation fuels, renewable chemicals and energy from biomass is the quantitative understanding of the mechanistic pathways for catalytic valorization of lignin.[121] Although, lignin is the second most abundant biopolymer on earth (surpassed only by cellulose) and constitutes of 15-30% by weight of cellulosic biomass, it is an underutilized component (usually burned to heat the reactors) from which several useful value-added products such as methanol, organic acids, benzene, and vanillin can be produced.[122,123] Lignin is a highly branched complex aromatic polymer comprised of substituted phenyl-propane units derived biosynthetically from three primary monomers: *p*-coumaryl, coniferyl, and sinapyl alcohols. The monomeric units are linked together by varieties of chemical bonds of which the 1-(4-hydroxy-3-methoxyphenyl)-2-(2-methoxyphenoxy)-1,3-propanediol (also known as arylglycerol β-aryl ether but hereafter referred to as β-O-4 linkage (Figure 4.1)) is the most common (50-60%).[122] Due to the complexity of its structural attributes, fundamental insight into the mechanistic studies of lignin conversion are usually obtained through studies of model compounds, and since β-O-4 is by far the most common linkage, it is commonly used as a representative of the complex structure.[124-126]

[†] This chapter is presented in its entirety from G. A. Oyedepo and A.K. Wilson, "Oxidative addition of the C_α-C_β bond in β-O-4 linkage of lignin to transition metals using relativistic pseudopotential ccCA-ONIOM method." *ChemPhysChem.* **2011**, 186, 583 with permission from WileyOnline.

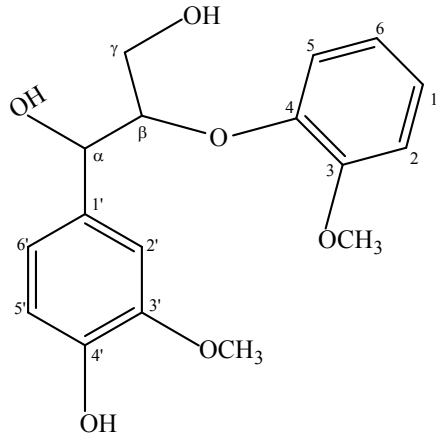

Figure 4.1 β-O-4 substructure of lignin

Many experimental and theoretical investigations have been dedicated to understanding the thermal decomposition of β-O-4 substructure of lignin using varieties of pyrolysis conditions.[126-130] Britt et al. used flash vacuum pyrolysis to investigate the primary pathways that occur under fast pyrolysis conditions using phenylethyl phenyl ether (PPE), the simplest model of β-O-4 dilignol. They found that the decomposition reaction proceeds C_β-O and C_α-C_β cleavages in 37:1 favorability ratio.[127] Using isotopic labeling and thermochemical kinetic analysis of the pyrolysis products obtained, they showed that PPE decomposition is a free-radical chain process following an initial C_β-O homolytic step.[128] Similarly, Drage et al. concluded that slow pyrolysis of a β-O-4 model compound in a closed system proceeds by C_β-O cleavage followed by demethylation of the aromatic methoxyl groups.[129] Beste and Buchanan used the M06-2X hybrid density functional to predict the bond dissociation energies (BDEs) of C_β-O and C_α-C_β bonds in substituted PPEs with a conclusion that, under a range of pyrolysis conditions, the initial reaction in the thermal decomposition of PPE will proceed via the homolytic cleavage of C_β-O bond and to a smaller extent, the C_α-C_β bond.[130] However, similar

calculations by Elder using the G3MP2 and CBS-4m methods indicate that the initial homolysis reaction of fully substituted β-O-4 compound will be less selective at higher temperatures than predicted using the PPE model since the difference between the C_β-O and C_α-C_β BDEs become smaller.[125]

Many more studies have been carried out on elucidating the mechanism of oxidative cleavages of C-C and C-O bonds in lignin by ligninolytic enzymes from the white rot-causing basidiomycetous fungi, a well-known natural lignin-degrading organism.[124,131,132] Kirk et al. utilized the fungus *Phanerochaete chrysosporium* to investigate biodegradative reactions in β-O-4 substructures in order to clarify the relative importance of competing C_4-O and C_α-C_β cleavages. They discovered that C_α-C_β cleavage is by far the more important reaction while C_4-O cleavage occurs to a very limited extent.[124] A lot of efforts have also been devoted to understanding the mechanism of bacterial degradation of lignin due to poor stability of the well-studied fungi under extreme substrate conditions as obtainable in a reactor.[133] Vicuna et al. have studied the mechanism of catabolic pathways of a more environmentally adaptive and biochemically versatile bacteria (*Pseudomonas acidovoran*) on β-O-4 model compounds.[134] It was found that the key reaction is the cleavage of the ether linkage between C_β of the phenylpropane moiety and an oxygen atom of the methoxyphenoxy moiety (C_β-O) of the substructure. However, while controlled pyrolysis of lignin streams from pre-treated biomass feeds could in principle lead to economical value-added chemicals, the selectivity of the resulting product is usually very limited.[135] Also, technologies based on enzymatic valorizations of biomass have been historically expensive.[136] Therefore, because of the high costs of their procurement and the inevitable complicated separating processes involved in removing

enzymatic catalysts from the end products, heterogeneous catalysts remain the most practical and widely used in the industries.[137] Heterogeneous catalysts are typically less expensive, more robust and longer lived than other types of catalysis.[138] Despite these obvious advantages of heterogeneous catalysts, fundamental atomic level investigations on the energetics of the catalytic pyrolysis of lignin are very scarce in the literature.[121] To gain molecular level understanding of why some transition metals form good catalysts while others do not, it is important to investigate relatively simpler model using accurate and reliable quantum mechanics methods before the consideration of more complicated conditions such as solvent and ligand effects. Also, quite little is known about the gas phase reactivity of neutral transition metal atoms with organic compounds, although they arguably provide more realistic models of condensed phase systems than the much more studied cations.[139] Therefore, to better understand the intrinsic properties influencing the activation and functionalization of each chemical bond in a complex system like lignin, gas phase studies of the electronic structures and thermodynamic properties could be a key to unraveling their catalytic activities.

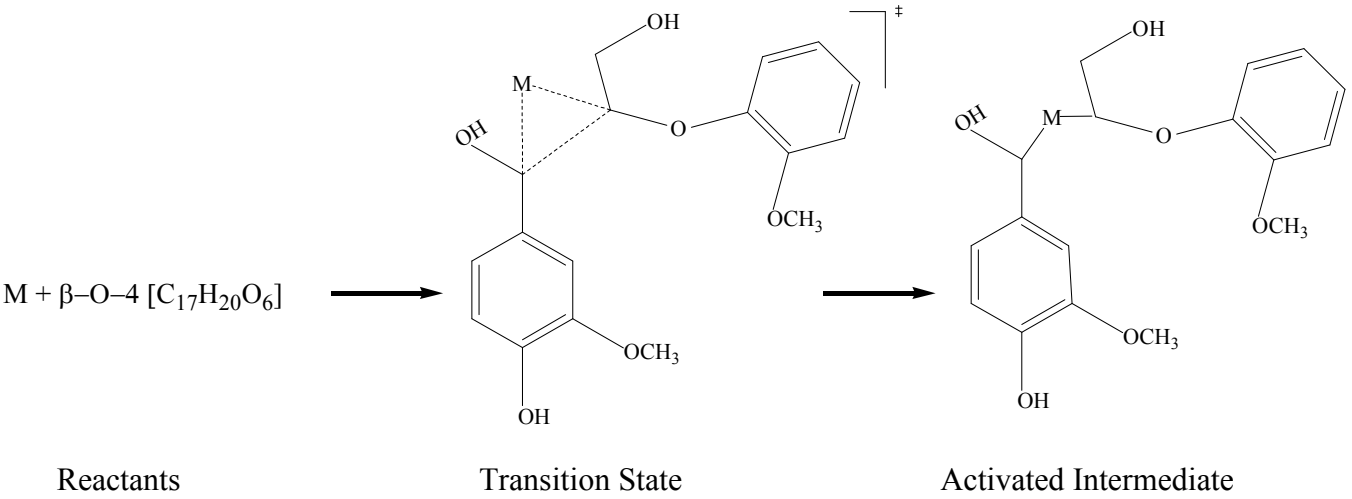

Chart 4.1 Model reaction scheme for the activation of the C_α-C_β bond in the β-O-4 linkage of lignin

The purpose of the present study is to investigate the fundamental energetics of oxidative addition of the C_α-C_β bond in β-O-4 substructure to bare transition metal atoms of group 10 metals (Ni, Pd and Pt) and Cu as depicted in Chart 4.1. These transition metal atoms are chosen based on the unique favorability of their active bonding states to insertion across covalent bonds (d^9s^1 for Ni, Pd and Pt) and because they are the most extensively used metals in contemporary heterogeneous catalysis for biomass valorization.[138,140] We also studied the reactivity of Cu atom due to the important role it plays in the active site of the ligninolytic enzyme laccasses in the decomposition of lignin.[131] Unlike the more commonly studied C-H bond cleavages in hydrocarbons and many organic compounds, the selective activations of C-C bonds can be very challenging because they usually proceed via higher energetic barriers. One of the reasons adduced to this is the possibility that in the initial bonding interactions between the metal atom and the highly directional C-C bond (Figure 4.2), the orbital overlaps accompanying the donation of electron density from the *σ*-orbital of the C-C bond to the metal *s*-orbital ($\sigma \rightarrow s$) and the concurrent back-donation of electron density from the metal *d*-orbital to the strained *σ**-orbital of the C-C bond (d_{xz} or $d_{yz} \rightarrow \sigma^*$) are not optimal.[141]

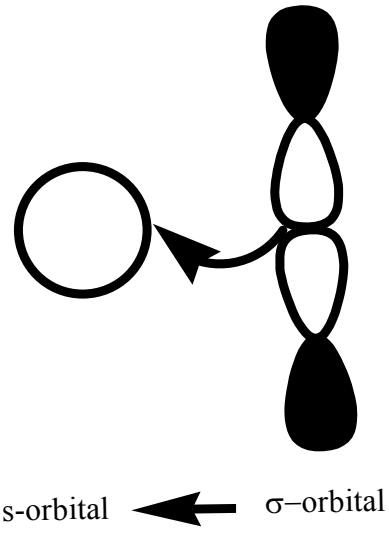

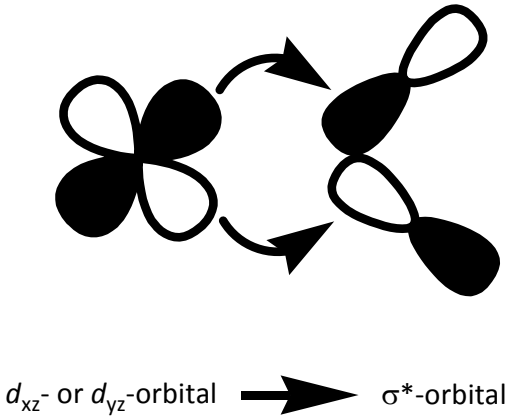

Figure 4.2 Orbital interaction diagrams depicting the activation of the C-C bond by a transition metal

Despite the advances in the development of effective theoretical methods and the upsurge in computational capabilities in recent decades, scientists are still limited to quantitative modeling of less than 20 non-hydrogen-atom systems due to the non-linear dependence of computational cost with system size. The oft-touted golden standard of computational methodologies, the coupled cluster method with single, double, and non-iterative treatment of triple excitations [CCSD(T)],[32,92,96, 142,143] has a significant drawback due to its $O(N^7)$ scaling (where N is the number of basis functions). As such, the use of CCSD(T) is generally limited to the accurate predictions of the energetics of systems with less than 10 non-hydrogen atoms. To address the problem of prohibitive costs, *ab initio* composite methodologies have been developed.[79,85,88,90,95,144-153] Composite methods take advantage of the additive effects of basis functions and correlation energies to significantly reduce costs without a corresponding loss of accuracies. On the other hand, density functional theory (DFT) methods have been shown to be more efficient than wavefunction methods due to their excellent cost-to-performance ratio.[154] Out of the plethora of the existing DFT methods, a recent review[155] showed that 80% of all the occurrences of density functionals in the chemistry

literature for the period 1990-2006 represents the usage of Becke-3-Lee-Yang-Parr (B3LYP) hybrid semi-empirical functional.[61-63] Despite its good accuracy in the prediction of geometric parameters, B3LYP has been shown to lead to large errors in the prediction of enthalpies of formation, bond dissociation energies and reaction barrier heights.[156] A methodical combination of the accuracy of composite approaches and the efficiency of DFT methods has the potential of broadening the applicability of quantitative theoretical methods to larger chemical systems.

For quantitative predictions of the energetics of moderately sized transition metal species, we introduce a multi-level multi-layer QM/QM methodology (Section 4.2) designed to exploit the accuracy of a variant of the successful *ab initio* composite methodology developed by Wilson et al. (the correlation consistent composite approach (ccCA))[90,92,95,96,142,143,149-152,157-162] in hybrid with the popular B3LYP method, using the efficiency of "divide-and-conquer" technique of Morokuma et al. (our own n-layered integrated molecular orbital and molecular mechanics (ONIOM)),[163] and the cost-saving Stuttgart-Dresden energy-consistent relativistic effective core potentials (ECPs) or pseudopotentials (PPs) constructed to reproduce experimental atomistic spectrum within relativistic Dirac-Fock theory together with their optimized correlation consistent basis sets of Peterson et al. for transition metal atoms.[164-168] The resultant method is aptly referred to as the relativistic pseudopotential correlation consistent composite approach within ONIOM framework (rp-ccCA-ONIOM). This method will be especially useful in the quantitative investigations of the chemistry at localized reaction centers involving large organometallic compound containing elements of the fourth period of the periodic table and beyond.

4.2 Theoretical Approach

It is well documented that the B3LYP method gives reliable geometries and vibrational frequencies for many chemical systems including transition metal compounds such as hydrides, halides, carbides, nitrides, oxides, and sulfides of the first-row transition metal compounds.[169,170] Therefore, fully optimized geometries of the β-O-4 substrate, transition states and activated intermediates have been carried out using the B3LYP method with the correlation consistent polarized valence triple-ζ quality basis set (cc-pVTZ) on the main group atoms while a small-core relativistic pseudopotential basis set (cc-pVTZ-PP) has been utilized on the transition metal atoms. Later we refer to this combination of basis sets as simply cc-pVTZ(PP). Analytic harmonic frequencies were computed at the same level of theory to obtain the zero-point vibrational energies (ZPVE), thermal corrections, identify the transition states, and to ensure that each intermediate geometry correctly corresponds to a true minimum on the potential energy surface. The transition states are characterized by exactly one imaginary frequency and are thus first-order saddle points. To ensure that the right transition states have been found, we inspected the animated normal mode corresponding to each imaginary frequency using the GaussView package[171] and by intrinsic reaction coordinate (IRC) calculations. A series of single-point energy calculations were subsequently carried out on the optimized geometries to determine the enthalpies of reaction and activation energies using the rp-ccCA-ONIOM method.

The rp-ccCA-ONIOM method is a two-layered extrapolated QM/QM approach[163] with a total electronic energy defined as:

$$E(\text{rp-ccCA-ONIOM}) = E(\text{B3LYP,Real}) + E(\text{rp-ccCA,Model}) - E(\text{B3LYP,Model}) \quad (4.1)$$

where *E*(B3LYP,Real) denotes the electronic energy of the full system that is obtained at the B3LYP/cc-pVTZ level of theory, *E*(rp-ccCA,Model) denotes the electronic energy of the most chemically relevant region of the system (model or primary subsystem) carefully selected for treatment with the high-level rp-ccCA method (*vide infra*) and *E*(B3LYP,Model) denotes the electronic energy of the model region obtained using B3LYP/cc-pVTZ(PP) method. The QM/QM approach outlined above corresponds to a mechanical embedding technique, an embedding scheme where a high-level quantum mechanical calculation performed on the primary subsystem is done in the absence of the secondary subsystem while the interaction between the two subsystems are treated using a lower level quantum mechanical method. The use of a sufficiently accurate quantum mechanical method (e.g. B3LYP/cc-pVTZ(PP)) as the low level of theory will ensure that polarization, charge transfer and other electronic effects are adequately included in the final electronic energy.

The effective electronic energy obtained using the rp-ccCA method can be expressed using the following general formula:

$$E_{\text{rp-ccCA}} = E(\text{HF/CBS}) + E(\text{MP2/CBS}) + \Delta E(\text{CC}) + \Delta E(\text{CV}) + \Delta E(\text{ZPVE}) \quad (4.2)$$

where *E*(HF/CBS) is the Hartree-Fock (HF) reference energy extrapolated to the complete basis set (CBS) limit, a limit at which errors due to incomplete one-electron functions would have been eliminated, *E*(MP2/CBS) is the MP2 reference correlation energy extrapolated to the CBS limit, Δ*E*(CC) is an additive term that accounts for higher-order electron correlation effects that are not fully described at the MP2 level of theory, Δ*E*(CV) is a term that accounts for core-core and core-valence electronic energy and Δ*E*(ZPVE) is a term that accounts for zero-point vibration energy.

The reference energies were determined from a series of single-point energy calculations using aug-cc-pV*n*Z(PP) [where *n* = *D*, *T* and *Q*] basis sets. Separate extrapolation of the HF and MP2 correlation energies to the CBS limit was done because, as shown in previous work,[142,151] the HF and MP2 energies converge at different rates to the CBS limit, thus, separate extrapolation schemes provide better accuracy. The MP2 correlation energies were extrapolated utilizing the mixed exponential/Gaussian function of the form:

$$E(n) = E_{MP2/CBS} + A*\exp[-(n-1)] + B*\exp[-(n-1)^2] \quad (4.3)$$

where *n* is the cardinal number of the basis set (i.e *n*=2 for aug-cc-pVDZ(PP), *n*=3 for aug-cc-pVTZ(PP) and *n*=4 for aug-cc-pVQZ(PP)) while A and B are fitting constants, first proposed by Peterson et al.[118] The HF/CBS energy was obtained using the simple two-point extrapolation scheme introduced by Feller[114]:

$$E(n) = E_{HF/CBS} + A*\exp[-1.63n] \quad (4.4)$$

where $E(n)$ in equation 4.4 is obtained from aug-cc-pVTZ(PP) and aug-cc-pVQZ(PP) basis sets. The two additive corrections (ΔE(CC) and ΔE(CV)) highlighted in equation 4.2 above are obtained using the equations 4.5 and 4.6 described below:

$$\Delta E(CC) = CCSD(T)/cc\text{-}pVTZ(PP) - MP2/cc\text{-}pVTZ(PP) \quad (4.5)$$

$$\Delta E(CV) = CCSD(T)/cc\text{-}pwCVTZ(PP) - CCSD(T)/cc\text{-}pVTZ(PP) \quad (4.6)$$

Since the selection of the layers in ONIOM calculations is somewhat arbitrary, it is desirable to show that hierarchical expansion of the high-level layer (as explained below) results in values that are not significantly different from one another. To demonstrate the locality of the activation reaction in this study, we successively expanded the rp-ccCA layer from three to five and finally to seven non-hydrogen atoms as shown in Figures 4.3a, 4.3b and 4.3c, respectively.

The ensuing results from these expansions are designated as rp-ccCA-ONIOM(3), rp-ccCA-ONIOM(5), and rp-ccCA-ONIOM(7) respectively. It should however be noted that the results from the type of expansion just discussed does not necessarily converge systematically, so a determination of the best approach for inclusion of atoms in the model system is necessary.

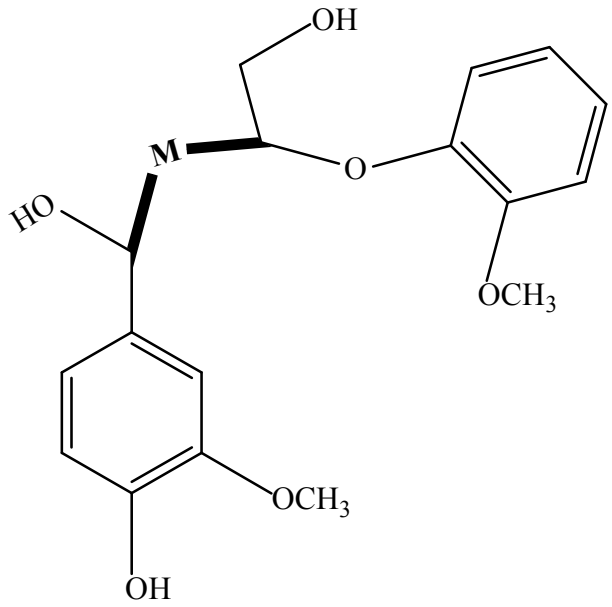

Figure 4.3a Two-layer partitioning for transition metal (M) activated intermediate of β-O-4 dilignol with three non-hydrogen atoms in the high-level layer (in bold)

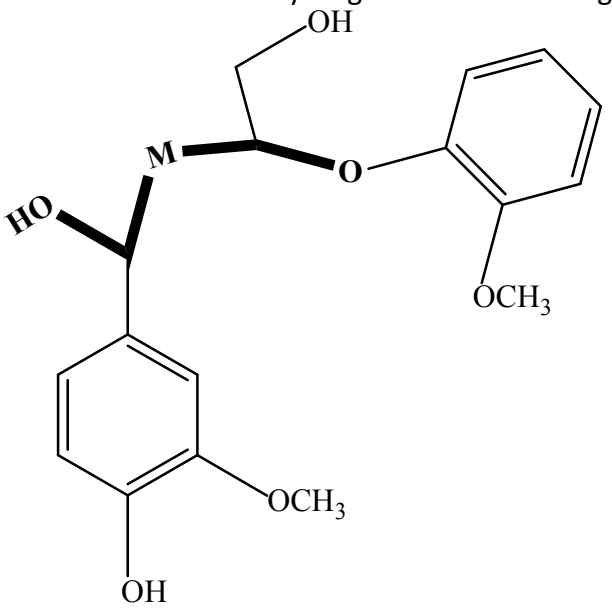

Figure 4.3b Two-layer partitioning for transition metal (M) activated intermediate of β-O-4 dilignol with five non-hydrogen atoms in the high-level layer (in bold)

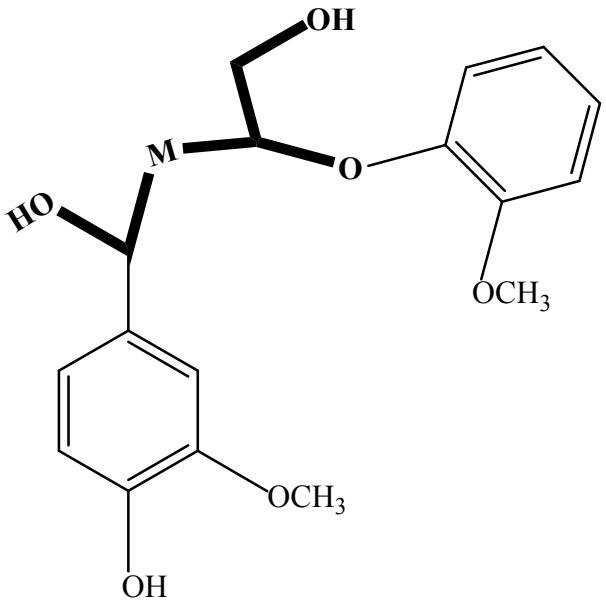

Figure 4.3c Two-layer partitioning for transition metal (M) activated intermediate of β-O-4 dilignol with seven non-hydrogen atoms in the high-level layer (in bold)

To demonstrate that rp-ccCA effectively reproduces the accuracy of the target method [CCSD(T)/aug-cc-pCV∞Z(PP)], we studied the energetics of a prototypical reaction involving the insertion of Ni, Cu, Pd, and Pt metal atoms across the C-C bond of a more computationally tractable compound, ethane (C_2H_6). For this reaction, the geometry optimizations and subsequent frequency calculations were done using B3LYP/cc-pVTZ(PP) method as outlined above. Single-point energy calculations using CCSD(T) method with aug-cc-pV*n*Z(PP) [*n* = D, T, Q] basis sets were extrapolated to the CBS limit using equation 3. The correlation effects due to core electrons in carbon and all non-valence electrons outside the ECP were included using equation 6. The resulting method, hereafter referred to as CCSD(T)/CBS, was utilized to compute the reaction energies and activation barriers involved in the oxidative addition of the C-C bond in ethane to the four transition metal atoms mentioned above, as schematically represented in Chart 2. The results obtained from CCSD(T)/CBS calculations were compared to their corresponding values using rp-ccCA method and six density functional methods: B3LYP,

M06, M06-L, B2PLYP, mPW2PLYP, and B2GPPLYP. All the DFT calculations were done with cc-pVTZ(PP) basis set. All geometry optimizations and DFT calculations in this work were carried out using Gaussian 03 (revision E.01) and Gaussian 09 (revision A.02).[118,172] All post-SCF single-point energy calculations were carried out using versions 2006.1 and 2009.1 of MOLPRO program packages.[173] Thermal corrections were included in the calculations of enthalpies of reaction and activation energies (from 0 to 298 K).

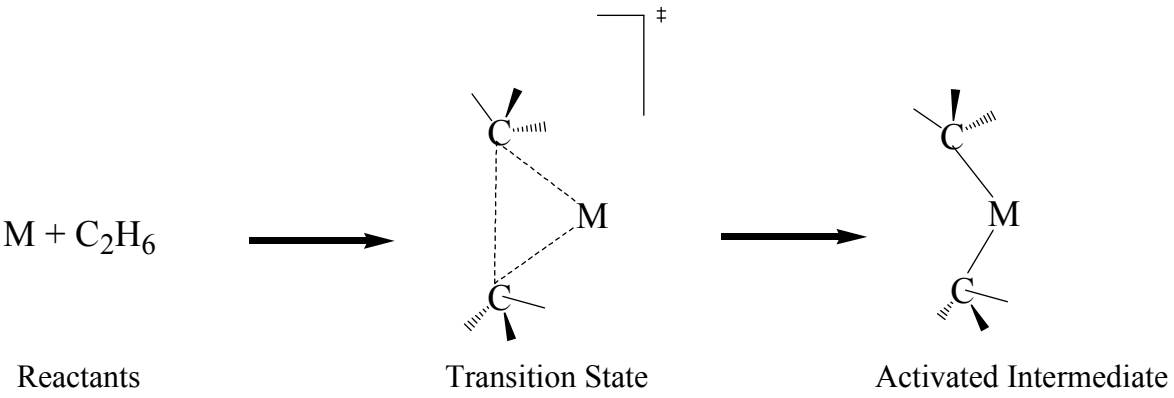

Chart 4.2 Model reaction scheme for the activation of C-C bond in ethane

4.3 Results and Discussion

4.3.1 Reaction Energies and Barrier Heights for the Activation of C-C Bond of Ethane

One of the main conclusions from previous theoretical and experimental studies on the activation of bonds in saturated hydrocarbon by transition metal atoms is that the reaction energetics are mostly determined by the electronic configurations of the metal atoms.[141] All the energy values reported in this study have been calculated relative to the ground electronic states of the metal atoms: $3d^8 4s^2$ (^{3}F) for Ni, $3d^{10} 4s^1$ (^{2}S) for Cu, $4d^{10}$ (^{1}S) for Pd and $5d^9 6s^1$ (^{3}D) for Pt. However, in order to successfully insert a metal atom across C-C bond to consequently

form two covalent bonds, the bonding electronic state of the metal should have two unpaired open-shell orbitals. Therefore, Ni and Pt are more disposed to undergo oxidative addition reaction with ethane than are Cu and Pd due to the favorable ground state electron configuration of the former. Also, since the valence *s*-orbitals in transition metal atoms are more diffuse than the outermost *d*-orbitals, the Pt atom with a lower occupation of the *s*-orbital will suffer less repulsion than Ni during the initiation of orbital overlaps as explained in Figure 4.2. Ni, however, has a low-lying and less repulsive d^9s^1 (^{3}D) bonding excited configuration with an experimental promotion energy of only 0.6 kcal mol^{-1}.[174] The promotion energy is the amount of energy required to convert a repulsive electronic configuration of the ground state of a metal to an appropriate reactive excited state configuration. The experimental promotion energy to the more reactive d^9s^1 (^{3}D) and $d^9s^1p^1$ (^{4}P) configuration for Pd and Cu are 18.8 kcal mol^{-1} and 111.6 kcal mol^{-1}, respectively.[174] The very high excitation energy required for Cu to achieve a bonding configuration for two covalent bonds will lead to a less effective overlap between its orbitals and the orbitals of C-C bond. It is thus not surprising that the exothermicity of reaction energies for the oxidative addition of the C-C bond of ethane to the metal atoms follow the trend Pt>Ni>Pd>Cu, where the reaction involving Cu is observed to be strongly endothermic as depicted in Figure 4.4a while the activation barriers in descending order follow the trend Cu>Pd>Ni>Pt as shown in Figure 4.4b.

In Tables 4.1-4.4, we summarize the performances of the various quantum mechanical methods mentioned above in the determination of the heat of reaction at 298 K (ΔH_{298}) and activation barriers (E_a) for the insertion of transition metal atoms into the C-C bond of ethane. To the best of our knowledge, there are no available experimental values for ΔH_{298} and E_a

determined in this study. Hence, the results of the computationally intensive CCSD(T)/CBS are used as the benchmark against which other methods are measured due to its well-known accuracy and reliability. The rp-ccCA determined ΔH_{298} for Ni (Table 4.1), Cu (Table 4.2), Pd (Table 4.3) and Pt (Table 4.4) are -21.2, 8.7, -7.5, and -52.1 kcal mol^{-1}, respectively in good agreement with the CCSD(T)/CBS results of -21.4, 9.4, -7.8, and 51.7 kcal mol^{-1} respectively. The largest deviation observed ($\Delta\Delta H_{298}$) between rp-ccCA values and the corresponding CCSD(T)/CBS values is 0.7 kcal mol^{-1} which is well within the so-called chemical accuracy of ±1.0 kcal mol^{-1}. We estimated the extent of systematic error in each method by calculating the mean signed error (MSE) while the average magnitude of errors are reported as mean absolute error (MAE) and root mean square error (RMSE) in Tables 4.5a and 4.5b for ΔH_{298} and E_a respectively. The rp-ccCA method results in an MSE value of +0.2 kcal mol^{-1} indicating that it, on the average, gives a slightly more exothermic value for ΔH_{298} while its MAE and RMSE values are both 0.4 kcal mol^{-1} indicating that it effectively reproduces the accuracy of CCSD(T)/CBS without any significant error. The rp-ccCA results for the E_a of Ni, Cu, Pd and Pt atoms are 10.8, 51.9, 14.2, and -1.2 kcal mol^{-1} respectively in good agreement with the CCSD(T)/CBS values of 10.8, 53.4, 14.7, and -0.2 kcal mol^{-1} respectively. The MSE value of +0.8 kcal mol^{-1} indicates that rp-ccCA tends to underestimate the reaction barriers, particularly for the Cu reaction, with the largest error (ΔE_a) of 1.5 kcal mol^{-1}. The MAE and RMSE values of 0.8 and 0.9 kcal mol^{-1} were obtained for rp-ccCA indicating its good agreement with CCSD(T)/CBS results. The efficient rp-ccCA method is thus decidedly representative of the results that would be obtained using the CCSD(T)/CBS method, more so than all of the other methods considered in this study as clearly shown in Figures 4.4a and 4.4b.

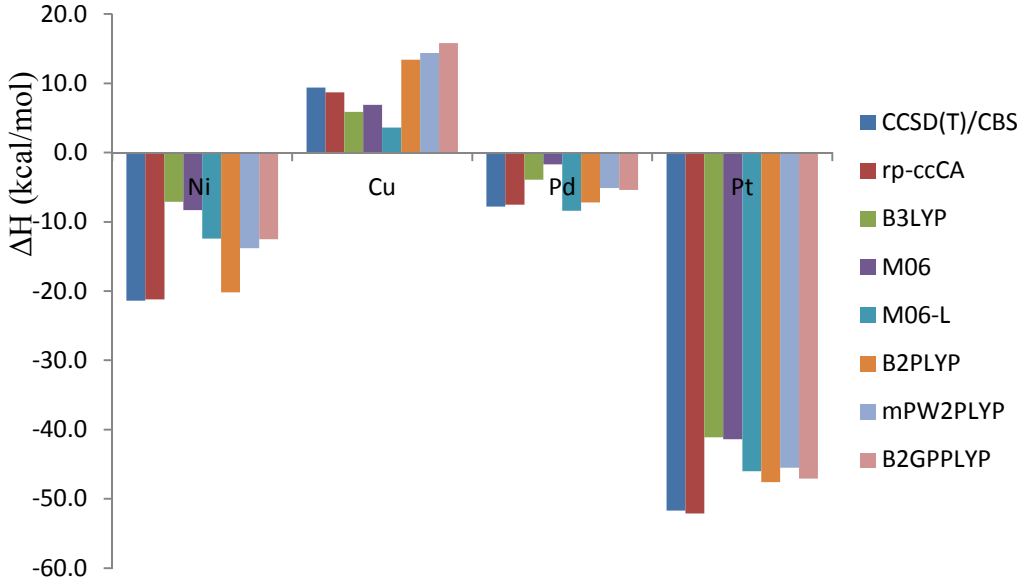

Figure 4.4a Analysis of the reaction energies (ΔH) involved in the oxidative addition of C-C bond in ethane to Ni, Cu, Pd and Pt atoms

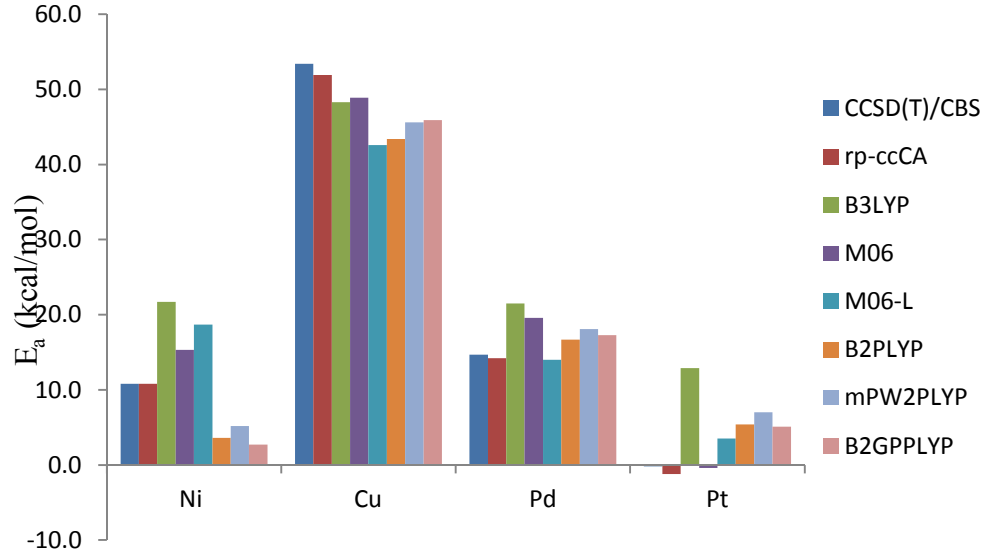

Figure 4.4b Analysis of the activation barriers (E_a) that must be overcome in the oxidative addition of C-C bond in ethane to Ni, Cu, Pd and Pt atoms

All the density functional methods in this study give results that are systematically more endothermic relative to CCSD(T)/CBS in the calculation of ΔH_{298} as exhibited by their very negative MSE values on Table 4.5a. However, B2PLYP outperforms the other five density functional methods with the MAE and RMSE values of 2.5 and 2.9 kcal mol^{-1} respectively as shown in Table 4.5a. Among the semi-empirical double-hybrid density functional methods (*x*, *y*) first proposed by Grimme[66] where *x* and *y* represent the proportions of MP2-type correlation and Hartree-Fock-type exchange utilized in their construction [B2PLYP (0.27, 0.53), mPW2PLYP (0.25, 0.55) and B2GPPLYP (0.36, 0.65)], it can be observed that as the proportion of the exact non-local Hartree-Fock-exchange increases, the difference with respect to CCSD(T)/CBS value decreases in the determination of ΔH_{298}. This observation agrees with and further corroborates previous findings by Goerigk and Grimme[175] that the lower the amount of Hartree-Fock-exchange in a hybrid or double-hybrid density functional, the better its performance in the calculation of the reaction enthalpies of transition metal compounds. Also, the double-hybrid functionals generally perform better than the single-hybrid density functionals (B3LYP, M06 and M06-L with 20%, 27% and 0% Hartree-Fock-type exchange respectively) in the determination of ΔH_{298}. M06-L, however, clearly outperforms B3LYP and M06 functionals for ΔH_{298} in further confirmation of its recommendation by Zhao and Truhlar as a method to be considered in the computation of transition metal thermodynamics.[176] The performance of the M06 functional is significantly better than that of the other five functionals in the determination of E_a (it should be noted that the training sets used in the parameterization of both M06 and M06-L functionals include reaction barriers). This observation supports the recommendation of Truhlar et al. that the M06 functional could be used to study chemical problems where bonds are broken or

formed and for transition metal reactions with multireference rearrangements.[186] Another interesting observation in this study is that the three double-hybrid density functional methods employed generally underestimate the barrier heights (positive MSE values) and also result in a similar level of accuracy as shown in Table 4.5b. This is not very surprising since they contain similar constituents in their formulations (the primary difference occurs for mPW2PLYP and B2PLYP where mPW and B88 exchange functionals were used, respectively). The largest observed errors of -14.3 kcal mol^{-1} (Table 4.1) and -13.1 kcal mol^{-1} (Table 4.4) are obtained with B3LYP method in the determination of ΔH_{298} and E_a for Ni and Pt, respectively which is not unexpected since B3LYP gives the highest MAE and RMSE values of all the methods considered in the present study.

4.3.2 Reaction Energies and Activation Barriers for Oxidative Addition of the C_α-C_β Bond in β-O-4 Substructure of Lignin to Transition Metals

As mentioned above, efforts have been made to show that the selection of the high-level layer when using the rp-ccCA-ONIOM method is representative of the most chemically relevant region of the system by sequentially expanding the layer (i.e. increasing the number of non-hydrogen atoms by two in successive runs). Although the results superficially appear to be in the same ballpark as shown on Tables 4.6-4.9, the difference between the values are very substantial, ranging from 1.1 to 3.9 kcal mol^{-1}. The reason for this large difference is because important chemical information is lost when, for instance, a hydrogen bonding interaction in the glycerol side chain is split between the layers and treated in a mechanically embedded fashion. Consequently, the results of rp-ccCA-ONIOM(7) (where all the pertinent interactions are included together in the high-level layer while only the sterics are treated at the low-level

layer) should be taken as the de facto rp-ccCA-ONIOM value, and it will be the one referenced in this discussion.

The first interesting observation in the oxidative addition reaction of C_α-C_β bond of β-O-4 dilignol to transition metal atoms is that unlike in the activation of C-H bond where reactivity was found to increase with the size of hydrocarbon compounds due to weakening of the C-H bond as the size of the alkane increases from methane through *n*-butane,[177] our results indicate the direct opposite of these findings. The reaction barriers leading to the activation of the carbon-carbon bond increases on increasing the size of the system from ethane to β-O-4 (with the exception of the Cu reaction discussed below) despite the fact that the C-C bond is significantly stronger in ethane than in β-O-4 substructure (84.4 kcal mol^{-1} versus 60.8 kcal mol^{-1}, as computed using B3LYP/cc-pVTZ method). A rational explanation for this observation is the increased steric hindrances to which the transition metal atoms are subjected before reaching the activation site.

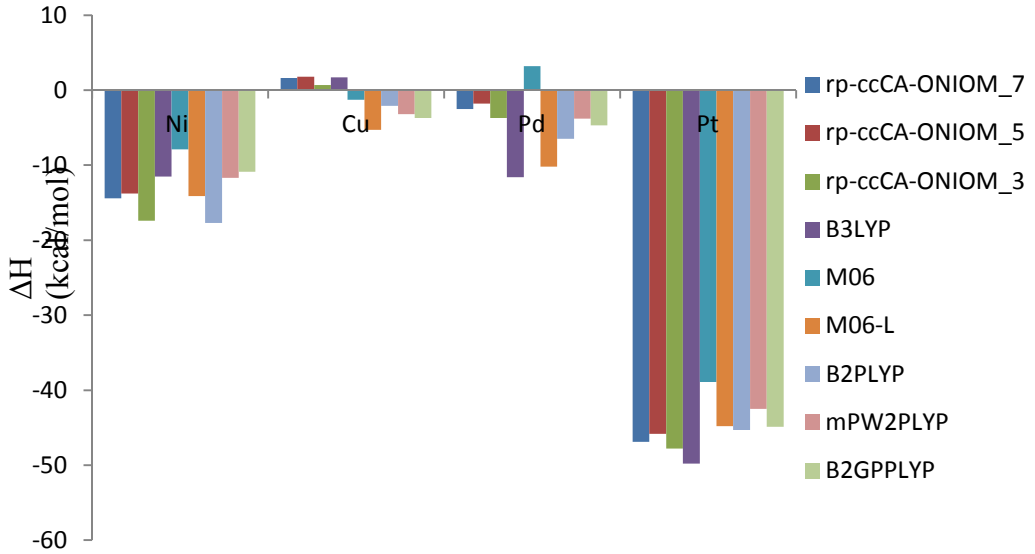

Figure 4.5a Analysis of the reaction energies (ΔH) involved in the oxidative addition of C_α-C_β bond in β-O-4 substructure of lignin to Ni, Cu, Pd and Pt atoms

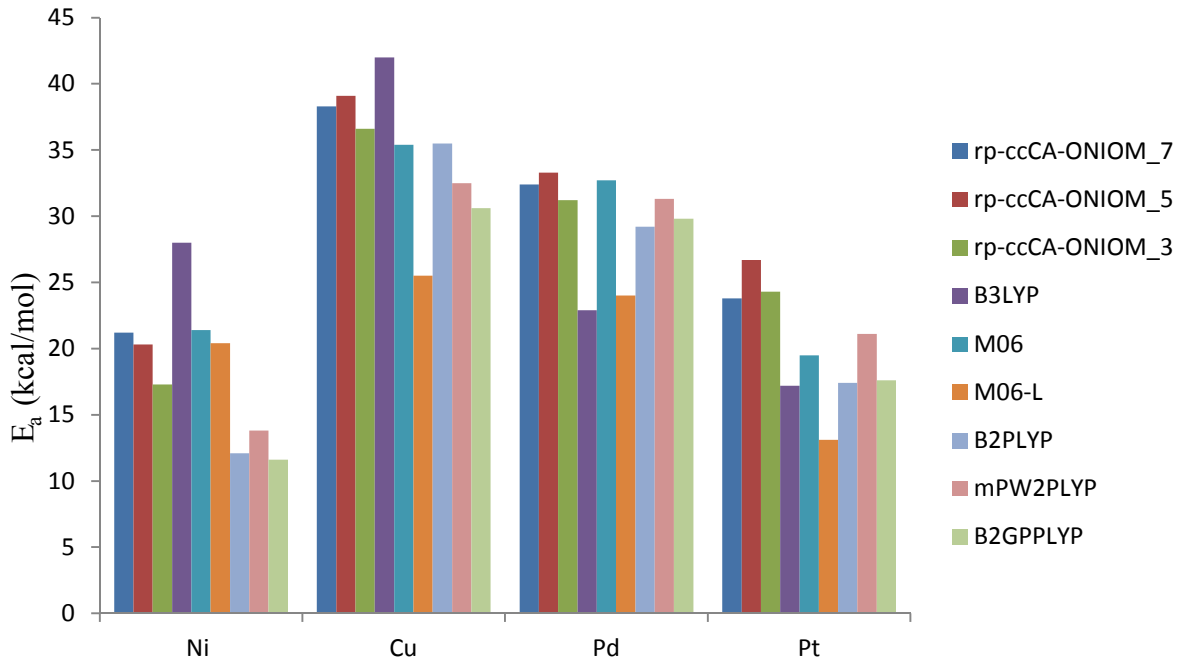

Figure 4.5b Analysis of the activation barriers (E_a) that must be overcome in the oxidative addition of C_α-C_β bond in β-O-4 substructure of lignin to Ni, Cu, Pd and Pt atoms

The reaction energies for the four transition metal atoms investigated in the present study follow the same pattern observed in their reaction with ethane as explained earlier. The exothermicity of the reactions follow the trend Pt>Ni>Pd>Cu as clearly shown in Figure 4.5a while the reaction barriers also follow similar trend Cu>Pd>Ni>Pt as can be observed in Figure 4.5b. However, the general trend observed in the activation of the C_α-C_β bond in β-O-4 by the metal atoms is that the reactions tend to be more endothermic with higher barrier heights than the corresponding reactions in ethane. The only exception to this trend is the reaction of Cu which our calculations indicate is more exothermic with lower activation barrier as can be seen in the results on Tables 4.2 and 4.7 [8.7 kcal mol^{-1} (ΔH_{298}) and 51.9 kcal mol^{-1} (E_a) for ethane versus 1.6 kcal mol^{-1} (ΔH_{298}) and 38.3 kcal mol^{-1} (E_a) for β-O-4]. The reason for this "anomaly" could be due to the small van der Waals radius of Cu atom which will ensure that it suffers less

steric repulsions than the other three metals (van der Waals radii of Cu, Ni, Pd and Pt atoms are 1.40, 1.63, 1.63 and 1.72, respectively).[178]

Since computationally demanding theoretical methods like CCSD(T)/CBS are impractical for studying the reaction of β-O-4 and transition metal atoms due to the relatively large size of the system, the reliability of the results obtained using rp-ccCA-ONIOM as shown in Tables 4.6-4.9 may be assessed by comparison to the results of the density functionals methods utilized in the reaction of ethane in the above discussion. The B2PLYP method gives ΔH_{298} values of -17.7, -2.1, -6.5 and -45.3 kcal mol^{-1} in contrast with -14.4, 1.6, -2.5 and -46.9 kcal mol^{-1} of rp-ccCA-ONIOM for Ni, Cu, Pd and Pt respectively. While for E_a, the M06 method results in values of 21.4, 35.4, 32.7 and 19.5 kcal mol^{-1} where rp-ccCA-ONIOM results are 21.2, 38.3, 32.4 and 23.8 kcal mol^{-1} for Ni, Cu, Pd and Pt respectively. However, because this type of comparison could be subjective, we ran the very time and resource consuming CCSD(T)/aug-cc-pVDZ calculation, which although has inadequate one-electron basis functions, can aid in assessing the accuracy of the rp-ccCA-ONIOM method.

Due to the very high computational cost of CCSD(T)/aug-cc-pVDZ method as a result of the size of the system, we only computed the energetics of Pd and Pt reactions with β-O-4 for comparison to the rp-ccCA-ONIOM and the density functional methods. As shown in Tables 4.1-4.4, the better the quality of the basis sets used with the CCSD(T) method, the lower the activation barriers and the more exothermic the reaction energies. However, as shown in Tables 4.8 and 4.9, the CCSD(T)/aug-cc-pVDZ(PP) computed E_a for Pd and Pt reactions are lower than the corresponding values of rp-ccCA-ONIOM (31.9 versus 32.4 kcal mol^{-1} for Pd and 18.3 versus 23.8 kcal mol^{-1} for Pt). Therefore, there is a possibility that the values of E_a reported

in Tables 4.6-4.9 may have been slightly overestimated, at least relative to CCSD(T)/CBS. This observation can be explained by considering that B3LYP method was used as the lower level of theory in rp-ccCA-ONIOM method. As shown in Table 4.5b, B3LYP tends to overestimate the E_a values with its very large MSE value of -6.4 while the rp-ccCA method tends to slightly underestimate the same property. This can lead to favorable cancellation of errors within rp-ccCA-ONIOM method. However, in the interplay of these opposing tendencies, the method used as the lower level of theory (B3LYP in the present study) may influence the accuracy of the computed reaction barrier using the rp-ccCA-ONIOM method. The computed ΔH_{298} for Pd and Pt using CCSD(T)/aug-cc-pVDZ(PP) are, however, more endothermic than the corresponding results for rp-ccCA-ONIOM (2.6 versus -2.5 kcal mol^{-1} for Pd and -41.6 versus -46.9 kcal mol^{-1} for Pt), which as explained above indicates that the rp-ccCA-ONIOM results are more comparable to the values that would have been obtained using the highly expensive but reliable CCSD(T)/CBS method.

4.4 Conclusions

The major objective of the present study is to provide insight into the catalytic activation of the carbon-carbon bond in an archetypal lignin model compound (β-O-4) by transition metal atoms using a multi-level multi-layer QM/QM methodology designed to benefit from the accuracy of a variant of the successful ccCA composite method and the efficiency of the popular density functional method (B3LYP), within the ONIOM framework. The resultant method, tagged rp-ccCA-ONIOM, has been used to predict the enthalpies of reaction and the activation barriers of the oxidative addition reaction of the C_α-C_β bond in a β-O-4 substructure

to four transition metal atoms: Ni, Cu, Pd and Pt. Three double-hybrid (B2PLYP, mPW2PLYP and B2GPPLYP), two single-hybrid (B3LYP and M06) and one local (M06-L) density functional methods were also utilized to provide comparison. The main findings in this study are summarized as follows.

a) While the electronic configuration of the transition metal atoms largely determine the energetics of the activation reaction of the C_α-C_β bond in β-O-4 in accordance with the observations reported for simpler hydrocarbon compounds, steric hindrances due to the atomic sizes of the elements may also play a big role.

b) The exothermicity of the β-O-4 reaction with the transition metals follows the trend Pt>Ni>Pd>Cu while the reaction barriers in descending order is Cu>Pd>Ni>Pt. This observation is due to the favorable d^9s^1 electron configuration of Pt in the formation of two covalent bonds while the extent of the promotional energy penalty that has to be paid to achieve similar configuration by the other atoms influence their reactivities.

c) The accuracy of the rp-ccCA-ONIOM method in the determination of reaction barriers may be influenced by the choice the DFT method used for the lower level of theory.

d) Among the DFT methods employed in the present study, the B2PLYP double-hybrid functional gives the better performance in the determination of ΔH_{298} (MAE = 2.5 kcal mol^{-1}) while M06 single hybrid functional results in the lowest mean absolute error in the estimation of E_a (MAE = 3.5 kcal mol^{-1}), relative to CCSD(T)/CBS results.

e) The rp-ccCA method [MAE = 0.4 (ΔH_{298}) and 0.8 (E_a) kcal mol^{-1}] used in the high-level layer of the QM/QM method, effectively and efficiently reproduces the accuracy of the CCSD(T)/CBS method and significantly outperforms all the DFT methods employed in

this study. Consequently, it is recommended to be used when chemical accuracy is desirable in the prediction of the energetics of moderately-sized organometallic reactions.

Further investigations are continuing in our laboratory to explore the size dependence of the reactivities of the transition metals in the activation of bonds in lignin. In conclusion, among the four transition metals investigated in the present study, the activation of the C_α-C_β bond in β-O-4 dilignol with Pt will be more kinetically and thermodynamically favored because of its low activation barrier and high exothermicity.

Table 4.1 Heat of reaction (ΔH_{298}) and activation energy (E_a) for C-C cleavage in ethane using Ni atom (kcal mol^{-1}).

	ΔH_{298}	E_a	$\Delta\Delta H_{298}$	ΔE_a
B3LYP/VTZ(PP)	-7.1	21.7	-14.3	-10.9
M06/VTZ(PP)	-8.3	15.3	-13.1	-4.5
M06-L/VTZ(PP)	-12.4	18.7	-9.0	-7.9
B2PLYP/VTZ(PP)	-20.2	3.6	-1.2	7.2
mPW2PLYP/VTZ(PP)	-13.8	5.2	-7.6	5.6
B2GPPLYP/VTZ(PP)	-12.5	2.7	-8.9	8.1
CCSD(T)/AVDZ(PP)	-17.8	15.8	-3.6	-5.0
CCSD(T)/AVTZ(PP)	-18.4	13.3	-3.0	-2.5
CCSD(T)/AVQZ(PP)	-20.0	10.7	-1.4	0.1
CCSD(T)/CBS	-21.4	10.8	0.0	0.0
rp-ccCA	-21.2	10.8	-0.2	0.0

$\Delta\Delta H_{298} = \Delta H_{298}$[CCSD(T)/CBS] − ΔH_{298}[X]; $\Delta E_a = E_a$[CCSD(T)/CBS] – E_a[X],
(X = B3LYP, M06, M06-L, B2PLYP, mPW2PLYP and B2GPPLYP)

Table 4.2 Heat of reaction (ΔH_{298}) and activation energy (E_a) for C-C cleavage in ethane using Cu atom (kcal mol^{-1}).

	ΔH_{298}	E_a	$\Delta\Delta H_{298}$	ΔE_a
B3L P/VTZ(PP)	5.9	48.3	3.5	5.1
M06/VTZ(PP)	6.9	48.9	2.5	4.5
M06-L/VTZ(PP)	3.6	42.6	5.8	10.8
B2PLYP/VTZ(PP)	13.4	43.4	-4.0	10.0
mPW2PLYP/VTZ(PP)	14.4	45.6	-5.0	7.8
B2GPPLYP/VTZ(PP)	15.8	4 .9	-6.	7.5
CCSD(T)/AVDZ(PP)	11.8	55.5	-2.4	-2.1
CCSD(T)/AVTZ(PP)	10.6	54.8	-1.2	-1.4
CCSD(T)/AVQZ(PP)	10.1	54.7	-0.7	-1.3
CCSD(T)/CBS	9.4	53.4	0.0	0.0
rp-ccCA	8.7	51.9	0.7	1.5

$\Delta\Delta H_{298} = \Delta H_{298}[CCSD(T)/CBS] - \Delta H_{298}[X]$; $\Delta E_a = E_a[CCSD(T)/CBS] - E_a[X]$,
(X = B3LYP, M06, M06-L, B2PLYP, mPW2PLYP and B2GPPLYP)

Table 4.3 Heat of reaction (ΔH_{298}) and activation energy (E_a) for C-C cleavage in ethane using Pd atom (kcal mol^{-1}).

	ΔH_{298}	E_a	$\Delta\Delta H_{298}$	ΔE_a
B3LYP/VTZ(PP)	-3.9	21.5	-3.9	-6.8
M06/VTZ(PP)	-1.7	19.6	-6.1	-4.9
M06-L/VTZ(PP)	-8.4	14.0	0.6	0.7
B2PLYP/VTZ(PP)	-7.2	16.7	-0.6	-2.0
mPW2PLYP/VTZ(PP)	-5.1	18.1	-2.7	-3.4
B2GPPLYP/VTZ(PP)	-5.4	17.3	-2.4	-2.6
CCSD(T)/AVDZ(PP)	-2.0	19.4	-5.8	-4.7
CCSD(T)/AVTZ(PP)	-3.7	17.1	-4.1	-2.4
CCSD(T)/AVQZ(PP)	-3.8	17.0	-4.0	-2.3
CCSD(T)/CBS	-7.8	14.7	0.0	0.0
rp-ccCA	-7.5	14.2	-0.3	0.5

$\Delta\Delta H_{298} = \Delta H_{298}[CCSD(T)/CBS] - \Delta H_{298}[X]$; $\Delta E_a = E_a[CCSD(T)/CBS] - E_a[X]$,
(X = B3LYP, M06, M06-L, B2PLYP, mPW2PLYP and B2GPPLYP)

Table 4.4 Heat of reaction (ΔH_{298}) and activation energy (E_a) for C-C cleavage in ethane using Pt atom (kcal mol^{-1}).

	ΔH_{298}	E_a	$\Delta\Delta H_{298}$	ΔE_a
B3LYP/VTZ(PP)	-41.1	12.9	-10.6	-13.1
M06/VTZ(PP)	-41.4	-0.4	-10.3	0.2
M06-L/VTZ(PP)	-46.0	3.5	-5.7	-3.7
B2PLYP/VTZ(PP)	-47.6	5.4	-4.1	-5.6
mPW2PLYP/VTZ(PP)	-45.5	7.0	-6.2	-7.2
B2GPPLYP/VTZ(PP)	-47.1	5.1	-4.6	-5.3
CCSD(T)/AVDZ(PP)	-46.6	4.1	-5.1	-4.3
CCSD(T)/AVTZ(PP)	-49.4	0.3	-2.3	-0.5
CCSD(T)/AVQZ(PP)	-50.5	-0.6	-1.2	0.4
CCSD(T)/CBS	-51.7	-0.2	0.0	0.0
rp-ccCA	-52.1	-1.2	0.4	1.0

$\Delta\Delta H_{298} = \Delta H_{298}[CCSD(T)/CBS] - \Delta H_{298}[X]$; $\Delta E_a = E_a[CCSD(T)/CBS] - E_a[X]$,
(X = B3LYP, M06, M06-L, B2PLYP, mPW2PLYP and B2GPPLYP)

Table 4.5a The mean signed error (MSE), mean absolute error (MAE) and root mean squared error (RMSE) of theoretical methods for reaction energies (ΔH) in the activation of C-C bond in ethane (kcal mol^{-1}).[a]

ΔH	CCSD(T)/CBS	rp-ccCA	B3LYP	M06	M06-L	B2PLYP	mPW2PLYP	B2GPPLYP
MSE	0.0	0.2	-6.3	-6.8	-2.1	-2.5	-5.4	-5.6
MAE	0.0	0.4	8.1	8.0	5.3	2.5	5.4	5.6
RMSE	0.0	0.4	9.3	9.0	6.1	2.9	5.7	6.1

[a] All DFT calculations were done using cc-pVTZ(PP) basis set

Table 4.5b The mean signed error (MSE), mean absolute error (MAE) and root mean squared error (RMSE) of theoretical methods for activation barriers (E_a) in the activation of C-C bond in ethane (kcal mol^{-1}).[a]

E_a	CCSD(T)/CBS	rp-ccCA	B3LYP	M06	M06-L	B2PLYP	mPW2PLYP	B2GPPLYP
MSE	0.0	0.8	-6.4	-1.2	0.0	2.4	0.7	1.9
MAE	0.0	0.8	9.0	3.5	5.8	6.2	6.0	5.9
RMSE	0.0	0.9	9.5	4.0	7.0	6.8	6.2	6.3

[a] All DFT calculations were done using cc-pVTZ(PP) basis set

Table 4.6 Heat of reaction (ΔH_{298}) and activation energy (E_a) for C_α-C_β cleavage in β-O-4 using Ni atom (kcal mol^{-1})

	ΔH_{298}	E_a
rp-ccCA-ONIOM(3)	-17.4	17.3
rp-ccCA-ONIOM(5)	-13.8	20.3
rp-ccCA-ONIOM(7)	-14.4	21.2
B3LYP/VTZ(PP)	-11.5	28.0
M06/VTZ(PP)	-7.9	21.4
M06-L/VTZ(PP)	-14.1	20.4
B2PLYP/VTZ(PP)	-17.7	12.1
mPW2PLYP/VTZ(PP)	-11.7	13.8
B2GPPLYP/VTZ(PP)	-10.9	11.6

Table 4.7 Heat of reaction (ΔH_{298}) and activation energy (E_a) for C_α-C_β cleavage in β-O-4 using Cu atom (kcal mol^{-1})

	ΔH_{298}	E_a
rp-ccCA-ONIOM(3)	0.7	36.6
rp-ccCA-ONIOM(5)	1.8	39.1
rp-ccCA-ONIOM(7)	1.6	38.3
B3LYP/VTZ(PP)	1.7	42.0
M06/VTZ(PP)	-1.3	35.4
M06-L/VTZ(PP)	-5.3	25.5
B2PLYP/VTZ(PP)	-2.1	35.5
mPW2PLYP/VTZ(PP)	-3.2	32.5
B2GPPLYP/VTZ(PP)	-3.5	30.6

Table 4.8 Heat of reaction (ΔH_{298}) and activation energy (E_a) for C_α-C_β cleavage in β-O-4 using Pd atom (kcal mol^{-1})

	ΔH_{298}	E_a
rp-ccCA-ONIOM(3)	-3.7	31.2
rp-ccCA-ONIOM(5)	-1.8	33.3
rp-ccCA-ONIOM(7)	-2.5	32.4
B3LYP/VTZ(PP)	-11.6	22.9
M06/VTZ(PP)	3.2	32.7
M06-L/VTZ(PP)	-10.2	24.0
B2PLYP/VTZ(PP)	-6.5	29.2
mPW2PLYP/VTZ(PP)	-3.8	31.3
B2GPPLYP/VTZ(PP)	-4.7	29.8
CCSD(T)/AVDZ(PP)	2.6	31.9

Table 4.9 Heat of reaction (ΔH_{298}) and activation energy (E_a) for C_α-C_β cleavage in β-O-4 using Pt atom (kcal mol^{-1}).

	ΔH_{298}	E_a
rp-ccCA-ONIOM(3)	-47.8	24.3
rp-ccCA-ONIOM(5)	-45.8	26.7
rp-ccCA-ONIOM(7)	-46.9	23.8
B3LYP/VTZ(PP)	-49.8	17.2
M06/VTZ(PP)	-38.9	19.5
M06-L/VTZ(PP)	-44.8	13.1
B2PLYP/VTZ(PP)	-45.3	17.4
mPW2PLYP/VTZ(PP)	-42.5	21.1
B2GPPLYP/VTZ(PP)	-44.9	17.6
CCSD(T)/AVDZ(PP)	-41.6	18.3

CHAPTER 5

MULTIREFERENCE CORRELATION CONSISTENT COMPOSITE APPROACH: TOWARD QUANTITATIVE PREDICTION OF THE ENERGETICS OF EXCITED AND TRANSITION STATE CHEMISTRY[†]

5.1 Introduction

The accurate prediction of thermodynamic and spectroscopic properties of open-shell species that involve molecular electronic excited states, bond breaking (or formation), reactive intermediates, or transition metal species has been a continuing challenge to computational chemistry.[179,180] The most widely used electronic structure methods are based on the ability of the independent particle model (Hartree-Fock theory) to provide a qualitative description of molecular species by using a single Slater determinant, and then utilizing the resultant orbitals within popular correlated methods such as second-order Møller-Plesset perturbation theory (MP2),[28] configuration interaction with single and double excitations (CISD),[181] coupled cluster with single, double and perturbative triple substitutions [CCSD(T)][32] and density functional approaches such as the Becke, three-parameter, Lee-Yang-Parr (B3LYP),[182,183] and Perdew-Burke-Ernzerhof (PBE)[64] methods.

When combined with at least very large, if not complete, basis sets, CCSD(T) is known to predict, complement, verify and even guide experimentalists in the measurement of chemically accurate energetic properties, which is usually described as ±1 kcal mol^{-1} of reliable experimental data. However, with its N^7 computational scaling, where N is the number of basis functions, such calculations are typically limited to rather small molecules (e.g., molecules

[†] This chapter is presented in its entirety from G. A. Oyedepo and A.K. Wilson, "Multireference Correlation Consistent Composite Approach [MR-ccCA]: Toward Accurate Prediction of the Energetics of Excited and Transition State Chemsitry." *J. Phys. Chem. A* **2010**, *114*, 8806 with permission from the American Chemical Society.

comprised of no more than ~10 non-hydrogen atoms. To increase the size of molecules that can be addressed successfully while achieving similar accuracy, a variety of *ab initio* composite approaches have been introduced. Such methods are based on the assumption that the one-electron functions (basis sets) and electron correlation methods are additive, and, thus, can be combined in such ways to mimic the energetic prediction that, in principle, would be achieved with much more sophisticated, albeit, computationally expensive means (e.g., CCSD(T) with a large basis set), and, to accomplish this feat with a series of much less costly computational calculations. Examples of composite methods include the Gaussian-1 (G1)[87] method, which was introduced nearly two decades ago, as the first in a family of Gaussian-*n* methods (*i.e.* G2,[85,184,185] G3,[186,187] G4[188]), the Complete Basis Sets (CBS) methods (*i.e.* CBS-4, CBS-q, CBS-Q,[147] CBS-QB3[144,189]), Weizmann-*n* methods (W1, W2,[79] W3,[148] W4[190]), high-accuracy extrapolated *ab initio* thermochemistry methods (HEAT)[153,191,192] and correlation consistent composite approach (ccCA)[25,90,91,92,94,95,193-195,165-169] to name but a few. The target accuracy of these multi-level methods is to reach at least chemical accuracy, on average. As mentioned, the composite methods have been designed to replicate the results that, in principle, would be obtained using much more sophisticated and computationally expensive methods and basis sets. For instance, the ccCA method attempts to replicate results that would be obtained via a calculation utilizing CCSD(T)(full)-DK/aug-cc-pCV∞Z-DK. Some composite methods (most notably HEAT and Weizmann-*n* methods) aim for sub-kcal mol^{-1}, or near-spectroscopic accuracy (1 kJ/mol), of well-established experimental data.

All of the methods discussed above are based on the assumption that the desired wavefunctions of chemical species can be described by a single Lewis dot structure. While these

presumptions are generally known to result in very good energetic and structural properties of closed shell ground state species, they can be inadequate for bond breaking or formation processes, transition states, diradical species and other situations where the frontier orbitals, the highest occupied molecular orbital (HOMO) and lowest unoccupied molecular orbitals (LUMO), are nearly or exactly degenerate. In this study, our goal is to determine a composite strategy that can be used for these types of situations.

Multireference composite methods previously have been reported. Sølling et al.[196] introduced a number of variants of the multireference equivalents of G2 and G3 methods and applied these methods to examine enthalpies of formation, ionization energies, electron affinities and proton affinities of the reduced G2-1 test set. These MR-G*n* approaches are dependent on experimentally derived parameters (a so-called higher level correction, HLC). To illustrate the magnitude of the HLC, for the single reference method, G3B3, it accounts for 47.3 kcal mol^{-1} in the computation of the enthalpy of formation for linear octane, and increases as molecule size increases).[90,91] The use of experimental parameters, such as the HLC, can be undesirable because it is not always clear whether the parameter will perform sufficiently if a new molecule of interest deviates from the test set used to create the parameter. This can impact the accuracy of predictions when used on novel chemical compounds. And, as reported by the authors, the additivity approximations utilized in the parent G*n*-type procedures did not perform as well when extended to the MR-G*n* methods. The multireference versions of Weizmann-*n* series of methods proposed[197] and utilized[198] by Martin and coworkers do not contain any such parameterization; however, their approaches, which are based, in part, upon MR-ACPF method and aim for sub-chemical accuracy, are extraordinarily expensive, severely

limiting the size of molecules that may be studied. Because of these potential limitations to existing methods and the success of the correlation consistent composite approach, our group has therefore proposed a multireference equivalent of the successful single reference based correlation consistent composite approach (ccCA).[25]

The multireference correlation consistent composite approach (MR-ccCA)[25] has been developed by replacing the single reference methods in the parent ccCA method with their multireference equivalents. In ccCA, the higher-order electron correlation is computed utilizing CCSD(T). To date, there have been a few studies that have considered a multireference CCSD(T) approach.[199-204] However, the replacement of CCSD(T) utilized in ccCA with a multireference coupled cluster [MR-CCSD(T)] method is hindered in that MR-CCSD(T) has not been implemented into readily available *ab initio* program packages, such as Gaussian and Molpro.[172,173] Therefore, to provide a more generally applicable approach, the use of multireference configuration interaction including single and double excitations and an *a posteriori* Davidson-type size-consistency correction (MRCI+Q), multireference averaged quadratic coupled cluster (MR-AQCC) and multireference averaged coupled pair functional (MR-ACPF) are considered in this study. A great benefit of MR-ccCA is that it does not contain any empirical parameters and, rather, its flexibility enables easy modifications as indicated above, (as opposed to reparameterization) as theoretical methods and computational hardware evolve.

In early work, MR-ccCA was applied to compute the potential energy curves (PECs) of N_2 and C_2 and their spectroscopic parameters.[25] Both PECs are known to require multireference methods to obtain even qualitatively correct results near dissociation limits. It was found that

MR-ccCA provided excellent agreement with the experimental values for the dissociation energies, bond lengths and vibrational frequencies for N_2 and C_2. The PECs obtained also compare favorably with that obtained using FCI/6-31g(d) indicating the utility of MR-ccCA for multi-configurational problems, such as for the quantitative study of systems with severe non-dynamical electron correlation.

The objective in this work was to further consider MR-ccCA, utilizing the method to predict the spectroscopic and thermochemical properties of diradicals, many of which are known to require multi-configurational wavefunctions for proper descriptions of their reference states,[205] and of some closed-shell species to assess the performance of the method for different systems. We have applied MR-ccCA to predict the singlet-triplet energy separations in open-shell atomic species, namely, carbon, oxygen, silicon, and sulfur. Calculations on atoms enable direct comparison with experimental results to ensure critical evaluation of the accuracy of our method. We also computed the adiabatic singlet-triplet energy separations (ΔE_{S-T}) for a number of diatomic species and investigated methylene and its halogen- and hydroxyl-substituted derivatives. We computed the relative energies of the open (C_{2v}) and closed (D_{3h}) forms of ozone and its heavier congener, thiozone, that are known to require multi-configurational wavefunctions to properly describe even their ground electronic states.[205] Since one of the most stringent tests of any multireference theoretical method is the ability to predict accurately the energetic barrier to internal rotations of ethylene which leads to the breakage of its unsaturated π-bond, a situation that has been reported to require multi-configurational wavefunction,[206,207] MR-ccCA has been utilized to study this phenomenon. We have also computed the enthalpy of formation at 298K ($\Delta H^{\Theta}_{f,298}$), for all of the species studied in

this work, in their ground states and, provide the first predictions of the $\Delta H^{\Theta}_{f,298}$ for their low-lying excited states.

5.2 Computational Details

To put into context the MR-ccCA methodology, the total electronic energy of an atom or molecule, as described by single-reference ccCA,[90,91,92,94,95,165,193,194] may be expressed using the following general formula,

$$E(\text{ccCA}) = E_0(\text{ccCA}) + \Delta E(\text{CC}) + \Delta E(\text{DK}) + \Delta E(\text{CV}) + \Delta E(\text{SO}_a) \quad (5.1)$$

where E_0(ccCA) is the reference ccCA energy, ΔE(CC) is a term that accounts for higher-order electron correlation that is not fully described by the ccCA reference, ΔE(DK) is a term that accounts for scalar relativistic effects, ΔE(CV) is a term that accounts for core-valence electronic effects, and $\Delta E(\text{SO}_a)$ is a term that accounts for atomic spin-orbit effects. A more detailed discussion of these terms can be found in previous ccCA papers. [90,91,95,165,168,169,193,195]

The first step in MR-ccCA, as in ccCA, includes a geometry optimization and frequency calculation. In this study, the geometry and frequencies for MR-ccCA are determined at the CASSCF/CASPT2 level of theory using correlation consistent polarized valence triple-ζ basis sets (cc-pVTZ). As this level of theory quickly becomes cost prohibitive for a full valence active space study, it is largely limited to molecules comprised of no more than several non-hydrogen molecules.

We have utilized state-averaged CASSCF references and the full valence complete active space for all steps in the development of MR-ccCA. The use of a full valence active space affords rigorous evaluation of MR-ccCA that may not be achieved if subjected to further

approximations that would be introduced by the selection of a smaller active space. Obviously, this greatly limits the size of molecules that may be studied but a practical implementation in which smaller active spaces are utilized is under investigation.

The MR-ccCA reference energy was determined by a series of single-point computations, which were performed using CASPT2/aug-cc-pV*n*Z [where *n* = D(2), T(3), and Q(4)]; aug-cc-pV(*n*+d)Z basis sets were used for elements in the second period (Al-Ar) of the periodic table. The CASPT2 energies were then extrapolated to the complete basis set (CBS) limit utilizing a three-point mixed Gaussian/exponential formula proposed by Peterson et al. (hereafter denoted as P_DTQ),[118]

$$E_n = E_0(\text{MR-ccCA}) + Ae^{-(n-1)} + Be^{-(n-1)^2} \tag{5.2}$$

where E_n is the total energy computed at the *n*th basis set level, *n* is the cardinal number of the basis set (*i.e.* D=2, T=3, Q=4), E_0(MR-ccCA) is the total energy at the CBS limit computed with Eqn. (5.2), and *A* and *B* are parameters that are determined in the extrapolation. We also utilized extrapolation to the CBS limit using the quartic inverse power of $\mathrm{l_{max}}$ (where $\mathrm{l_{max}}$ is the highest angular momentum used in the basis set functions) developed by Schwartz,[208] Klopper,[209,210] Kutzelnigg and coworkers, [43,211] which is expressed as:

$$E(l_{max}) = E_0(\mathrm{MR-ccCA}) + \frac{B}{(l_{max}+1/2)^4} \tag{5.3}$$

For all main group species studied in this work, both *n* the cardinal number of the basis set and l_{max}, the maximum angular momentum function found within the basis sets utilized are equal[212] (e.g. for cc-pVDZ, *n*=2 and l_{max}=2) and *B* is a fitting parameter. The total electronic energies

derived using this extrapolation scheme are denoted as S_DT and S_TQ when double-, triple-zeta and triple-, quadruple- zeta quality basis sets are utilized, respectively.

To the reference energy obtained from either of equations 5.2 and 5.3, several terms are added. The first term accounts for higher-order electron correlation that is not completely described by CASPT2. In this study, each of the three multireference higher-order correlation energy corrections, generally denoted as Δ*E*(MR-CC), is computed using the following formula,

$$\Delta E_{(\text{MRCI+Q})} = E_{[\text{MRCI+Q}/\text{cc-pVTZ}]} - E_{[\text{CASPT2}/\text{cc-pVTZ}]} \quad (5.4)$$

$$\Delta E_{(\text{MR-AQCC})} = E_{[\text{MR-AQCC}/\text{cc-pVTZ}]} - E_{[\text{CASPT2}/\text{cc-pVTZ}]} \quad (5.5)$$

$$\Delta E_{(\text{MR-ACPF})} = E_{[\text{MR-ACPF}/\text{cc-pVTZ}]} - E_{[\text{CASPT2}/\text{cc-pVTZ}]} \quad (5.6)$$

Another term included is the scalar relativistic energy term, which encompasses the mass-velocity term to correct for kinetic energy changes and the one-electron Darwin term to correct for variation in coulomb attraction. The scalar relativistic term is obtained from frozen-core CASPT2 computations combined with the cc-pVTZ-DK basis set[42] and the spin-free, one-electron Douglas-Kroll-Hess (DKH) Hamiltonian.[213-215] The standard CASPT2 relativistic correction is labeled ΔE(MR-DK) and formulated as

$$\Delta E_{(\text{MR-DK})} = E_{[\text{CASPT2-DK}/\text{cc-pVTZ-DK}]} - E_{[\text{CASPT2}/\text{cc-pVTZ}]} \quad (5.7)$$

The final term, Δ*E*(MR-CV), accounts for core-valence correlation effects, and is computed by taking the difference between the frozen-core CASPT2/aug-cc-pVTZ and CASPT2(FC1)/aug-cc-pCVTZ total energies. The multireference core-valence correction is defined as

$$\Delta E_{(\text{MR-CV})} = E[\text{CASPT2(FC1)/aug-cc-pCVTZ}] - E[\text{CASPT2/aug-cc-pCVTZ}] \quad (5.8)$$

The CASPT2(FC1) computation refers to the inclusion of the core-valence electrons in the correlation space as follows: a) for first-row (Li-Ne) atoms the 1*s* electrons are included in the correlation space, b) for second-row (Na-Ar) atoms the 2*s* and 2*p* electrons are included in the correlation space, and c) for third-row (Ga-Kr) atoms the 3*s* and 3*p* electrons are included in the correlation space.

The overall MR-ccCA method utilized to compute the energetic properties studied in this work can be described using the relation:

$$E(\text{MR-ccCA}) = E_0(\text{MR-ccCA}) + \Delta E(\text{MR-CC}) + \Delta E(\text{MR-DK}) + \Delta E(\text{MR-CV}) \quad (5.9)$$

To compute atomization energy and enthalpy of formation at 0K, $\Delta H_{f,0}^{\Theta}$, we include the zero-point vibrational energy (ZPVE) correction, which is obtained from the frequency calculation as highlighted above. Addition of thermal correction to the enthalpy at 0K leads to $\Delta \mathrm{H}_{\mathrm{f},298}^{\Theta}$.

Davidson and Borden[216] have shown that open-shell molecules often exhibit symmetry breaking due to close spacing of their electronic states. To circumvent artifactual minima in the geometry optimization and frequency calculations due to this phenomenon, all of our calculations were performed using the C_1 point group, *i.e.*, no symmetry restrictions were imposed on the wavefunctions. Artifactual symmetry breaking due to orbital instabilities, usually caused by the use of RHF wavefunction as the reference wavefunction,[217] has been avoided since our reference wavefunctions are based on MCSCF method. Real symmetry breaking (pseudo-Jahn-Teller effect) which is usually caused by near degeneracies[218] has also been accounted for by the use of full valence CASSCF/CASPT2 method to generate all the geometries and in the subsequent MR-ccCA calculations.[219] All the parameters (bond lengths, bond angles and dihedral angles) of the optimized geometries are compared to available

experimental and previous symmetry-restricted calculated values to ensure that the computed symmetry-unconstrained calculations do not inadvertently lead to erroneous geometries. To ensure a balanced treatment of closed- and open-shell wavefunctions when CASPT2 was used, the *g3* variant proposed by Andersson,[220] as one of his suggested modifications to the zeroth-order Hamiltonian was utilized. All multireference ccCA computations for this study were performed with the MOLPRO 2006.1 program[173] while all calculations on single reference ccCA were done using the GAUSSIAN 03 package.[118]

5.3 Results and Discussion

We have examined the use of viable multireference equivalents to the CCSD(T)/cc-pVTZ step in single reference ccCA by utilizing MRCI+Q, MR-ACPF and MR-AQCC. Hereafter, we refer to the three variants of MR-ccCA namely as MR-ccCA-CI+Q, MR-ccCA-AQCC and MR-ccCA-ACPF. The effects of Peterson and Schwartz extrapolation schemes on the accuracy of predicted properties have also been examined.

5.3.1 Singlet-Triplet (^{1}D-^{3}P) Energy Gaps in Atomic Radicals

The accuracy of any theoretical method may be measured by how well it predicts atomic properties. This is because there are no complications arising from uncertainties in geometries, ZPVEs and anharmonicity corrections. All of the variants of MR-ccCA have been applied to compute the singlet-triplet energy gaps in carbon, oxygen, silicon and sulfur (Table 5.1). Each of the variants of MR-ccCA performed better than its constituent individual methods for the four atoms considered. However, of the three potential MR steps for CCSD(T) and of the

CBS schemes considered, MR-ccCA-AQCC(S_DT) results provide the best overall agreement with experiment,[221] with absolute deviations of 0.2, 0.5, 0.2 and 0.0 kcal mol^{-1} for C, O, Si and S atoms, respectively. These results are in excellent agreement with values obtained using spin-flip optimized orbital coupled cluster doubles calculations (SF-OD) with cc-pVQZ basis set.[221]

5.3.2 Methylene and Isovalent Species

Schaefer long ago described methylene (CH_2) as the "paradigm for computational quantum chemistry" due to the role it has played in the recognition of the utility of computational chemistry in the study of chemical species.[222] The elucidation of the structure and energetics of CH_2, the simplest neutral hydrocarbon diradical, took nearly two decades of collaboration between experiment and theory to be resolved.[222] It has since become a convention to test new theoretical methods against this species.

The electronic configuration for the triplet ground state ($\tilde{X}^3B_1$) of the bent methylene molecule (C_{2v}) may simply be described as

$$^3\psi \approx 1a_1^2 2a_1^2 1b_2^2 3a_1^1 1b_1^1 \qquad (5.10)$$

and has been determined, experimentally,[223] to lie 9.0 kcal mol^{-1} (T_e =9.2 kcal mol^{-1}) below the lowest-lying singlet excited state (ã$^1A_1$) which may be qualitatively described as

$$^1\psi \approx c_1|1a_1^2 2a_1^2 1b_2^2 3a_1^2| + c_2|1a_1^2 2a_1^2 1b_2^2 1b_1^2| \qquad (5.11)$$

These terms are the dominating configurations with c_1 and c_2, determined using CASSCF/cc-pVTZ, having values of 0.95 and -0.16, respectively indicating a small (≈5%) diradical character.[51] Each of the other contributing configuration state functions in the wavefunction has a coefficient that is less than 0.1.

Table 5.2 shows the results obtained for adiabatic singlet-triplet energy difference (ΔE_{S-T}) and enthalpies of formation for CH_2 and silylene (SiH_2) using the nine variants of MR-ccCA. MR-ccCA-AQCC(S_DT), utilizing the least costly extrapolation procedure, is our recommended method for predicting energetic properties. It predicts an energy difference of 8.7 kcal mol^{-1} (T_e=9.2 kcal mol^{-1}) for methylene which is in excellent agreement with the experimental value of 9.0 kcal mol^{-1} and also compares favorably with 8.8 kcal mol^{-1} (T_e=9.2 kcal mol^{-1}) obtained by Kalemos et al., using the more computationally intensive MRCISD/d-aug-cc-pV6Z approach[224] To highlight the utility of MR-ccCA method, the ΔE_{S-T} for CH_2 using CASPT2 method and aug-cc-pVTZ, aug-cc-pVQZ and aug-cc-pV5Z basis sets are also presented with the attendant results of 11.8, 11.3, 11.3 kcal mol^{-1}, respectively, signifying the convergence of the one-electron functions but leading to an error of 2.1 kcal mol^{-1}. The enthalpy of formation at 298K for the triplet ground state ($\tilde{X}^3B_1$) of CH_2 has been computed using all the variants of MR-ccCA. MR-ccCA-ACPF(S_TQ), our recommended method for computing thermochemical properties, leads to a value of 94.3 kcal mol^{-1} which compares favorably with the experimental[90,153] value of 93.7 kcal mol^{-1}. The thermochemical accuracies of MR-ccCA-ACPF(P_DTQ) and MR-ccCA-ACPF(S_TQ) variants are observed to be comparable throughout this study, however, we recommend the latter due to the slight cost savings that would occur, as one fewer single-point calculation is required. MR-ccCA-MRCI+Q variants are found to underestimate substantially the ΔE_{S-T} in CH_2.

Silylene (SiH_2), the isoelectronic heavier congener of methylene, is known to exist as a ground state singlet. One of the reasons offered for the different multiplicity of the ground states of SiH_2 and CH_2 is the larger size of the $5a_1$ orbital in SiH_2 as compared to the $3a_1$ of CH_2.[225] Electron-electron repulsion for paired electrons in the spatially larger $5a_1$ orbital of SiH_2

should be less than that in the $3a_1$ orbital of CH_2, favoring the singlet state for the heavier elements. Lineberger[226] and coworkers reported an experimental energy gap value of -13.8 kcal mol^{-1} (*negative* ΔE_{S-T} *values indicate that the singlet state is the ground state*) while most theoretical predictions resulted in a value between -17 and -21 kcal mol^{-1}.[227] This was settled after Berkowitz and coworkers[228] experimentally determined the energy difference to be -21.0±0.7 kcal mol^{-1}, effectively harmonizing the theoretical and experimental values. MR-ccCA-AQCC(S_DT) predicts the adiabatic singlet-triplet energy separation as -21.6 kcal mol^{-1} which is in very good agreement with the experimental value and previous estimate of -21.0±1 by Balasubramanian using the Davidson-type corrected CASSCF/SOCI method.[229]

MR-ccCA-ACPF(S_TQ), Table 5.1, predicts the $\Delta H^{\Theta}_{f,298}$ for the singlet ($^1A_1$) and triplet ($^3B_1$) states of SiH_2 as 64.9 and 87.6 kcal mol^{-1}, respectively. Our computed triplet values compare favorably with the experimental value of 86.2±1.2 kcal mol^{-1} and the theoretical value obtained by Wood *et al.*[230] (86.7 kcal mol^{-1}) using the ROCBS-QB3 method. The experimental $\Delta H^{\Theta}_{f,298}$ for the singlet state has been difficult to measure accurately. Values ranging from 58 kcal mol^{-1} to 69 kcal mol^{-1} have been reported in the literature,[231] though the recommended value is 65.5±1 kcal mol^{-1}.[232-234] Our computed value of 64.9 kcal mol^{-1} is in very good agreement with this recommended value.

5.3.3 T_1 Diagnostics and Percentage Diradical Character

To determine the multireference characteristics of the species considered in this study, we determined the Euclidian norm of the t_1 vector (Table 5.3), commonly known as the T_1 diagnostics,[235,236] of the CCSD wavefunction using cc-pVTZ basis set. We also calculated the

percentage diradical character, using the expression $2B^2x100$ where B is the co-efficient of the second leading CSF in the CASPT2/cc-pVTZ wavefunction, as indicated by Schmidt et al.[51] A species is believed to exhibit significant multireference character if the T_1 diagnostics has a value greater than or equal to 0.02.[235,237] Pulay and coworkers[238-240] also suggested that a molecule demonstrating about 10% or more diradical character could have substantial non-dynamic electron correlation effect and should be treated by a multireference method.

5.3.3.1 Species with T_1 Diagnostic Values Less Than 0.02

The values of the T_1 diagnostics and percentage diradical in Table 5.3 show that nitrenium ion (NH_2^+), phosphenium ion (PH_2^+), imidogen (NH), diatomic oxygen (O_2), hydroxyl cation (OH+), and sulfur dimer possess minimal multireference character. These species have been studied to illustrate the versatility of the MR-ccCA method in calculating molecular properties.

5.3.3.1.1 NH_2^+ and PH_2^+

In Tables 5.4 and 5.5, the ΔE_{S-T} (along with previous theoretical calculations using SF-OD/cc-pVQZ method)[221] and $\Delta H^{\Theta}_{f,298}$, respectively, for the singlet and triplet states of isovalent nitrenium ion (NH_2^+) and phosphenium ion (PH_2^+) are shown. MR-ccCA predicts that the singlet state of nitrenium ion is 28.1 kcal mol^{-1} above the ground triplet state, indicating an absolute deviation of 2 kcal mol^{-1} from the experimental result, in contrast with 30.1 kcal mol^{-1} obtained using SF-OD method. Similar observation is noted for PH_2^+ with MR-ccCA-AQCC(S_DT) resulting in an absolute deviation of 1.5 kcal mol^{-1} from the reported experimental value which is just

outside the experimental error bar. The ΔE_{S-T} follows similar trends as observed for CH_2 and SiH_2, with the ground state of the heavier congener, PH_2^+, and its lighter homologue, NH_2^+, being singlet and triplet states, respectively.

5.3.3.1.2 Imidogen and Other Diatomic Diradicals

The ΔE_{S-T} for imidogen (NH), fluoroimidogen (NF), dioxygen (O_2) and hydroxyl cation (OH^+) have also been studied using MR-ccCA (Table 5.3). There is overall agreement with previous theoretical calculations[221] and experimental values,[241] with absolute deviations from experimental results, of 0.7, 1.4, 0.0 and 0.1 kcal mol^{-1} for NH, NF, O_2 and OH^+ respectively using MR-ccCA-AQCC(S_DT). The sulfur dimer (S_2) and sulfur oxide (SO) have also been studied using MR-ccCA. The ΔE_{S-T} values obtained are in excellent agreement with experimental values[242,243] leading to absolute deviation of 0.1 for S_2, while SO results in an absolute deviation of 0.4 kcal mol^{-1}.

The computed $\Delta H_{f,298}^{\Theta}$ for the ground triplet states of NH, NF, O_2 and OH^+ using MR-ccCA-ACPF(S_TQ) are shown in Table 5.5 while the corresponding values for the lowest-lying singlet states are shown in Table 5.4. Imidogen, the simplest member of the nitrene family, has an absolute deviation of 0.3 kcal mol^{-1} from the accurate but extremely expensive *HEAT* theory [153] which is suggested to provide a better estimate for this species, than the experimental value provided in the NIST-JANAF compendium[244], 90.0±4.0 kcal mol^{-1}. As well, the MR-ccCA result is in excellent agreement with its own single reference counterpart, ccCA, with an absolute deviation of 0.2 kcal mol^{-1}. Oxygen (O_2), like H_2 and N_2, is known to have $\Delta H_{f,298}^{\Theta}$ of 0.0 kcal mol^{-}

[1]. MR-ccCA-AQCC(S_TQ) gives a deviation of 0.4 kcal mol^{-1} which compares very well with previous theoretical estimates.[90,153]

The $\Delta H^{\Theta}_{f,298}$ for the triplet ground states of S_2 (Table 5.5) using MR-ccCA-ACPF(S_TQ), 31.6 kcal mol^{-1} is in good agreement with the experimental results of 30.7 kcal mol^{-1}.[243] Table 5.5 shows the computed $\Delta H^{\Theta}_{f,298}$ for the first singlet excited states of S_2 with favorable (0.9 kcal mol^{-1} difference) comparison to experiment.

5.3.3.2 Species with T_1 Diagnostic Values Greater Than 0.02

Though the halocarbenes demonstrate very small diradical character, as shown in Table 5.3, they do have significant multireference disposition as do diatomic nitrogen fluoride (NF), sulfur oxide (SO) and hydroxymethylene.

5.3.3.2.1 The Halocarbenes

Unlike methylene, electronegative substituted halocarbenes usually have singlet ground states due to the slight stabilization of the σ relative to the π orbital of the nearly degenerate nonbonding pair in the frontier orbitals. There has also been significant divergence between the experimental (-3±3 kcal mol^{-1})[245] and theoretical values (-19.5±2 kcal mol^{-1})[246-2248] for the ΔE_{S-T} of dichloromethylene (CCl_2). This may be connected with the fact that CCl_2 is a lot less stable than some other halocarbenes, for example difluoromethylene (CF_2), making it difficult to study using matrix-isolation techniques.[249]

MR-ccCA-AQCC(S_DT) estimates ΔE_{S-T} for CCl_2 as -19.7 kcal mol^{-1} which is in good agreement with the -19.2 kcal mol^{-1} of a recent theoretical prediction using CASBCC4 method

by Jun *et al*.[247] The contribution of the various components of MR-ccCA to the estimated value indicates that a high-level correlated theoretical method is needed to predict quantitative results for halogen-containing compounds. To illustrate, the CASPT2/aug-cc-pVnZ (where the aug-cc-pV(n+d)Z basis set was used for chlorine) CBS limits using S_DT, S_TQ and P_DTQ extrapolation schemes are -17.2, -17.6 and -17.6 kcal mol^{-1}, respectively. The MRCI+Q, MR-AQCC and MR-ACPF approaches accounted for an additional -2.8, -2.7 and -2.9 kcal/mol, respectively, of correlation energy. Core-valence corrections (1*s* orbitals of chlorine are not correlated) and scalar relativistic effects contributed 0.2 and -0.3 kcal mol^{-1} respectively while ZPVE accounted for 0.3 kcal mol^{-1}. This resulted in computed singlet-triplet gaps of -20.1, -20.1 and -19.7 kcal mol^{-1} for MR-ccCA-AQCC(P_DTQ), MR-ccCA-AQCC(S_TQ) and MR-ccCA-AQCC(S_DT), respectively. Indeed, it is the additive nature of the high-level correlated treatment in the MR approach that enables better agreement with experiment.

The predicted ΔE_{S-T} values for CF_2, CHF and CHCl using MR-ccCA-AQCC(S_DT), -56.3, -15.1 and -5.7 kcal mol^{-1}, are in very good agreement with established experimental[250-252] values of -56.7, -14.9±0.4, and -6.2 kcal mol^{-1}, respectively.

Tables 5.4 and 5.5 show the computed $\Delta H^{\Theta}_{f,298}$ for the singlet and triplet states of CCl_2, CF_2, CHF and CHCl using MR-ccCA-ACPF(S_TQ). Our results are, generally, in very good agreement with previous high level theoretical calculations[247-249,253], for instance CCSD(T)/cc-pV5Z method of Demaison *et al*.,[249] and recommended experimental values.[254]

5.3.3.2.2 Hydroxymethylene

Like other electronegative substituted derivatives of methylene, hydroxymethylene is

known to have a singlet ground state, in a *trans* conformation, which has been estimated theoretically using CCSD(T) method extrapolated to the CBS limit with aug-cc-pVnZ (n=D,T,Q) basis sets,[255] to lie 25 kcal mol^{-1} below the lowest triplet electronic state.

MR-ccCA has been utilized to compute the ΔE_{S-T} (Table 5.3) for CHOH, the $\Delta H^{\Theta}_{f,298}$ for the singlet states (Table 5.4) of its *cis*, *trans* isomers and tautomer, formaldehyde (CH_2O) and lowest lying triplet excited state (Table 5.5). All computed values are in very good agreement with earlier theoretical[247,255,256] predictions and experimental results.

5.3.4 Ozone and Thiozone

The singlet state of ozone and its heavier congener thiozone are shown to have substantial multi-configurational or diradical character (Table 5.3). There have been questions about the relative energy difference between the open (C_{2v}) singlet form and the closed cyclic (D_{3h}) form, which has been predicted theoretically to be isolable but experimentally elusive.[257,258] Also, there have been debates over whether the cyclic D_{3h} form lies above or below the asymptotic dissociation limit of the open singlet C_{2v} form of ozone [257]

$$O_3(X^1A_1) \rightarrow O(^3P) + O_2(X^3\Sigma_g^-) \qquad (5.12)$$

which has been experimentally[259] determined to be 26.1 kcal mol^{-1}.

MR-ccCA-AQCC(S_DT) predicts the relative energy between the open and cyclic forms (Table 5.8) as 29.9 kcal mol^{-1}, in agreement with the CCSD(T) predicted value of 28.7 kcal mol^{-1} by Lee[257] using quadruple zeta quality basis set. This result corroborates the discovery in previous calculations that the cyclic isomer of ozone is above the $O_3(X^1A_1) \rightarrow O(^3P) + O_2(X^3\Sigma_g^-)$ asymptotic dissociation limit[260] which we predict as shown in Table 5.8, as 26.0 kcal mol^{-1}.

Thiozone (S_3) has received much less attention than its lighter homologue, ozone. Like for ozone, the energy difference between its C_{2v} and D_{3h} isomers has not yet been resolved[258] since the cyclic form has not yet been isolated experimentally. We predict the C_{2v}-D_{3h} isomerization energy (Table 5.8) for S_3, using MR-ccCA-AQCC(S_DT), as 5.2 kcal mol^{-1} which is comparable with 4.4 kcal mol^{-1} predicted by Peterson and coworkers[243] using CCSD(T)/cc-pV∞Z where the CBS limit was determined using quintuple and sextuple zeta quality basis sets. Our estimated photodissociation energy (Table 5.7) for $S_3(X^1A_1) \rightarrow S(^3P) + S_2(X^3\Sigma_g^-)$ asymptotic limits of 60.3 kcal mol^{-1} lies very well above the cyclic form of thiozone.

Table 5.4 shows the predicted ΔE_{S-T}, isomerization energies (Table 5.8) between C_{2v} and D_{3h} isomers and $\Delta H^{\Theta}_{f,298}$ for the ground singlet (Table 5.5) states of O_3 and S_3 using MR-ccCA, respectively. We have also estimated the photodissociation energies of four low-lying dissociation channels of each homologue (Tables 5.7) and compare to previous theoretical estimates[261-263] and experimental[264] values. Since the MOLPRO 2006.1 code cannot correlate electrons distributed in more than 16 orbitals using CASPT2 method, all current MR-ccCA values for S_3 do not include the core-valence terms described above. The contribution due to this term is expected to be about 0.5 kcal mol^{-1}.[243]

5.3.5 Acetylene, Ethylene and Disilene

The experimentally measured ΔE_{S-T} for acetylene (C_2H_2) by Suits and coworkers[265]has been reported as 82.6 kcal mol^{-1} in significant disagreement with all known high-level theoretical estimates that predict a relatively higher value. Acetylene, in its ground electronic

state ($X^1\Sigma_g^+$), is linear in its equilibrium geometry and can be described by the electronic configuration

$$1\sigma_g^2 1\sigma_u^2 2\sigma_g^2 2\sigma_u^2 3\sigma_g^2 1\pi_u^4 \qquad (5.13)$$

However, its first excited electronic states result from the orbital excitation $\pi_u \rightarrow \pi_g^*$, culminating in C-C bond elongation, and are stabilized by bending out of linearity. The lowest triplet excited electronic state is known to be the *cis* $\tilde{a}^3B_2$. We are reporting the MR-ccCA computed ΔE_{S-T} (Table 5.4) for acetylene as -88.6 kcal mol^{-1} which is in very good agreement with previous theoretical prediction of -87.2 kcal mol^{-1} of Lundberg et al.[266-268] using CCSD(T)/TZ2Pf level of theory, further supporting the theoretical claim[266] that the experimental value is underestimated. Our MR-ccCA computed $\Delta H_{f,298}^{\Theta}$ for the ground singlet (Table 5.5) and lowest-lying triplet (Table 5.6) states of acetylene are 56.1 and 144.7 kcal mol^{-1}. The former value is in quantitative agreement with previous estimates[90,153] while the latter, to the best of our knowledge, is the first explicitly computed value reported.

The electronic ground state of ethylene is a planar singlet with D_{2h} symmetry. Like in acetylene, excitation of an electron from a π orbital to a π* orbital leads to geometry distortion and a resultant loss in symmetry. This transition may be better understood if the C=C is torsionally rotated away from planarity, through a biradical transition state at 90^o, thereby raising the energy of π bonding orbital and lowering the energy of the π* antibonding orbital. At the transition state, the π and π* orbitals are nearly degenerate (should be degenerate if its D_{2d} symmetry is enforced) with the resulting relaxed electronic state expectedly stabilized, according to Hund's rule of maximum multiplicity, as a triplet state. However, for ethylene, the transitional singlet state has been predicted[269-272] to be lower in energy, a clear violation of

Hund's rule. When another theoretical calculation using two-configurational self-consistent field method was done by Yamaguchi, Osamura and Schaefer,[273,274] in which only the valence π electrons were correlated, they predicted that the triplet state is lower in energy than the singlet state, in accordance with Hund's rule. We have therefore computed the adiabatic singlet-triplet energy gap (Table 5.3), *cis-trans* isomerization energy barrier (Table 5.8) and the enthalpy of formation at 298K for the ground singlet and the lowest triplet (Table 5.5) excited states for ethylene using MR-ccCA.

MR-ccCA does predict the violation of Hund's rule in twisted ethylene with the transition state singlet for rotation about the C=C double bond being lower in energy than the relaxed triplet state by 1.9 kcal mol^{-1}. This could be adduced to anti-ferromagnetic coupling stemming from dynamic spin polarization[272,275] of the σ and π electrons in the valence space. The electronic configuration of the singlet ground state of ethylene (eqn. 5.14) can also be said to be formed from the thermodynamically favorable overlap of two triplet ground state wavefunctions of methylene which also correlates with the transitional singlet state (Figure 5.1), thereby leading to lower activation energy.

$$1\sigma_g^2 1\sigma_u^2 2\sigma_g^2 2\sigma_u^2 1\pi_u^2 3\sigma_g^2 1\pi_g^2 2\pi_u^2 \qquad (5.14)$$

However, the optimized triplet state of C_2H_4 correlates with two orthogonal states, one triplet ground state and one singlet excited state of CH_2, and hence constitutes an energetically unfavorable pathway.

(a)

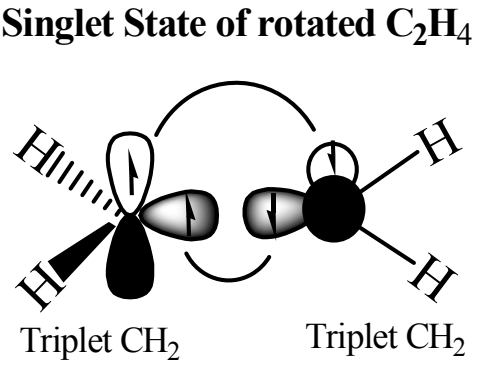

(b)

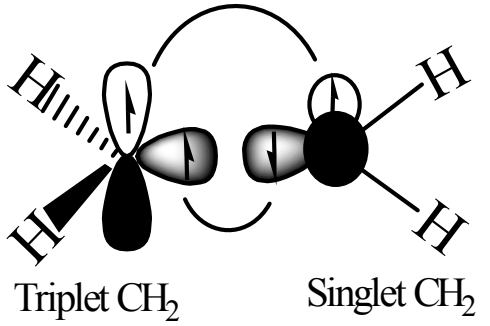

Figure 5.1 Diagramatic representation of probable overlaps of two orthogonal methylene fragments corresponding to rotated ethylene: (a) Singlet state for ethylene correlating with two triplet ground states of methylene; (b) Triplet state for ethylene correlating with one triplet ground state and one singlet excited state of methylene

The barrier height or activation energy for *cis-trans* isomerization is computed to be 64.3 kcal mol^{-1} in excellent agreement with the estimated experimental value of 65 kcal mol^{-1}.[276] Using MR-ccCA lowest optimized triplet state in ethylene is predicted to be 66.2 kcal mol^{-1} above the singlet ground state in excellent agreement with the value obtained using a Diffusion Monte Carlo method[277], 66.4±0.3 kcal mol^{-1}. The enthalpy of formation at 298 K for the singlet ground state is calculated, using MR-ccCA-ACPF(S_TQ), to be 12.6 kcal mol^{-1}, in excellent agreement with the experimental values of 12.5 kcal mol^{-1}.[146] The $\Delta H^{\Theta}_{f,298}$ for the optimized lowest triplet state is computed to be 80.2 kcal mol^{-1}.

Conventional single-reference methods and single-reference-based composite methods, most especially in the spin-restricted cases, usually yield unphysical cusps[378] in the torsional potential of ethylene at the transition state which often lead to very large errors in the barrier height. Figure 5.2 shows the potential energy curves, obtained using single reference ccCA and MR-ccCA variants, for twisted ethylene from 0^o to 180^o torsional angles while Figure 5.3 displays the potentials curves for C_2H_4 around the transition barrier, using MR-ccCA variants and the single reference ccCA method, as smooth continuous curves without any kinks while single reference ccCA exhibits an erroneous cusp.

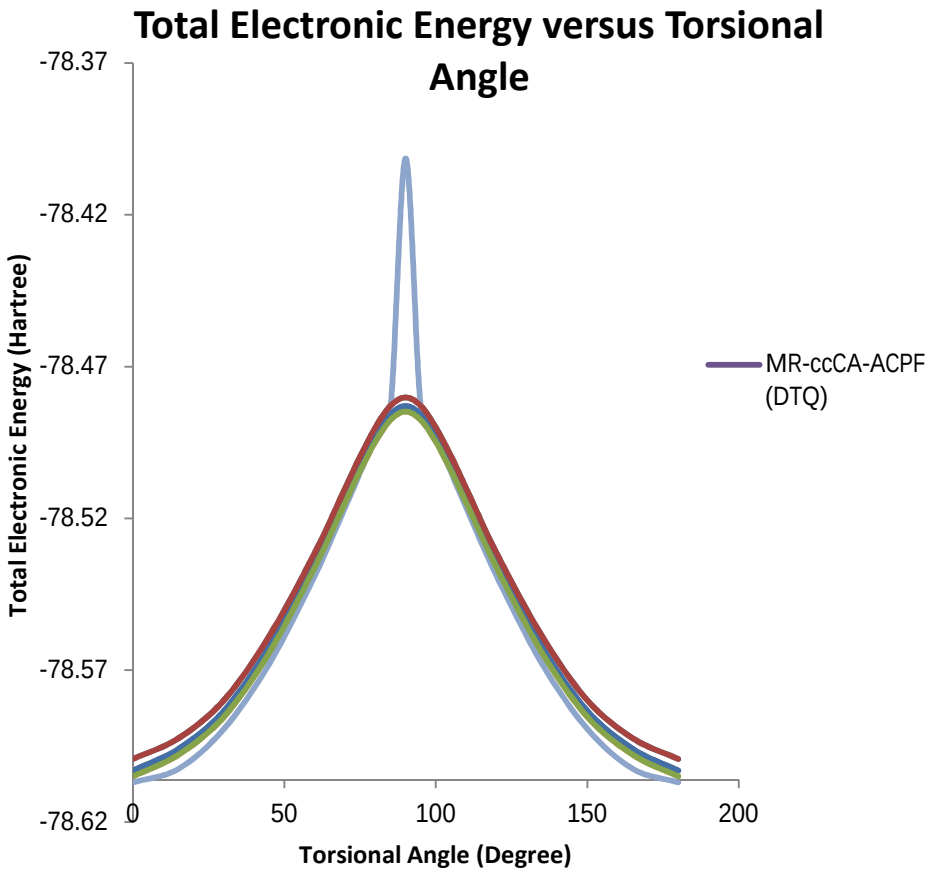

Figure 5.2 Potential energy curves depicting the internal rotation around ethylene double bond using single reference ccCA and MR-ccCA variants

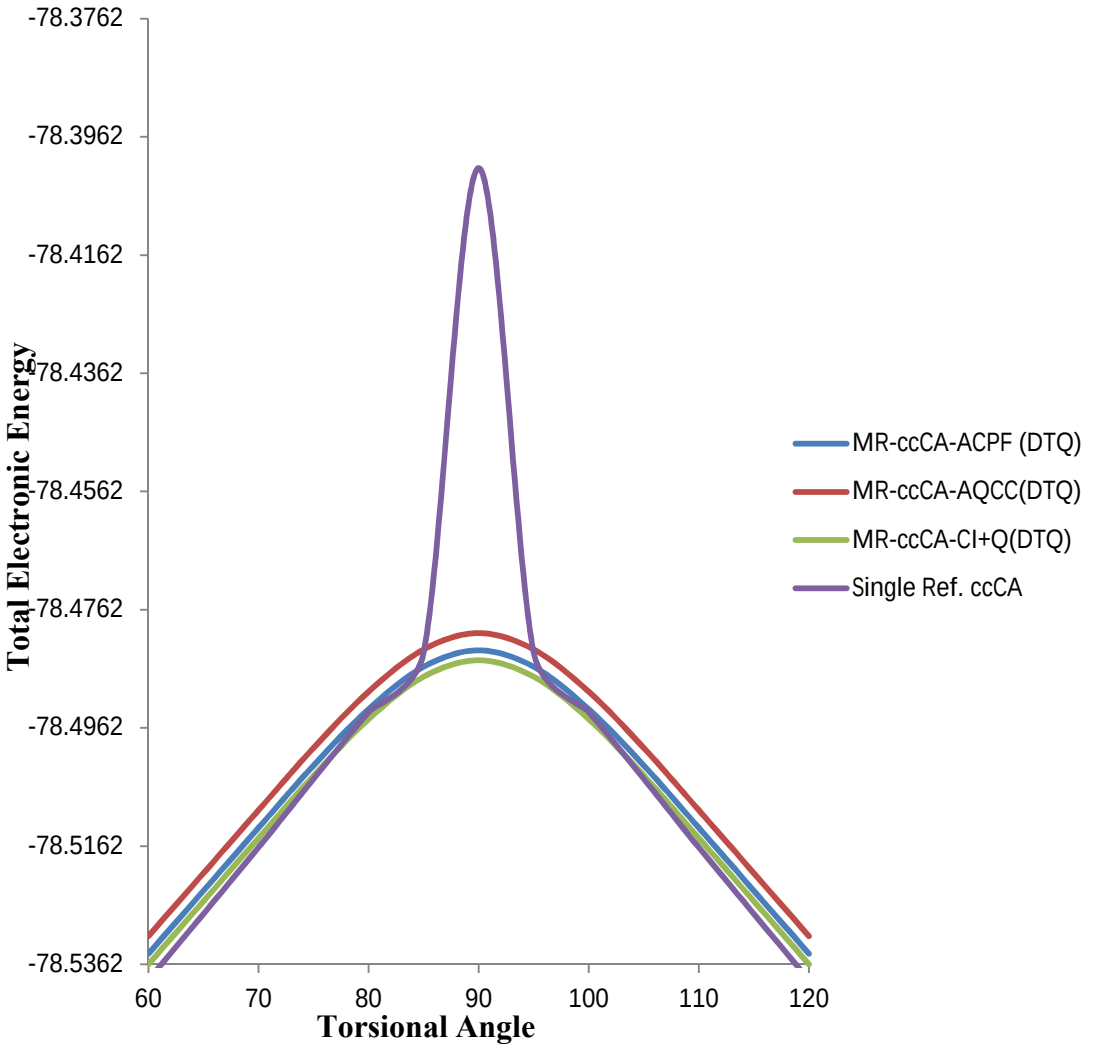

Figure 5.3 Potential energy curves around the transition state of twisted ethylene.

Unlike its lighter homologue ethylene, the energy ordering in disilene (Si_2H_4) follows the Hund's rule since its triplet state is predicted to be lower in energy than the twisted singlet transition state by 1.2 kcal mol^{-1}. MR-ccCA corroborates previous theoretical predictions[279] and recent experimental confirmation[280,281] that disilene has a trans-bent geometry with barrier to planarity of 0.4 kcal mol^{-1}. The π-bond strength (barrier to twisting) for Si_2H_4 is predicted to be 25.5 kcal mol^{-1} in excellent agreement with 25.1 kcal mol^{-1} of a previous MCSCF/SOCI/6-31g(d) calculation by Schmidt[274] et al. and an estimated experimental value of 25.8±4.8 kcal mol^{-1} by

Olbrich et al. for substituted disilene.[282] The $\Delta H^{\Theta}_{f,298}$ for the ground singlet state of disilene has also been predicted to be 66.8 kcal mol^{-1} in excellent agreement with the computed values of 66.0, 67.1 and 67.2 kcal mol^{-1} by Dolgonos,[279] Sax *et al*[283] and Katzer et al.[284] respectively and an experimental value of 65.7±0.9 kcal mol^{-1} by Ruscic and Berkowitz.[285]

5.3.6 Predicted $\Delta H^{\Theta}_{f,298}$ for Excited States

In addition to the $\Delta H^{\Theta}_{f,298}$ discussed earlier for the triplet states for which experimental results have been reported, here we predict the $\Delta H^{\Theta}_{f,298}$ for species (listed in Table 5.6) that have been unreported (to our knowledge) or unresolved, as is the case for the excited states of CCl_2, C_2H_2, and Si_2H_4. In the absence of experiments for these species, a comparison of the absolute energy arising from the difference between $\Delta H^{\Theta}_{f,298}$ of the singlet and triplet states ($|\Delta\Delta H^{\Theta}_{f,298}|$) can be made with prior computed $\Delta E_{S\text{-}T}$ values. For CCl_2, C_2H_2, and Si_2H_4, the ($|\Delta\Delta H^{\Theta}_{f,298}|$) are 20.8, 88.5, and 24.8 kcal mol^{-1}, respectively, in agreement with earlier computed ΔE_{S-T} values of 20.9 kcal mol^{-1} using CASSCF/MRCI+Q/cc-pVQZ,[286] 87.2 kcal mol^{-1} using CCSD(T)/TZ2P*f*,[268] and 22.7 kcal mol^{-1} using CASSCF/SOCI/6-31g(d),[274] respectively.

The $\Delta H^{\Theta}_{f,298}$ for the triplet excited state of O_3 and CHCl, validated in Table 5.3 to exhibit the most substantial multireference character (T_1 diagnostics of 0.05 and 0.03, respectively) of the triplet species examined, have been predicted using MR-ccCA-ACPF(S_TQ) method to be 65.7 and 84.3 kcal mol^{-1}.

5.4 Summary and Conclusions

We have demonstrated that the recently introduced multireference equivalent of the

highly successful single reference correlation consistent composite approach (ccCA) can be used to *quantitatively* predict spectroscopic and energetic properties of chemical species in the ground and excited states. Accurate predictions of processes that may require multi-configurational wavefunctions, such as bond-breaking, transition states, near or exact degeneracy in diradical species and excited states have been shown to be accomplished using MR-ccCA. For chemical systems consisting of first-row elements, we have introduced three variants of MR-ccCA: MR-ccCA-CI+Q, MR-ccCA-AQCC and MR-ccCA-ACPF. Three extrapolation schemes have been used to estimate the complete basis set limits of computed energetic properties.

Among the nine variants of MR-ccCA utilized, we have found that for spectroscopic properties such as singlet-triplet energy gaps considered in this study, MR-ccCA-AQCC(S_DT) results in better accuracy among the extrapolation schemes considered when compared to available well-established experimental results and previous high-level calculations. We therefore recommend MR-ccCA-AQCC(S_DT) as the method for computing energy differences such as barrier heights and singlet-triplet energy gaps in chemical systems. Our results also indicate that MR-ccCA-ACPF(S_TQ) and MR-ccCA-ACPF(P_DTQ), which have similar accuracy, provided the best overall predictions of thermochemical properties of the ground and excited states of chemical species.

Table 5.1 Singlet-triplet (ΔE_{S-T}) energy separations in atomic diradicals (kcal mol^{-1}).

	O	Si	C	S
CASPT2/AVDZ	48.9	21.8	33.2	30.6
CASPT2/AVTZ	47.0	19.2	30.6	28.6
CASPT2/AVQZ	46.1	18.4	29.8	27.7
CASPT2/AV5Z	45.7	18.1	29.4	27.3
MRCI+Q/VTZ	46.7	18.3	30.4	27.1
AQCC/VTZ	46.8	18.9	30.7	27.6
ACPF/VTZ (P_DTQ)	46.8	18.6	30.6	27.3
MR-ccCA-MRCI+Q	45.0	16.2	28.5	25.1
MR-ccCA-AQCC	45.1	16.8	28.8	25.7
MR-ccCA-ACPF (S_TQ)	45.1	16.6	28.7	25.4
MR-ccCA-MRCI+Q	45.0	16.2	28.5	25.2
MR-ccCA-AQCC	45.1	16.8	28.8	25.7
MR-ccCA-ACPF (S_DT)	45.1	16.6	28.7	25.4
MR-ccCA-MRCI+Q	45.7	16.5	29.0	25.9
MR-ccCA-AQCC	45.9	17.1	29.3	26.4
MR-ccCA-ACPF	45.8	16.9	29.2	26.1
Previous Calculations[a]	45.7	17.2	29.3	-
Experiment[a]	45.4	17.3	29.1	26.4

[a] *Ref. 221*

Table 5.2 Singlet-triplet separations (ΔE_{S-T}) and enthalpies of formation ($\Delta H^{\Theta}_{f,298}$) for the triplet state of methylene and silylene.

	ΔE_{S-T}[a]		$\Delta H^{\Theta}_{f,298}$	
	CH_2	SiH_2	CH_2	SiH_2
CASPT2/AVDZ	12.8	-16.5	-	-
CASPT2/AVTZ	11.8	-17.8	-	-
CASPT2/AVQZ	11.3	-18.2	-	-
CASPT2/AV5Z (P_DTQ)	11.2	-18.5	-	-
MR-ccCA-MRCI+Q	7.7	-23.1	94.4	88.0
MR-ccCA-AQCC	8.2	-22.4	94.6	87.7
MR-ccCA-ACPF (S_TQ)	7.9	-22.7	94.4	87.6
MR-ccCA-MRCI+Q	7.7	-23.1	94.2	87.9
MR-ccCA-AQCC	8.2	-22.4	94.4	87.6
MR-ccCA-ACPF (S_DT)	8.0	-22.7	94.3	87.6
MR-ccCA-MRCI+Q	8.2	-22.8	94.1	88.8
MR-ccCA-AQCC	8.7	-22.1	94.3	88.5
MR-ccCA-ACPF	8.4	-22.5	94.1	84.5
Previous Calculations	8.8[b]	-21.0±1[c]	92.4[d]	84.9[e]
Experiment	9.0[f]	-21.0±0.7[g]	93.7[d]	86.2[e]

[a]Negative values indicate that the singlet state is the lower state; [b]Ref. 224; [c]Ref. 229; [d]Ref. 153; [e]Ref. 89; [f]Ref. 71; [g]Ref. 77

Table 5.3 The T_1 diagnostics and percentage diradical character of the species considered.

	T_1 Diagnostics		%Diradicals (largest abelian point grp.)	
	Singlet state	Triplet state	Singlet state	Triplet state
CH_2	0.01	0.01	6.8	2.1
SiH_2	0.01	0.02	3.3	5.0
PH_2^+	0.01	0.02	2.3	6.8
NH_2^+	0.01	0.01	7.2	9.9
NH	0.01	0.00	99.1	1.4
O_2	0.01	0.01	91.8	4.9
OH^+	0.01	0.01	98.9	1.4
NF	0.03	0.02	96.0	1.6
CF_2	0.02	0.02	3.6	3.8
CCl_2	0.02	0.02	2.3	2.4
CHF	0.02	0.02	3.1	1.3
CHCl	0.02	0.03	4.5	3.8
Cis-CHOH	0.02	0.02	1.8	0.7
O_3	0.04	0.05	19.3	5.9
S_2	0.01	0.01	92.2	4.4
SO	0.02	0.02	88.2	3.9
S_3	0.02	0.02	13.2	5.1

Table 5.4 Singlet-triplet energy gaps (ΔE_{S-T}) in first and second row species (kcal mol^{-1})[a]

Species	MR-ccCA-AQCC(S_DT)	Expt.	Prev. Calc.
NH	36.6	35.9[b]	37.0[b]
O_2	22.6	22.6[b]	24.5[b]
OH^+	50.4	50.5[b]	50.5[b]
NF	32.9	34.3[b]	34.4[b]
SO	17.1	16.8[o]	-
S_2	12.6	12.6[c]	12.5[c]
O_3	29.0	28.6[n]	26.5[n]
S_3	-26.2	-	-
NH_2^+	28.1	30.1±0.2[b]	30.1[b]
PH_2^+	-18.8	-17.3±1.2[b]	-17.5[b]
CF_2	-56.3	-56.7[d]	-56.0[d]
CHCl	-5.7	-6.2[l]	-5.7[d]
CCl_2	-19.7	-3±3[m]	-19.2[e]
CHF	-15.1	-14.9±0.4[d]	-14.3[d]
trans-CHOH	-24.2	-	-25.3[f]
CH_2O-(formaldehyde)	-77.9	-72.0[g]	-77.7[g]
C_2H_2	-88.6	-82.6[i]	-87.2[h]
C_2H_4	-66.2	-58±3[j]	-66.4±0.3[j]
Si_2H_4	-24.3	-	-22.7[k]

[a]Negative values indicate that the singlet state is the lower state; [b]Ref. 221; [c]Ref. 243; [d]Ref. 248; [e]Ref. 247; [f]Ref. 255; [g]Ref. 256; [h]Ref. 268; [i]Ref. 265; [j]Ref. 277; [k]Ref. 274; [l]Ref. 249; [m]Ref. 245; [n]Ref. 261; [o]Ref. 242

Table 5.5 Enthalpies of formation for first and second row molecules (kcal mol^{-1}).

Molecules		MR-ccCA-ACPF(S_TQ)	Expt.	Prev. Calc.
Singlet states	CH_2	102.2	102.8[a]	101.8[a]
	SiH_2	64.9	65.2[a]	65.4[a]
	OH^+	357.7	-	-
	NF	89.2	-	-
	O_3	35.4	34.1±0.4[a]	34.9[a]
	S_3	36.3	33.0±3[b]	34.7±1.0[b]
	NH_2^+	330.8	-	-
	PH_2^+	257.7	-	-
	CF_2	-44.5	-43.5±1.5[c]	-46.9[c]
	CHCl	77.4	80.4±2.8[c]	76.4[c]
	CCl_2	57.5	55.0±2.0[c]	55.0[c]
	CHF	35.6	34.2±3.0[c]	34.9[c]
	trans-CHOH	27.2	-	26.1[d]
	CH_2O (formaldehyde)	-25.6	-26.0[e]	-26.7[e]
	C_2H_2	56.2	54.3±0.2[e]	55.1[e]
	C_2H_4	12.6	12.5[e]	12.6[e]
	Si_2H_4	66.8	65.7±0.9[f]	66.0[f]
Triplet states	NH	86.1	85.2[e]	85.9[e]
	O_2	0.4	0.0	0.9[e]
	SO	3.1	1.2[a]	1.7[a]
	S_2	31.6	30.7±0.1[b]	29.9[b]
	cis-CHOH	52.7	-	51.6[d]
	C_2H_2	144.7	-	145.3[g]
	C_2H_4	80.2	70.0±3[g]	78.5[g]

[a]Ref. 146; [b]Ref. 243; [c]Ref. 250; [d]Ref. 255; [e]Ref. 90; [f]Ref. 279 [g]Ref. 266.

Table 5.6 Predicted enthalpies of formation for excited states (kcal mol^{-1}).

Molecules	MR-ccCA-ACPF(S_TQ)	
	Triplet	Singlet
OH^+	308.0	-
NF	56.8	-
O_3	65.7	-
S_3	63.8	-
NH_2^+	302.6	-
PH_2^+	277.2	-
CF_2	11.8	-
CHCl	84.3	-
CCl_2	78.3	-
CHF	51.3	-
Si_2H_4	91.6	-
NH	-	122.3
O_2	-	23.0
SO	-	19.9
S_2	-	44.6

Table 5.7 Photodissociation channels for ozone and thiozone (kcal mol^{-1}).

Channels	MR-ccCA-AQCC(S_DT)	Expt.	Prev. Calc.
$O_3(X^1A_1) + h\nu \rightarrow O(^3P) + O_2(X^3\Sigma_g^-)$	26.0	26.1[a]	24.3[a]
$O_3(X^1A_1) + h\nu \rightarrow O(^3P) + O_2(a^1\Delta_g)$	48.8	>46.8[b]	-
$O_3(X^1A_1) + h\nu \rightarrow O(^1D) + O_2(X^3\Sigma_g^-)$	71.8	>69.6[b]	-
$O_3(X^1A_1) + h\nu \rightarrow O(^1D) + O_2(a^1\Delta_g)$	94.7	94.1[a]	93.5[a]
$S_3(X^1A_1) + h\nu \rightarrow S(^3P) + S_2(X^3\Sigma_g^-)$	60.3	-	61.3[c]
$S_3(X^1A_1) + h\nu \rightarrow S(^3P) + S_2(a^1\Delta_g)$	73.0	-	73.6[c]
$S_3(X^1A_1) + h\nu \rightarrow S(^1D) + S_2(X^3\Sigma_g^-)$	86.8	-	87.7[c]
$S_3(X^1A_1) + h\nu \rightarrow S(^1D) + S_2(a^1\Delta_g)$	99.6	-	100.0[c]

[a]Ref. 263; [b]Ref. 260; [c]Ref. 243

Table 5.8 Energetic barrier to isomerization in ozone, thiozone and unsaturated molecules (kcalmol^{-1}).

Molecule	MR-ccCA-AQCC(S_DT)	Expt.	Prev. Calc.
$O_3(D_{3h}$-$C_{2v})$	29.9	-	28.7[r]
$S_3(D_{3h}$-$C_{2v})$	5.3	-	4.4[s]
C_2H_4(π-bond)	64.3	≈65[t]	65.4[u]
Si_2H_4(π-bond)	25.5	25.8±4.8[v]	25.1[u]

[r]Ref. 257; [s]Ref. 243; [t]Ref. 276; [u]Ref. 274; [v]Ref. 282

CHAPTER 6

ACCURATE PREDICTIONS OF THE ENERGETICS OF SILICON COMPOUNDS USING THE MULTIREFERENCE CORRELATION CONSISTENT COMPOSITE APPROACH[†]

6.1 Introduction

Silicon compounds have been used in numerous industrial applications such as in semiconductors, optoelectronics, and surface growth processes, and thus are of significant interest in the scientific community.[287,288] Small silicon compounds are of great astronomical importance, as they are estimated to constitute nearly 10% of molecular species in interstellar atmospheres.[289] Silicon compounds are also used as precursors in chemical vapor deposition (CVD) and chemical etching.[161] Detailed understanding of the thermochemistry and reactivity of homogenous and heterogeneous clusters of silicon is important for the control of particle nucleation, growth processes, stoichiometric composition of vapor phase and doping of the epitaxial layer.[290,291] Inefficient control of the gas-phase content, particularly in vapor-phase epitaxy, can result in highly defective materials.[290] In many technological applications, the importance of accurate thermodynamic values to uniform deposition of semi-conductor layers during epitaxial growth on a substrate cannot be over-emphasized.[292] For instance, in the silicon doping of GaAs using a molecular beam epitaxy technique, quantitative thermodynamic information (e.g. the free energies) is important to the production of electronic grade layers, as this information can be used to determine whether other reactions that can enhance defect layer formation are intruding upon the process.[292] Indeed, accurate measurements and

[†] This chapter is adapted from G. A. Oyedepo, C. Peterson and A.K. Wilson, "Accurate predictions of the energetics of silicon compounds using the multireference correlation consistent composite approach." *J. Chem. Phys.* **2011**, *135*, 094103 with permission from the American Institute of Physics.

predictions of the energetics of silicon-containing compounds are highly imperative.

While reliable geometrical parameters of many carbon and silicon compounds are known, quantitative energetics (thermochemical and spectroscopic) of many small gas-phase silicon-containing species, unlike their lighter carbon-containing valence isoelectronic analogues, are sparse as they have been difficult to study, either experimentally or theoretically. Although carbon and silicon are members of group 14 of the periodic table, they both have remarkably different chemical properties. For instance, silicon is not known to form stable multiply-bonded compounds and concatenate, unlike carbon. On the other hand, silicon has the ability to expand its coordination sphere for hypervalency (pentavalent[293-295] and hexavalent[296]) and many of its compounds are crystalline, properties that are not particularly known in carbon chemistry. It is well-known that obtaining experimental gas phase molecular properties for silicon compounds is challenging due to their refractory characteristics (great hardness, high melting temperatures, very low coefficients of thermal expansion, high thermal-shock resistance, and exceptionally high chemical resistance even in corrosive media).[297,298] Theoretically, sophisticated correlated, but computationally costly, *ab initio* quantum mechanical methods such as single and multireference coupled cluster methods are often required to properly describe their wavefunctions.[161,299,300]

One of the major problems plaguing the purification of molten silicon is the removal of phosphorus to a tolerable maximum limit, for instance, 10^{-5} mass percentage phosphorus for solar grade silicon.[301] Quantitative knowledge of the thermodynamic properties of stable silicon-phosphorus compounds like siladiphosphirene (SiP_2) and disilaphosphirene (Si_2P) could assist in the design of more efficient purification methods. Unfortunately, there is little

quantitative thermodynamic and spectroscopic data available for many mixed silicon clusters containing elements of groups 13 and 15 in the literature and, of the available experimental thermochemical data, many very large uncertainties.[302-304] Even for small silicon hydrides, there have been major disagreements between theoretical and experimental results.[226,254] For instance, Kasdan et al.[226] experimentally estimated the singlet-triplet energy gap in SiH_2 as having an upper-bound value of 13.8 kcal mol^{-1} (≤0.6eV) while Balasubramanian et al.[254] predicted a value of 21.0±1 kcal mol^{-1} using MCSCF/SOCI-*f*. Prior theoretical studies have suggested that some of the experimental results need to be reanalyzed[246,254] and, in the wake of these predictions, subsequent experimental evidence has been obtained in substantiation of theoretical results.[305] Simple hydrides of carbon, have seen their share of conflicting results. For example, Gauss et al. used CCSD(T)/cc-pVTZ to predict an experimentally disputed geometry of cyclopropane which was later found to be in good agreement with a reanalyzed geometry obtained via analysis of microwave spectra.[306] Also, Al-Saadi et al. reinterpreted the far-infrared spectra of 2-silacyclopent-2-ene, guided by results from CCSD/6-311++G(d,p) and DFT methods, to show that this ring molecule has a small barrier to planarity of about 0.14 kcal mol^{-1} in contrast to the highly rigid planar structure previously proposed.[307] Although recent results from both experiment and theory have been more refined due to the increased use of high-resolution spectroscopy and advances in computing power and computational methodology, there are still thermodynamic and spectroscopic data that have eluded laboratory synthesis or need to be reexamined (for instance, silicon-aluminum and silicon-phosphorus mixed clusters). In this study, we determine the atomization energies, standard enthalpies of formation, and ground-excited state splittings for spin-forbidden transitions of carbon and silicon compounds

(such as the mixed clusters of silicon and group 13 and 15 elements) using the multireference correlation consistent composite approach (MR-ccCA).[149,152,308]

MR-ccCA has been shown[143,149,152] to result in quantitative theoretical predictions, within "chemical accuracy" (±1 kcal/mol of reliable experiment for energies). MR-ccCA is the multireference equivalence of the tested and proven single-reference correlation consistent composite approach (ccCA) designed by Wilson and coworkers[90,92,95,96,157-161] to replicate results that would otherwise be obtained using a sophisticated but computationally intensive high level theoretical method such as coupled cluster with singles, doubles and non-iterative triples correction with a very large basis set, such as CCSD(T)-DK/aug-cc-pCV∞Z-DK, albeit at a fraction of the computational cost. The current study is undertaken to predict the properties of evasive and previously studied but yet unresolved silicon compounds. The utilization of multi-configurational reference wavefunctions in this study is essential for many of the considered silicon compounds because of their strong multireference characteristics (demonstrated by the magnitudes of percentage contributions of their SCF configurations to the CASSCF wavefunctions (C_0^2) together with their T_1 and D_1 diagnostics i.e. Frobenius norm and matrix 2-norm of the t_1 amplitudes of their coupled cluster wavefunctions, respectively),[309] especially for those with open-shell electronic configurations, due to manifolds of close lying states (in their electronic structures). Thermochemical properties of a number of carbon-containing compounds are also considered for contrast with their corresponding silicon analogues. Silicon species for which the properties are better established are also considered to aid in gauging the utility of MR-ccCA.

6.2 Computational Methods

MR-ccCA has been formulated to exploit the unique ability of the correlation consistent basis sets (cc-pV*n*Z) to systematically recover electron correlation energy as the size of the basis set increases. The monotonic convergence characteristics of cc-pV*n*Z enables extrapolation to the complete basis set (CBS) limit, the limit at which the error due to an incomplete basis set description is deemed eliminated. Within the MR-ccCA composite scheme, the CBS limit provides a useful foundation upon which to build missing correlation effects (e.g. higher-order correlations, core-core and core-valence correlations) and relativistic effects. In this work, while the regular cc-pV*n*Z family of basis sets are generally utilized, the tight *d* correlation consistent basis sets, cc-pV(*n*+*d*)Z, where the "+*d*" indicates the addition of an extra high-exponent *d* function to the re-optimized standard cc-pV*n*Z basis set of Dunning et al.[37,310] have been used for all third-period elements in this study to accommodate inner polarization effects.[311,312]

Two extrapolation schemes have been used in this study; (i) a three-point mixed Gaussian/exponential scheme (equation (6.1)) proposed by Peterson et al.,[118]

$$E_n=E_{CBS}+A*exp[-(n-1)]+B*exp[-(n-1)^2] \quad (6.1)$$

where n is the ζ-level (D=2, T=3, Q=4, etc.) of the basis set used, E_{CBS} is the total electronic energy at the CBS limit, E_n is the total energy at the nth ζ-level and A and B are analytical or least squares fitting parameters. (ii) a two-point extrapolation scheme using the quartic inverse power of the highest angular momentum (equation (6.2)) in a basis set as developed by Schwartz,[208] Klopper,[117] Kutzelnigg and co-workers[313]

$$E(l_{max})=E_{CBS}+D/(l_{max}+1/2)^4 \quad (6.2)$$

where l_{max} and $E(l_{max})$ are the highest angular momentum in a given basis set while E_{CBS} and D are the electronic energy at CBS limit and fitting constant, respectively.

The MR-ccCA formulation is based on a CASPT2 reference energy [$E_o(MR\text{-}ccCA)$] obtained by extrapolation to the CBS limit which is then improved via the inclusion of a series of additivity terms that account for core-core and core-valence correlation effects, scalar relativistic effects and higher-order correlation beyond the CASPT2 level of theory. The full valence active space has been used for all calculations and to ensure a balanced treatment of closed- and open-shell wavefunctions within CASPT2, the g3 variant of the modification to the zeroth-order Hamiltonian as proposed by Andersson[245] was applied. The core-valence term [$\Delta E(MR\text{-}CV)$] has been included at the CASPT2/cc-pCVTZ level of theory, scalar relativistic effects [$\Delta E(MR\text{-}DK)$] from second-order Douglas-Kroll-Hess theory,[314-316] has been included at CASPT2-DK/cc-pVTZ-DK level and higher-order correlation effects [$E(MR\text{-}CC)$] has been included at two levels of theory, MR-ACPF/cc-pVTZ and MR-AQCC/cc-pVTZ, since MR-CCSD(T) has not been implemented into readily available ab initio program package. The overall MR-ccCA methodology used to compute energetic properties can therefore be described using equation (6.3)

$$E(MR\text{-}ccCA) = E_o(MR\text{-}ccCA) + \Delta E(MR\text{-}CC) + \Delta E(MR\text{-}DK) + \Delta E(MR\text{-}CV) \quad (6.3)$$

where

$\Delta E(MR\text{-}CC) = E(MR\text{-}ACPF/cc\text{-}pVTZ) - E(CASPT2/cc\text{-}pVTZ)$ or

$$E(MR\text{-}AQCC/cc\text{-}pVTZ) - E(CASPT2/cc\text{-}pVTZ) \quad (6.4)$$

$$\Delta E(MR\text{-}DK) = E(CASPT2\text{-}DK/cc\text{-}pVTZ\text{-}DK) - E(CASPT2/cc\text{-}pVTZ) \quad (6.5)$$

$$\Delta E(MR\text{-}CV) = E(CASPT2/cc\text{-}pCVTZ) - E(CASPT2/cc\text{-}pVTZ) \quad (6.6)$$

The MR-ccCA method has thus been designed to effectively approximate the MR-ACPF-DKH/aug-cc-pCV(∞)Z-DK or MR-AQCC-DKH/aug-cc-pCV(∞)Z-DK level of theory.

All extrapolation procedures in this study have been done using the least-squares method with a residual error squared less than 10^{-7} Hartree. As two different extrapolation schemes and higher-order correlation methods are used, the resultant variants of MR-ccCA can be described by a variety of names. For example, 'MR-ccCA-ACPF(P_DTQ)' denotes the use of the Peterson extrapolation, using double-, triple- and quadruple-ζ basis sets and the MR-ACPF method as the higher-order correlation method. 'MR-ccCA-AQCC(S_DT)' denotes an extrapolation using the quartic inverse scheme with double- and triple-ζ basis sets and MR-AQCC method as the higher-order correlation method, while 'MR-ccCA-ACPF(S_TQ)' denotes an extrapolation using the quartic inverse scheme with triple- and quadruple-ζ basis sets. Further information about the MR-ccCA methodology can be obtained from our earlier studies.[149] As the MR-ccCA-ACPF(S_TQ) and MR-ccCA-AQCC(S_DT) variants provided the best combinations of computational efficiencies and accuracy in our prior study,[149] these are the approaches that are the focus of this study.

All computations have been performed using the Gaussian09 and MOLPRO 2009 software packages.[172,173] All reference geometries and subsequent frequency calculations for silicon compounds have been done at the CASPT2/cc-pVTZ level of theory, where cc-pV(T+d)Z has been used for silicon with only the valence electrons correlated. Harmonic vibrational frequencies were computed from the optimized structures and were established as minima by the absence of imaginary frequencies. The total atomization energy (TAE) (equation (6.7) and enthalpy of formation ($\Delta_f H^o$) (equation (6.8)) of a silicon compound Si_mX_n have been calculated using the relations

$$TAE(0K) = \{m[E_{MR\text{-}ccCA}(Si) - \Delta E(SOC)_{Si}] + n[E_{MR\text{-}ccCA}(X) - \Delta E(SOC)_X]\} -$$

$$\{E_{MR\text{-}ccCA}(Si_mX_n) + ZPE(Si_mX_n)\} \quad (6.7)$$

$$\Delta_f H^o(298.15K) = \{m[\Delta_f H^o_{(expt)}(Si,0K) - H^o_{corr(expt)}(Si)] + n[\Delta_f H^o_{(expt)}(X,0K) - H^o_{corr(expt)}(X)]\} -$$

$$\{TAE(0K) - H^o_{corr(calc)}(Si_mX_n)\} \quad (6.8)$$

where ΔE(SOC) accounts for atomic spin-orbit corrections from experimental results,[317] ZPE is the molecular zero-point energy, $\Delta_f H^o_{(expt)}$ is the experimental enthalpy of formation of an atom at 0K, $H^o_{corr(expt)}$ is the experimental enthalpy correction of the atom and $H^o_{corr(calc)}$ is the computed enthalpy correction for the molecule.

6.3 Results and Discussion

6.3.1 Hydrides of Silicon and Carbon

6.3.1.1 SiH and CH

The MR-ccCA predicted $\Delta_f H^o_{298}$ of 90.5 kcal mol^{-1} for the ground electronic state $X^2\Pi$ of silylidyne (SiH) is in excellent agreement with NIST recommended value of 90.0 kcal mol^{-1}.[269] However, experimental results (68.7±0.7[305] 77.1±0.6[318] and ≤70.6[266] in kcal mol^{-1}) for the atomization energy of the SiH radical suggest that a conclusive value for this property might be unknown. In Table 6.2, we report the MR-ccCA computed TAE value for SiH as 70.4 (D_e=73.3) kcal mol^{-1} in support of two of the referenced experimental values (68.7±0.7 and ≤70.6). The MR-ccCA value is also in excellent agreement with theoretically determined values of 69.2 kcal mol^{-1} obtained by Larsson[319] using CASSCF/contracted CI method with a large contracted basis set [10*s*7*p*4*d*1*f*/$_{Si}$; 7*s*4*p*1*d*/$_H$] and the D_e value of 73.3 kcal mol^{-1} estimated by Kalemos, Mavridis and Metropoulus[320] using *ic*MRCI/aug-cc-pV6Z method that was corrected for atomic and molecular spin-orbit splittings, scalar relativistic effects, core-valence effect and basis set

superposition error. Kalemos *et al*.[320] also reported the $a^4\Sigma^- \rightarrow X^2\Pi$ separation of 38.8 kcal mol^{-1} and claimed that the experimental value of 14.3 kcal mol^{-1} obtained by Park[321] "is wrong". The MR-ccCA determined value for the ground state doublet of the lowest-lying excited state quartet electronic energy gap (Table 6.6) is 40.8 kcal mol^{-1}, in corroboration of the theoretically determined value of Kalemos. We also report $\Delta_f H^o_{298}$ for the ground state and the electronic energy term (T_o) for CH as 142.5 and 17.6 kcal mol^{-1} respectively, in excellent agreement with experimental values of 142.0[269] and 17.1±0.2[322] kcal mol^{-1}.

6.3.1.2 Si_2H and C_2H

The computed multireference diagnostics (T_1, D_1, and C_o^2) for the ground $^2A_1$ and low-lying $^4A''$ states (Table 6.1) of the disilynyl radical (Si_2H) are (0.027, 0.057, 0.889) and (0.048, 0.116, 0.895), respectively. The observation that the C_o^2 values are less than 0.90 while the T_1 diagnostic values are larger than the generally accepted cutoff of 0.02 and the D_1 diagnostic values are also above the suggested cutoff value of 0.05 indicates that the electronic states considered have large contributions from non-dynamic correlation effects.[323] Prediction of the energetics of these states dictate the application of a multi-configurational approach. We report $\Delta_f H^o_{298}$ for the doublet ground and quartet excited states as 122.5 and 149.9 kcal mol^{-1}, respectively. The $\Delta_f H^o_{298}$ for the ground state doublet of ethynyl radical (C_2H) has been reported (in kcal mol^{-1}) as 135.8±1.4 (photodissociation laser-induced fluorescence),[324] 136.0 (Weizmann-2 method)[325] and 141.0 (diffusion Monte Carlo (DMC) method).[326] In a recent paper by Golovin and Takhistov, the authors claimed that the $\Delta_f H^o_{298}$ is now "firmly established" as 123±2 kcal mol^{-1}.[327] The MR-ccCA computed $\Delta_f H^o_{298}$ for the ground state of C_2H is reported as

137.6 kcal mol^{-1} (Table 6.2) in very good agreement with the experimental result of 135.8±1.4 kcal mol^{-1} obtained by Hsu et al.[324] using a laser-induced fluorescence method.

6.3.1.3 Si_2H_2

The MR-ccCA predicted TAE and $\Delta_f H^o_{298}$ for the ground singlet state of dibridged disilyne (Si_2H_2) as 222.8 and 96.6 kcal mol^{-1}, respectively. These values support the reported theoretical values, using a high-level model coupled cluster composite method which approximates results that would be obtained with CCSDT-DK/CBS-DK method, of Dolgonos[328] (223.4 and 96.6 kcal mol^{-1}) and also agree with the upper-bound $\Delta_f H^o_{298}$ experimental value of <99.7 kcal mol^{-1} estimated by Ruscic and Berkowitz.[310] The corresponding results for the carbon analogue of disilyne, acetylene, have been reported in our earlier publication. [156]

6.3.1.4 Si_2H_3 and C_2H_3

The true global minimum for the ground state geometry of the Si_2H_3 radical is still an open question for both theoretical and experimental chemists. Various authors[283,287,306,329] have claimed different nearly degenerate isomers as the most stable geometries of this interesting species. We have studied the relative energies (corrected for ZPE) of four of the lowest energy isomers near the bottom of the potential energy surface using CASPT2 with a triple zeta quality basis set and then used MR-ccCA to refine the energetics of the two lowest energy geometries. The four considered isomers (Figure 6.1) consist of a quasi-planar form **A** (H_2SiSiH, C_1 symmetry) and three mono-bridged forms: **B** = H_2Si-H-Si with C_s symmetry, **C** = HSi-H-SiH (trans-like conformation) with C_2 symmetry and **D** = HSi-H-SiH (cis-like conformation) with C_1 symmetry.

The relative energies (Table 6.8) are found to be 0.0, 0.5, 2.66 and 10.7 kcal mol^{-1} for isomers **A**, **B**, **C** and **D**, respectively. However, when the MR-ccCA method, which includes all the missing corrections at the CASPT2/cc-pVTZ level, is applied to isomers **A** and **B** to improve the accuracy of the computed relative energies, the mono-bridged form **B** was discovered to be the most stable isomer by 0.7 kcal mol^{-1} in very good agreement with the trend observed by Sari et al.[287] using a hierarchy of coupled cluster methods including CCSDT. To our knowledge, the predicted ground state mono-bridged isomer **B** has not yet been characterized in the laboratory. We also report the TAE and $\Delta_f H^o_{298}$ for the ground state doublet, and the spin-forbidden electronic transition between the ground and lowest-lying quartet excited state as 271.3, 99.9 and 28.7 kcal mol^{-1}, respectively.

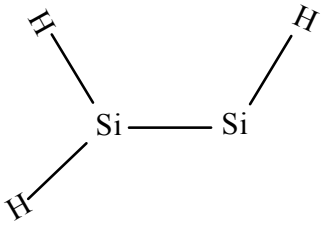

Isomer A (H_2Si-SiH), C_1

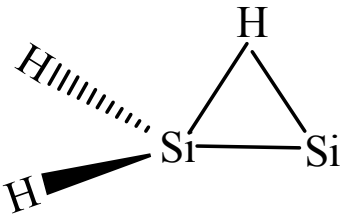

Isomer B (H_2Si-H-Si), C_s

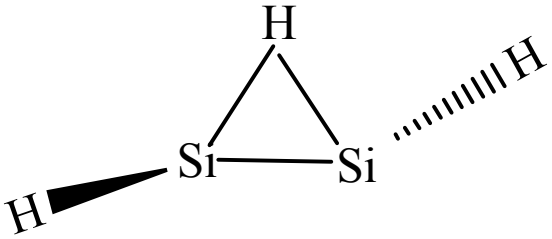

Isomer C (HSi-H-SiH), C_2

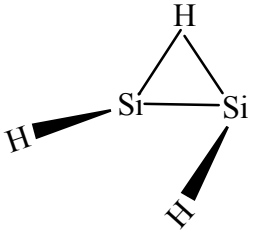

Isomer D (HSi-H-SiH), C_1

Figure 6.1 Conformations of Si_2H_3 isomers.

Unlike its heavier congener, the geometry of the C_2H_3 radical is planar with C_s symmetry. Considering that the values of the T_1, D_1 and C_0^2 diagnostics for the ground state of C_2H_3 are 0.016 and 0.036, 0.906 respectively, we note that its wavefunction can be adequately

represented by a single reference method. We have demonstrated in our previous publication[149] that the MR-ccCA method is versatile for modeling systems with significant static and dynamic correlation effects. The MR-ccCA predicted TAE and $\Delta_f H^o_{298}$ for the ground state of C_2H_3 are 421.1 and 72.8 kcal mol^{-1} in good agreement with the TAE of 422.2 and 421.3 kcal mol^{-1} obtained experimentally and using a DMC method, respectively.[326] The predicted $\Delta_f H^o_{298}$ is also in accord with the experimental value of 71.6±0.8 kcal mol^{-1} and 72.7 kcal mol^{-1} achieved using the G2 composite method.[330]

6.3.2 Small Homonuclear Clusters of Carbon and Silicon

6.3.2.1 Si_2 and C_2

To further demonstrate the performance of MR-ccCA for the prediction of the energetic properties of silicon species, we computed the TAE, $\Delta_f H^o_{298}$ and transition energies of small clusters of silicon and carbon. Homonuclear diatomic and triatomic clusters of carbon and silicon exhibit moderate to strong multireference characteristics, as shown in Table 6.1, as their T_1, D_1 and C_0^2 diagnostic values are outside the threshold values discussed above (T_1>0.02, D_1>0.05 and C_0^2<0.90). The MR-ccCA values for TAE and $\Delta_f H^o_{298}$ of the ground state triplet ($X^3\Sigma^-_g$) of Si_2 (T_1=0.023, D_1=0.039 and C_0^2=0.922) are 73.1 and 145.5 kcal mol^{-1}, in some disagreement with the recent experimental values of 76.2±1.7 and 140.3±1.7 kcal mol^{-1} by Schmude et al.[304] but in better agreement with the TAE value of 74.4±0.4 kcal mol^{-1} obtained by Dixon et al. using UCCSD(T) (n=D, T, Q, 5, 6) extrapolated to the CBS limit and corrected for ZPE, core-valence, scalar relativistic and spin-orbit effects.[331] The MR-ccCA value for TAE is also in good agreement with an experimental value of 74.0 kcal mol^{-1} reported by Huber and Herzberg[266] in 1979 and

73.3±0.2 kcal mol^{-1} determined by Grossman[332] using fixed-node diffusion Monte Carlo. The transition energies for two adiabatic spin-forbidden low-lying excited states ($a^1\Delta_g$ and $c^1\Sigma^+_g$) that have similar electronic configurations (equation 6.9) as the ground state of Si_2 but different electronic energies have also been computed using MR-ccCA.

[Core] $4\sigma_g^2 4\sigma_u^2 5\sigma_g^2 2\pi_u^2$ (6.9)

MR-ccCA predicts that $a^1\Delta_g$ and $c^1\Sigma^+_g$ lie 9.9 and 15.0 kcal mol^{-1} above the ground state in good agreement with experimental values of 10.0 and 14.7 kcal mol^{-1} reported by Kitsopoulos et al.[333] and theoretical values of 11.7 and 15.8 kcal mol^{-1} obtained by Sefyani and Schamps[334] using MRCI in combination with quadruple zeta quality basis set with the neon core represented by a pseudopotential. The MR-ccCA values for TAE and $\Delta_f H^o_{298}$ of C_2 are also reported in Table 6.3. Unlike Si_2, the ground state of C_2 is a singlet ($X^1\Sigma^+_g$) with TAE and $\Delta_f H^o_{298}$ values of 142.4 and 199.1 kcal mol^{-1}, in very good agreement with experimental values of 144.6±1.9 and 200.2 kcal mol^{-1}, respectively.[335] Our reported TAE value also agrees with previous computed values of 143.9 kcal mol^{-1} using the Weizmann-4 (W4) level of theory but differ from the Gaussian-4 (G4) predicted value by 3.6 kcal mol^{-1} indicating that the latter is more sensitive than the former to multi-configurational characteristics of the wavefunction.[335] The transition energy for $a^3\Pi_u \leftarrow X^1\Sigma^+_g$ has been computed to be 1.3 kcal mol^{-1}, using MR-ccCA, in agreement with the reported experimental value of 2.1 kcal mol^{-1}.[336]

6.3.2.2 Si_3 and C_3

The electronic singlet ground state of Si_3 ($^1A_1$) with C_{2v} symmetry has been reported to lie within 1 kcal mol^{-1} of the nearly isoenergetic low-lying cyclic triplet excited state ($^3A_2$) with D_{3h} symmetry.[337] MR-ccCA predicts the singlet-triplet energy gap as 0.2 kcal mol^{-1} in support of a previous theoretical estimate.[338] We also report the TAE and $\Delta_f H^o_{298}$ values for the ground singlet state as 169.7 and 158.0 kcal mol^{-1}, in agreement with the experimental values of 168.5±3.8 and 156.1±3.8 kcal mol^{-1}, respectively.[339] The geometry of the ground singlet state ($^1\Sigma^+_g$) of C_3 has been shown[340] to be linear ($D_{\infty h}$), unlike the bent structure of Si_3. However, both C_3 and Si_3 have a very similar cyclic D_{3h} geometry in their lowest-lying triplet excited state. The triplet electronic excited state of C_3 is predicted to lie 21.0 kcal mol^{-1} above the ground state. The MR-ccCA computed TAE value for the ground singlet state of C_3 is 314.7 kcal mol^{-1} in agreement with previous theoretical estimates of 315.8 using the W4 method and an experimental value of 311.4±3.1 kcal mol^{-1}.[335] MR-ccCA can thus be used to quantitatively predict the energetics of small carbon and silicon compounds.

6.3.3 Binary Compounds SiX (X=B, C, N, Al and P)

6.3.3.1 SiB

The electronic ground state of the SiB radical is a high-spin $X^4\Sigma^-$ state with configuration [Core] $5\sigma^2 6\sigma^2 7\sigma^1 2\pi^2$. The quartet ground state is moderately multireference in character (T_1=0.036, D_1=0.076 and C_0^2=0.895) suggesting a need for an accurate multi-configurational method for determining properties of the species. The MR-ccCA method predicts the TAE of SiB to be 74.3 kcal mol^{-1} in excellent agreement with experiment (74.6±2.8 kcal mol^{-1}). However,

the $\Delta_f H^o_{298}$ for SiB, a property determined from the TAE and enthalpies of formation of the constituent elements (Si and B), as described in equation 6.8 above, shows disagreement between our computed theoretical and prior experimental values; MR-ccCA $\Delta_f H^o_{298}$=172.3 kcal mol^{-1} while the experimental value is reported as 166.8±3.3 kcal mol^{-1}.[341] This difference is due, in part, to different atomistic enthalpies of formation utilized in computing the values for the $\Delta_f H^o_{298}$ of the SiB radical. While we utilized the more recently determined value, and we believe more accurate values of 108.2 and 136.3 kcal mol^{-1} for the silicon and boron atoms respectively,[299] the authors of the experimental paper reported that they used 107.6 and 135.0 kcal mol^{-1}. The MR-ccCA computed transition energy for $a^2\Pi \rightarrow X^4\Sigma^-$ is 16.6 kcal mol^{-1} in very good agreement with the theoretical value of 16.9 kcal mol^{-1} reported by Ornellas and Iwata using the *ic*MRCI/cc-pVQZ method.[342]

6.3.3.2 SiC

The $a^1\Sigma^+ \rightarrow X^3\Pi$ transition for SiC is predicted to be 14.9 kcal mol^{-1} in support of theoretical value of 14.3 kcal mol^{-1} reported by Sefyani and Schamps using MRCI.[334] We also report the TAE for the ground state $X^3\Pi$ with electronic configuration [Core] $5\sigma^2 6\sigma^2 7\sigma^1 2\pi^3$ and excited state $a^1\Sigma^+$ with configuration [Core] $5\sigma^2 6\sigma^2 7\sigma^0 2\pi^3$ as 100.0 and 85.0 kcal mol^{-1}, respectively as shown in Table 6.4. The corresponding $\Delta_f H^o_{298}$ for $X^3\Pi$ and $a^1\Sigma^+$ states are calculated as 180.1 and 195.0 kcal mol^{-1}, respectively.

6.3.3.3 SiN

A previous theoretical study by Melius and Ho of the ground state $X^2\Sigma^+$ ([Core]

$5\sigma^2 6\sigma^2 2\pi^4 7\sigma^1$) SiN radical using empirical bond additivity-corrected MP4 (BAC-MP4) method reported $\Delta_f H^o$(0K) as 115.2 kcal mol^{-1}.[343] The MR-ccCA computed $\Delta_f H^o_{298}$ of 118.5 kcal mol^{-1} ($\Delta_f H^o$(0K)=116.4 kcal mol^{-1}) is in support of the BAC-MP4 result. We also predicted the adiabatic transition energy for the $a^4\Sigma^+ \rightarrow X^2\Sigma^+$ transition as 59.7 kcal mol^{-1} (T_e=60.3 kcal mol^{-1}) in quantitative disagreement with T_e values of 63.5 kcal mol^{-1} and 53.0 kcal mol^{-1} reported by Cai et al.[344] and Bruna et al.[345] using *ic*MRCI/cc-pVQZ//*ic*MRCI/cc-pVTZ and MRD-CI/DZP+B+R (B and R denote augmented bond- and Rydberg-type functions) methods, respectively. The differences between the MR-ccCA value and the results obtained by Cai et al. and Bruna et al. can easily be traced to their lack of accounting for core-valence correlation, scalar relativistic effects and basis set incompleteness error. However, the MR-ccCA predicted TAE of 40.8 kcal mol^{-1} for $^4\Sigma^+$ state is in very good agreement with 39.7 kcal mol^{-1} reported by Cai et al.[344]

6.3.3.4 SiAl

Like its smaller group 13 homologue SiB, the electronic ground state of the SiAl radical is the high-spin $^4\Sigma^-$ ([Core] $7\sigma^2 8\sigma^2 3\pi^2 9\sigma^1$) state. The transition energy between the ground and lowest spin-forbidden excited states for both homologues are also very similar in magnitude; the MR-ccCA predicted $a^2\Sigma^- \rightarrow X^4\Sigma^-$ energy separation is 17.3 kcal mol^{-1} (*cf*. 16.6 kcal mol^{-1} for SiB), which is in very good agreement with 16.7 kcal mol^{-1} obtained by Ornellas et al. using the *ic*MRCI/cc-pVQZ method.[346] However, our computed binding energy (TAE) of 57.1 kcal mol^{-1} for the ground state of SiAl, which is in very good agreement with the 58.3 kcal mol^{-1} of Ornellas et al.[346], indicates a relatively weaker interaction between the constituent silicon and aluminium atoms wavefunctions, compared to the ground state of SiB with TAE of 74.3 kcal mol^{-1}. The TAE

of 40.3 kcal mol^{-1} for the low-spin $a^2\Sigma^-$ excited state of SiAl indicates that this electronic state is more weakly bonded relative to the ground state. We also report $\Delta_f H^o_{298}$ for the ground state of SiAl as 134.2 kcal mol^{-1} while no previous theoretical or experimental values are available for comparison.

6.3.3.5 SiP

The MR-ccCA predicted TAE and $\Delta_f H^o_{298}$ for the electronic ground state $X^2\Pi$ ([Core] $7\sigma^2 8\sigma^2 9\sigma^2 3\pi^3$) of the SiP radical are 84.0 and 100.5 kcal mol^{-1}, respectively. No previous theoretical and experimental values for these properties have been found for comparison. The energy gap between the ground state and the low-lying $a^4\Sigma^+$ state, $a^4\Sigma^+ \rightarrow X^2\Pi$, has also been computed as 44.4 kcal mol^{-1} using MR-ccCA in excellent agreement with 44.1 kcal mol^{-1} obtained by dos Santos et al. using *ic*MRCI/aug-cc-pVQZ. We also report the binding energy for the excited $a^4\Sigma^+$ state as 38.3 kcal mol^{-1} for which no previous value has been found for comparison.

6.3.4 Triatomic compounds Si_nX_m (X=B, C, N, Al, P)

6.3.4.1 SiB_2 and Si_2B

The lowest energy isomer of SiB_2 is the isosceles triangle-like C_{2v} form with the silicon atom at the apex (See Table 6.1 for geometrical parameters). The TAE and $\Delta_f H^o_{298}$ for the singlet ground state ($^1A_1$) have been computed using MR-ccCA as 191.4 and 192.0 kcal mol^{-1}, respectively, in quantitative disagreement with $\Delta_f H^o_{298}$ of 195.3 kcal mol^{-1} obtained by Davy et al. using B3LYP/cc-pVQZ method.[347] The lowest energy singlet-triplet energy gap ($^3A_1 \rightarrow {}^1A_1$) is

predicted to be 18.7 kcal mol^{-1}, in disagreement with 10.2 and 13.6 kcal mol^{-1} computed by Davy et al. using CISD/TZ2P and B3LYP/cc-pVTZ methods, respectively.[347] The apparent quantitative failures of CISD and B3LYP methods could be ascribed to the lack of size extensitivity in the CISD method, the same shortcoming that plagues truncated configuration interaction methods, the quality of the basis sets utilized, and the strong multi-configurational character exhibited by the $^1A_1$ state of SiB_2 wavefunction as estimated by T_1, D_1 and C_0^2 diagnostics of 0.064, 0.192 and 0.759, respectively.

The MR-ccCA predicted TAE for the ground state ($^2B_2$) of Si_2B is 181.8 kcal mol^{-1} (Table 6.5) in good agreement with the experimental value of 183.3±4.3 kcal mol^{-1} reported by Viswanathan et al.[341] However, as discussed above for the diatomic SiB radical, the computed $\Delta_f H^o_{298}$ of 173.6 kcal mol^{-1} is in significant disagreement with the reported experimental value of 164.4 kcal mol^{-1} by the same authors. The MR-ccCA predicted TAE for the $^4B_2$ state is 157.2 kcal mol^{-1} while the $^2B_2 \rightarrow {}^4B_2$ transition energy is 25.7 kcal mol^{-1}. No previous theoretical or experimental values have been found for comparison.

6.3.4.2 SiC_2 and Si_2C

SiC_2 has been one of the most studied triatomic silicon molecules. Nonetheless, the last known TAE experimental value of 301.0±7 kcal mol^{-1} for the singlet ground state ($^1A_1$) of the T-shaped molecule has been challenged by Deutsch et al.,[348] as it is believed that the value may have been overestimated, with an obviously large experimental uncertainty. MR-ccCA predicts a binding energy of 293.1 kcal mol^{-1} (Table 6.5) which is consistent with 294.7 kcal mol^{-1} predicted by Deutsch et al.[348] MR-ccCA also predicts an $\Delta_f H^o_{298}$ of 157.3 kcal mol^{-1}

($\Delta_f H^o$(0K)=154.6 kcal mol^{-1}) in good agreement with an estimated $\Delta_f H^o$(0K) value of 155±3 kcal mol^{-1} obtained by Schaefer et al. using focal-point thermochemical analysis method.[349] The MR-ccCA singlet-triplet ($^3B_2 \rightarrow X^1A_1$) energy gap has been computed to be 41.4 kcal mol^{-1} while the binding energy for $^3B_2$ state is predicted to be 251.5 kcal mol^{-1}.

Previous theoretical studies have found that the ground electronic state $^1A_1$ ([Core]$5b_2^2 7a_1^2 6b_2^2 2b_1^2 8a_1^2$) geometry for Si_2C is a bent equilibrium structure.[350-352] The optimized geometry at the CASPT2/cc-pVTZ level is bent with a Si-C bond length of 1.72 Å and symmetric stretch frequency of 829.6 cm^{-1}, in support of the experimental assignment of 839.5 cm^{-1} done by Presilla-Marques et al.[353] and confirmed by Rittby[352] using MP2/6-311g(2d), in contrast with the experimental assignment of 658.2 cm^{-1} by Kafafi et al.[354] The TAE for the ground state (X^1A_1) of Si_2C has been computed using MR-ccCA to be 249.3 kcal mol^{-1}. The MR-ccCA value is consistent with an experimental value of 256.1±6 and a previous theoretical value of 252.4 kcal mol^{-1} determined using the G2 composite method.[348] However, since the referenced experimental value (the only experimental value we found) has very large uncertainties and the G2 method is relatively less sophisticated than MR-ccCA, our current prediction should be considered the best available TAE result. We also report $\Delta_f H^o_{298}$ for the X^1A_1 state as 139.5 kcal mol^{-1}. The MR-ccCA predicted adiabatic singlet-triplet ($^3B_2 \rightarrow X^1A_1$) value of 46.4 kcal mol^{-1} is not consistent with the vertical excitation energies of 65.0, 66.4 and 74.3 kcal mol^{-1} of Spielfiedel et al.[300] obtained by using different C-Si bond lengths and Si-C-Si angles to construct MRCI derived potential energy functions with [$11s7p2d1f/_{Si}$; $9s6p2d1f/_C$] contracted basis sets. Considering the well-documented size-inconsistency problems of truncated CI methods[18,355,356] and the relatively smaller size of the basis sets utilized compared

with those utilized within MR-ccCA, we believe that MR-ccCA is more accurate than that of the MRCI calculations by Spielfiedel et al.[300]

6.3.4.3 SiN_2 and Si_2N

Theoretical studies (including CCSD(T) and MRCI calculations) and experimental studies have agreed on the linear geometry for the ground $X^3\Sigma^-$ state of diazasilene (SiN_2).[357-360] However, there have been disagreements on the assignments of the experimental fundamental frequencies (ν_i) and theoretical harmonic frequencies (ω_i) using different correlated methods. The N-N stretching fundamental frequency of 1731 cm^{-1} assigned by Lembke et al.[358] has been questioned by Ornellas et al.[360] who predicted the harmonic frequency to be very close to 1830 cm^{-1} using CCSD(T)/cc-pVQZ. Our CASPT2/cc-pVTZ harmonic stretching frequency of 1753 cm^{-1} is in agreement with the assignment of Lembke et al.[358] and more recent experimental results of 1755cm^{-1} by Maier et al.[361] (2000) and 1754.5 cm^{-1} of Amicangelo et al. (2008).[359]. Curiously, our result does not agree with ω=2024 cm^{-1} obtained using *ic*MRCI/cc-pVTZ.[360] This is however not surprising since the *ic*MRCI bond length of 1.125 Å is shorter than 1.15 Å obtained in this study (a value corroborated by the 1.142 Å and 1.135 Å obtained by Ornellas et al. using CCSD(T) with 6-311G* and cc-pVQZ basis sets, respectively) and also, as mentioned above, truncated CI methods may suffer from size consistency errors. The MR-ccCA predicted TAE and $\Delta_f H^o_{298}$ for the ground state of SiN_2 are 232.7 and 101.2 kcal mol^{-1} respectively. No previous theoretical or experimental values have been found for comparison. The singlet-triplet ($a^1A_1 \rightarrow X^3\Sigma^-$) energy gap has also been computed to be 1.7 kcal mol^{-1}, indicating that the bent singlet excited state may also be found at slightly higher temperature.

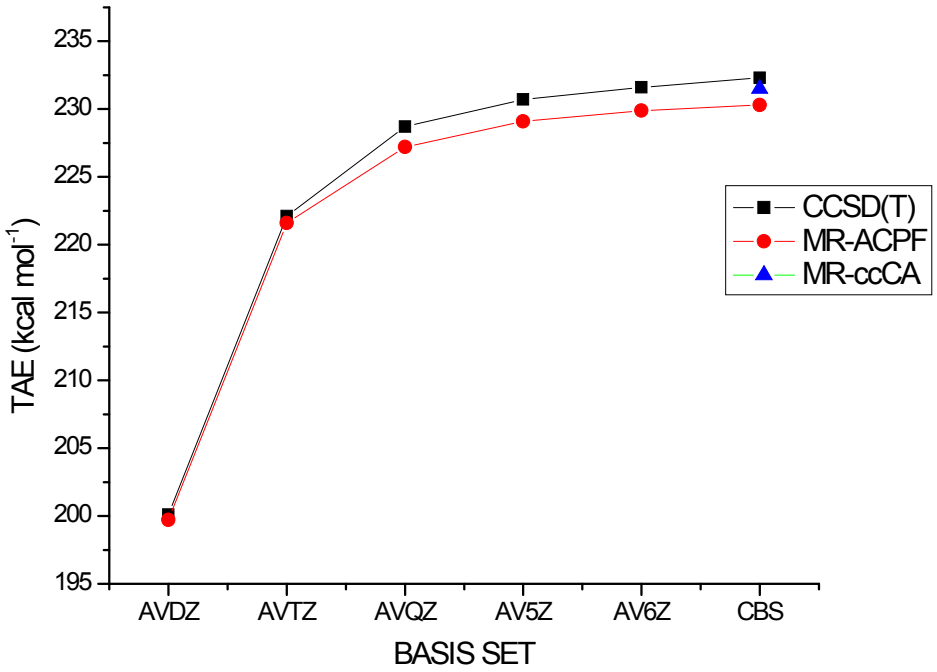

Figure 6.2 CBS limit for the total atomization energy of the Si_2N radical.

The two experimental values in the literature for the TAE of the ground $X^2\Pi$ state of Si_2N are 236±10 and 241.1±3.0 kcal mol^{-1} determined by Zmbov et al. (1967)[362] and Viswanathan et al. (1995),[303] respectively. The MR-ccCA predicted TAE value of 231.5 kcal mol^{-1} for the linear centrosymmetric structure of $X^2\Pi$ state, however, is only consistent with the result of Zmbov et al. while it is in greater disagreement with the data of Viswanathan et al. Since we found no other theoretical results for comparison, we utilized MR-ACPF/aug-cc-pVnZ and UCCSD(T)/aug-cc-pVnZ (n=Q, 5, 6) methods (Figure 6.2) to compute the TAE for Si_2N using CASPT2/cc-pVTZ and UCCSD(T)/cc-pV(Q+d)Z optimized geometries respectively. Table 6.7 shows the results obtained using UCCSD(T) and MR-ACPF methods. The computed TAE values for CCSD(T)/CBS and MR-ACPF/CBS, including core-valence and scalar relativistic corrections, of 233.4 and 231.3

kcal mol^{-1} are observed to also be consistent with the MR-ccCA and Zmbov et al. results. Our best predicted value of 231.6±1.0 kcal mol^{-1}, computed from the mean and standard deviation of MR-ccCA, UCCSD(T)/CBS and MR-ACPF/CBS values, can thus be taken as the final theoretical prediction with an estimate of the error in the methods used for calculating the atomization energy of the ground state for Si_2N. The MR-ccCA predicted $\Delta_f H^o_{298}$ value of 99.3 kcal mol^{-1} for the ground state of Si_2N is, unsurprisingly, in disagreement with the 85.0±3.5 kcal mol^{-1} estimated by Viswanathan et al. due to the differing values for TAE and atomic $\Delta_f H^o_{298}$ highlighted earlier.

6.3.4.4 $SiAl_2$ and Si_2Al

The existence of $SiAl_2$ has been confirmed by Gizenko et al. during high temperature calorimetry of Al-Si melts.[363] The T_1, D_1 and $C_0{}^2$ diagnostics for the ground X^1A_1 state of $SiAl_2$ are 0.040, 0.084 and 0.730 respectively, indicating the high importance of non-dynamic correlation in the reference wavefunction. The optimized geometry is almost cyclic with <AlSiAl=63.9^o and Si-Al bond length of 2.39 Å, 0.04 Å shorter than the diatomic. The TAE and $\Delta_f H^o_{298}$ for X^1A_1 state of $SiAl_2$ are predicted to be 115.3 and 157.5 kcal mol^{-1} (Table 6.5) respectively. No previous theoretical or experimental values have been found for comparison. The $a^3B_2 \rightarrow X^1A_1$ transition energy has been computed to be 3.4 kcal mol^{-1} while the binding energy among the constituent atoms at the a^3B_2 state is predicted to be 111.9 kcal mol^{-1}, about 3.4 kcal mol^{-1} weaker than for the ground state.

The ground electronic state for Si_2Al exhibits significant multireference character as shown in Table 6.1. The Si-Si bond length for the quasi-cyclic optimized geometry of the ground

X^2A_1 state is 2.21 Å, comparable to the 2.17 Å of disilene,[279] indicating double bond character. We report the binding energy and $\Delta_f H^o_{298}$ for the X^2A_1 state as 124.7 and 175.6 kcal mol^{-1}, respectively. The MR-ccCA value for $a^4B_2 \rightarrow X^2A_1$ energy separation has been computed to be 12.6 kcal mol^{-1}.

6.3.4.5 SiP_2 and Si_2P

Previous theoretical studies on SiP_2 and Si_2P have been focused mostly on the geometries and relative stabilities of their isomers.[364-366] We predict the TAE for the ground X^1A_1 ([Core]$8a_1^2 6b_2^2 9a_1^2 10a_1^2 3b_1^2 11a_1^2 7b_2^2$) and X^2A_1 ([Core]$8a_1^2 9a_1^2 6b_2^2 10a_1^2 3b_1^2 7b_2^2 11a_1^1$) states of SiP_2 and Si_2P as 188.1 and 182.6 kcal mol^{-1} (Table 6.5) respectively. The corresponding $\Delta_f H^o_{298}$ for SiP_2 and Si_2P have also been calculated as 71.2 and 110.9 kcal mol^{-1} respectively. The MR-ccCA computed $^3A'' \rightarrow X^1A_1$ and $^4A_2 \rightarrow X^2A_1$ energy separation for SiP_2 and Si_2P are 34.9 and 45.3 kcal mol^{-1}, respectively.

6.4 Conclusions

MR-ccCA is a versatile method, capable of predicting quantitative thermochemical and spectroscopic properties of silicon-containing and similar compounds with or without significant non-dynamical correlation effects in their reference wavefunctions. MR-ccCA has thus been utilized to predict the total atomization energies, enthalpies of formation, and spin-forbidden energy transitions for silicon hydrides and small clusters of silicon mixed with group 13 and 15 elements (e.g., Si_nP_m and Si_nAl_m; n+m=3) with no known previous theoretical and experimental values. Three diagnostics – T_1, D_1 and C_0^2 – have been utilized to provide insight

into the multi-configurational characteristics of the wavefunctions of the compounds studied. Of the twenty silicon-containing species studied in this work, the three compounds in their electronic ground states, with the most multireference characters with each possessing T_1>0.05, D_1>0.10 and C_0^2<0.90, are NSi, Si_2Al and SiB_2. Chemically accurate predictions of the energetic properties of these types of species can only be achieved using a multi-configurational method like MR-ccCA.

The lowest and highest adiabatic transition energies of the silicon compounds studied are predicted to occur in the near infrared and ultra-violet regions of the electromagnetic spectrum for the triatomic heteronuclear compounds N_2Si ($1.8x10^{13}$ Hz) and Si_2N ($7.8x10^{14}$ Hz), respectively.

Table 6.1 CASPT2/cc-pVTZ optimized geometries for ground and lowest-lying spin-forbidden excited states (distances in angstroms and angles in degrees)[a].

	Ground State					Excited State				
	Sym	Optimized parameters	T_1	D_1	C_0^2	Sym	Optimized parameters	T_1	D_1	C_0^2
CH	$C_{\infty v}$	CH = 1.12	0.008	0.017	0.954	$C_{\infty v}$	CH = 1.09	0.018	0.038	0.968
CC	$D_{\infty h}$	CC = 1.25	0.039	0.087	0.705	$D_{\infty h}$	CC = 1.32	0.020	0.040	0.875
CCH	$C_{\infty v}$	CC = 1.22, CH = 1.07, ∠CCH =180.0	0.016	0.030	0.885	C_s	CC = 1.46, CH = 1.11, ∠ CCH =113.3	0.019	0.040	0.894
$(H_{2a})C_aC_bH_b$	C_s	C_aC_b = 1.32, C_aH_a=1.09, C_bH_b =1.08 $\angle H_aC_aC_b$ = 121.4, $\angle H_bC_bC_a$ = 137.2	0.016	0.036	0.906	C_s	C_aC_b =1.50, C_aH_a=1.09, C_bH_b = 1.09 $\angle H_aC_aC_b$ =118.3, $\angle H_bC_bC_a$ = 126.6	0.011	0.012	0.949
CCC	$D_{\infty h}$	CC = 1.31 ∠CCC = 180.0	0.024	0.054	0.841	C_{2v}	CC = 1.38 ∠CCC = 60.0	0.012	0.030	0.876
SiH	$C_{\infty v}$	SiH = 1.53	0.017	0.023	0.955	$C_{\infty v}$	SiH = 1.50	0.035	0.071	0.969
SiSi	$C_{\infty v}$	SiSi = 2.18	0.023	0.039	0.922	$C_{\infty v}$	SiSi = 2.31	0.034	0.053	0.864
CSiC	C_{2v}	SiC = 1.85 ∠CSiC = 40.6	0.021	0.055	0.871	C_{2v}	SiC = 1.91 ∠CSiC = 40.7	0.072	0.219	0.841
SiCSi	C_{2v}	SiC = 1.72 ∠SiCSi = 113.4	0.020	0.040	0.867	C_{2v}	SiC = 1.82 ∠SiCSi = 78.7	0.041	0.098	0.824
SiHSi	C_{2v}	SiSi = 2.17, SiH = 1.68 ∠ SiHSi = 49.9	0.027	0.057	0.889	C_s	SiSi = 2.34, SiH = 1.53 ∠SiHSi = 106.2	0.048	0.116	0.895
$Si(H_2)Si$ $H_2Si_aSi_b$	C_{2v}	SiSi = 2.24, SiH = 1.68 ∠SiHSi = 83.71, ∠HSiH = 73.0	0.018	0.035	0.908	C_{2v}	Si_aSi_b = 2.29, Si_aH = 1.50 $\angle His_aSi_b$ = 127.0, $\angle His_aH$ =106.0	0.015	0.028	0.924
$(H_{2a})Si_aH_bSi_b$	C_s	Si_aSi_b = 2.26, Si_aH_a = 1.49, Si_aH_b = 1.63, Si_bH_b = 1.82 $\angle H_aSi_aSi_b$ = 125.5, $\angle Si_aSi_bH_b$ = 45.7, $\angle H_aSi_aH_a$ = 107.21 $\angle H_aSi_aH_b$ = 104.59	0.016	0.030	0.913	C_s	Si_aSi_b = 2.33, Si_aH_a = 1.50, Si_aH_b = 3.38, Si_bH_b = 1.50 $\angle H_aSi_aSi_b$ = 114.6, $\angle Si_aSi_bH_b$ = 122.8, $\angle H_aSi_aH_a$ = 108.8 $\angle H_aSi_aH_b$ = 103.6	0.021	0.040	0.939
SiC	$C_{\infty v}$	SiC = 1.71	0.046	0.102	0.759	$C_{\infty v}$	SiC = 1.67	0.074	0.171	0.855
SiAl	$C_{\infty v}$	SiAl = 2.43	0.036	0.067	0.892	$C_{\infty v}$	SiAl = 2.42	0.044	0.074	0.678
AlSiAl	C_{2v}	SiAl = 2.39, ∠AlSiAl = 63.9	0.040	0.084	0.730	C_{2v}	SiAl = 2.36, ∠AlSiAl = 73.6	0.023	0.035	0.834
SiAlSi	C_{2v}	SiAl = 2.48, ∠SiAlSi = 52.8	0.055	0.162	0.830	C_{2v}	SiAl = 2.48, ∠SiAlSi = 54.6	0.022	0.039	0.841
SiB	$C_{\infty v}$	SiB = 1.93	0.036	0.076	0.895	$C_{\infty v}$	SiB = 1.85	0.034	0.076	0.802
BSiB	C_{2v}	SiB = 1.92, ∠BSiB = 47.4	0.064	0.192	0.759	C_{2v}	SiB = 1.93, ∠BSiB = 48.5	0.023	0.045	0.795
SiBSi	C_{2v}	SiB = 1.88, ∠SiBSi = 80.9	0.029	0.062	0.808	C_{2v}	SiB = 2.01, ∠SiBSi = 68.1	0.033	0.075	0.771
SiN	C_{∞}	SiN = 1.66	0.060	0.141	0.855	C_{2v}	SiN = 1.76	0.060	0.148	0.934
SiNN	$C_{\infty v}$	SiN = 1.77, NN = 1.15, ∠SiNN = 180.0	0.022	0.046	0.888	C_{2v}	SiN = 1.86, ∠NSiN = 39.3	0.023	0.070	0.877
SiNSi	$D_{\infty h}$	SiN = 1.65, ∠SiNSi = 180.0	0.006	0.011	0.892	$D_{\infty h}$	SiN = 1.60, ∠SiNSi = 180.0	0.001	0.001	0.890
SiP	C_{2v}	SiP = 2.10	0.034	0.060	0.903	C_{2v}	SiP = 2.19	0.029	0.078	0.942
PSiP	C_{2v}	SiP = 2.25, ∠PSiP = 55.3	0.018	0.037	0.871	C_s	SiP = 2.16, SiP = 2.53, ∠PSiP = 52.8	0.039	0.107	0.854
SiPSi	C_{2v}	SiP = 2.19, ∠SiPSi = 68.3	0.022	0.047	0.872	C_{2v}	SiP = 2.31, ∠SiPSi = 57.7	0.022	0.052	0.827
SiSiSi	C_{2v}	SiSi = 2.21, ∠SiSiSi = 79.7	0.032	0.082	0.822	C_{2v}	SiSi = 2.31, ∠SiSiSi = 60.0	0.031	0.082	0.843

[a]A molecule is considered to have significant multireference character when T_1>0.02, D_1>0.05 and C_0^2<0.90.

Table 6.2 Total atomization energies (TAE) and enthalpies of formation ($\Delta_f H^o_{298}$) for carbon and silicon hydrides (in kcal mol^{-1}).

	MR-ccCA		Experimental		Other theory	
	TAE	$\Delta_f H^o_{298}$	TAE	$\Delta_f H^o_{298}$	TAE	$\Delta_f H^o_{298}$
CH ($^2\Pi$)	79.9	142.5	79.9[a]	142.8[b], 142.0[c]	80.0[a]	143.2[b]
CH ($^4\Sigma$)	61.5	160.9	-	-	-	-
C_2H ($^2\Sigma$)	255.0	137.6	257.5[d]	114.0[c], 135.8±1.4[e]	255.3[d]	136.0[b], 141.0[d]
C_2H ($^4A'$)	161.9	230.6	-	-	-	-
C_2H_3 ($^2A'$)	421.1	72.8	422.2[d]	72.1[c], 71.6±0.8[f]	421.3[d]	72.7[f]
C_2H_3 ($^4A''$)	345.4	148.5	-	-	-	-
SiH ($^2\Pi$)	70.4	90.5	68.7±0.7[g]	90.0[c]	69.2[h]	-
SiH ($^4\Sigma$)	29.2	131.7	-	-	-	-
Si_2H ($^2A_1$)	147.1	122.5	-	-	-	-
Si_2H ($^4A''$)	119.9	149.9	-	-	-	-
Si_2H_2 ($^1A_1$)	222.8	96.6	-	<99.7[i]	223.4[j]	97.2[j]
Si_2H_2 ($^3A_2$)	199.2	121.5	-	-	-	-
Si_2H_3 ($^2A''$)	271.3	99.9	-	-	-	-
Si_2H_3 ($^4A'$)	242.2	129.3	-	-	-	-

[a]Ref. 153; [b]Ref.325; [c]Ref. 244; [d]Ref. 326; [e]Ref. 324; [f]Ref. 330; [g]Ref.228; [h]Ref. 319; [i]Ref. 285; [j]Ref. 328;

Table 6.3 TAE and $\Delta_f H^o_{298}$ (kcal mol^{-1}) for small homogeneous clusters of carbon and silicon

	MR-ccCA		Experimental		Other theory	
	TAE	$\Delta_f H^o_{298}$	TAE	$\Delta_f H^o_{298}$	TAE	$\Delta_f H^o_{298}$
C_2 ($^1\Sigma$)	142.4	199.1	144.6±1.9[a]	200.2[a]	143.9[a]	-
C_2 ($^3\Pi$)	141.5	200.0	-	-	142.6[a]	-
C_3 ($^1\Sigma$)	314.7	196.6	311.4±3.1[a]	196.0[b]	315.8[a], 316.9[a]	-
C_3 ($^3B_1$)	294.4	217.2	-	-	-	-
Si_2 ($^3\Sigma$)	73.1	145.6	76.2±1.7[c], 74.0[e]	141.0[c]	74.4±0.4[d], 73.3±0.2[f]	-
Si_2 ($^1\Delta$)	63.6	155.0	-	-	-	-
Si_3 ($^1A_1$)	169.7	158.0	168.5±3.8[c]	156.1±3.8[c]	-	-
Si_3 ($^3B_2$)	169.4	158.3	-	-	-	-

[a]Ref. 335; [b]Ref.244; [c]Ref. 304; [d]Ref. 331; [e]Ref. 241; [f]Ref. 332;

Table 6.4 TAE and $\Delta_f H^o_{298}$ (kcal mol^{-1}) for diatomics of silicon SiX (X=B, C, N, Al, P).

	MR-ccCA		Experimental		Other theory	
	TAE	$\Delta_f H^o_{298}$	TAE	$\Delta_f H^o_{298}$	TAE	$\Delta_f H^o_{298}$
SiC ($^3\Pi$)	100.0	180.1	-	-	-	-
SiC ($^1\Sigma$)	85.0	195.0	-	-	-	-
SiAl ($^4\Sigma$)	57.1	134.2	-	-	58.3[a]	-
SiAl ($^2\Sigma$)	40.3	151.0	-	-	-	-
SiB ($^4\Sigma$)	74.3	172.3	74.6±2.8[b]	166.8±3.3[b]	-	-
SiB ($^2\Pi$)	57.9	188.7	-	-	-	-
SiP ($^2\Pi$)	84.0	100.5	-	-	-	-
SiP ($^4\Sigma$)	38.3	146.2	-	-	-	-
SiN ($^2\Sigma$)	103.3	118.5	-	-	-	-
SiN ($^4\Sigma$)	40.8	181.1	-	-	39.7[c]	-

[a]*Ref. 346;* [b]*Ref. 341;* [c]*Ref. 344;*

Table 6.5 TAE and $\Delta_f H^o_{298}$ (kcal mol^{-1}) for triatomics of silicon Si_nX_m (X=B, C, N, Al, P and n+m=3).

	MR-ccCA		Experimental		Other theory	
	TAE	$\Delta_f H^o_{298}$	TAE	$\Delta_f H^o_{298}$	TAE	$\Delta_f H^o_{298}$
SiB_2 ($^1A_1$)	191.4	192.0	-	-	-	195.3[a]
SiB_2 ($^3A_1$)	172.7	210.8	-	-	-	-
Si_2B ($^2B_2$)	181.8	173.6	183.3±4.3[b]	164.4±4.7[b]	-	-
Si_2B ($^4B_2$)	157.2	198.2	-	-	-	-
$SiAl_2$ ($^1A_1$)	115.3	157.5	-	-	-	-
$SiAl_2$ ($^3B_2$)	111.9	161.0	-	-	-	-
Si_2Al ($^2A_1$)	124.7	175.6	-	-	-	-
Si_2Al ($^4B_2$)	112.7	187.9	-	-	-	-
SiC_2 ($^1A_1$)	293.1	157.3	301.0±7[c]	-	294.7[c]	-
SiC_2 ($^3B_2$)	251.5	198.8	-	-	-	-
Si_2C ($^1A_1$)	249.3	139.5	256.1±6[c]	-	252.4[c]	-
Si_2C ($^3B_2$)	202.7	186.1	-	-	-	-
SiN_2 ($^3\Sigma$)	232.7	101.2	-	-	-	-
SiN_2 ($^1A_1$)	232.0	101.7	-	-	-	-
Si_2N ($^2\Pi$)	231.5	99.3	236±10[d], 241.1±3.0[e]	85.0±3.5[e]	-	-
Si_2N ($^4\Sigma$)	143.8	184.8	-	-	-	-
SiP_2 ($^1A_1$)	188.1	71.2	-	-	-	-
SiP_2 ($^3A''$)	153.0	106.5	-	-	-	-
Si_2P ($^2A_1$)	182.6	110.9	-	-	-	-
Si_2P ($^4A_2$)	136.7	156.6	-	-	-	-

[a]*Ref. 347;* [b]*Ref. 341;* [c]*Ref. 348;* [d]*Ref. 362;* [e]*Ref. 303;*

Table 6.6 Transition energies between ground and lowest-lying spin-forbidden excited states (kcal mol^{-1}).

	MR-ccCA	Experimental	Previous Calc.
CH ($^2\Pi$ - $^4\Sigma$)	17.6	17.1±0.2[a]	17.2[b]
C_2H ($^2\Sigma$ - $^4A'$)	93.3	-	-[c]
C_2H_3 ($^2A'$ - $^4A''$)	77.2	-	-[c]
SiH ($^2\Pi$ - $^4\Sigma$)	40.9	-	38.8[b]
Si_2H ($^2A_1$ - $^4A''$)	26.5	-	25.4[c]
Si_2H_2 ($^1A_1$ - $^3A_2$)	23.4	-	-
Si_2H_3 ($^2A''$ - $^4A'$)	25.9	-	-
C_2 ($^1\Sigma$ - $^3\Pi$)	1.3	2.1[d]	-
C_3 ($^1\Pi$ – $^3B_1$)	21.0	-	-
Si_2 ($^3\Sigma$ - $^1\Delta$)	9.9	10.0[e]	11.7[f]
Si_3 ($^1A_1$ - $^3B_{2)}$	0.2	-	-
SiC ($^3\Pi$ - $^1\Sigma$)	14.9	-	14.3[f]
SiAl ($^4\Sigma$ - $^2\Sigma$)	16.1	-	16.7[g]
SiB ($^4\Sigma$ - $^2\Pi$)	16.6	-	16.9[h]
SiP ($^2\Pi$ - $^4\Sigma$)	44.4	-	44.1[i]
SiN ($^2\Sigma$ - $^4\Sigma$)	59.7	-	63.5[j], 53.0[k]
SiB_2 ($^1A_1$ - $^3A_1$)	18.7	-	10.2[l], 13.6[l]
Si_2B ($^2B_2$ - $^4B_2$)	25.7	-	-
$SiAl_2$ ($^1A_1$ - $^3B_2$)	3.4	-	-
Si_2Al ($^2A_1$ - $^4B_2$)	12.6	-	-
SiC_2 ($^1A_1$ - $^3B_2$)	41.4	-	-
Si_2C ($^1A_1$ - $^3B_2$)	46.4	-	-
SiN_2 ($^3\Sigma$ - $^1A_1$)	1.7	-	-
Si_2N ($^2\Pi$ - $^4\Sigma$)	74.4	-	-
SiP_2 ($^1A_1$ - $^3A''$)	34.9	-	34.5[m]
Si_2P ($^2A_1$ - $^4A_2$)	45.3	-	48.0[m]

[a]Ref. 322; [b]Ref. 320; [c]Ref. 380; [d]Ref. 336; [e]Ref. 333; [f]Ref. 334 [g]Ref. 346; [h]Ref. 342; [i]Ref. 381; [j]Ref. 344; [k]Ref. 345; [l]Ref. 347; [m]Ref. 365;

Table 6.7 TAE (kcal mol^{-1}) for the $X^2\Pi$ ground state of Si_2N[a].

	UCCSD(T)[b]	MR-ACPF[c]
aug-cc-pV(Q+d)Z	228.7	227.2
aug-cc-pV(5+d)Z	230.7	229.1
aug-cc-pV(6+d)Z	231.5	229.9
CBS(Q56_P)	232.3	230.3
CBS(Q5_S4)	232.7	230.6
CBS(56_S4)	232.8	230.7
Core-Valence[d]	1.3	1.3
Scalar Relativistic[e]	-0.5	-0.5

[a]Tight d-function are only included in the silicon basis set. [b]UCCSD(T)/cc-pVQZ method was used to optimized the geometry. [c]CASPT2/cc-pVTZ method was used to optimized the geometry. [d]Corve-valance effects are computed at UCCSD(T)/aug-cc-pCVTZ and CASPT2/aug-cc-pCVTZ levels. [e]Scalar relativistic effects are computed using UCCSD(T)-DK/cc-pVTZ-DK and CASPT2-DK/cc-pVTZ-DK methods.

Table 6.8 Relative energies of different conformers using MR-ccCA method.

	Isomer	ΔE(kcal mol^{-1})
Si_2H	SiHSi (C_{2v}) $^2A_1$	0.0
	SiSiH ($C_{\infty v}$) $^2\Pi$	32.8
Si_2H_2	Si(H_2)Si (C_{2v}) $^1A_1$	0.0
	HSiSiH (C_{2h}) ^1A_g	18.1
Si_2H_3	H_2SiHSi (C_s) $^2A''$	0.0
	H_2SiSiH (C_s) $^2A''$	0.7
	HSiHSiH (trans) (C_2) ^2A	3.1
	HSiHSiH (cis) (C_1) ^2A	
Si_2B	SiBSi (C_{2v}) $^2B_1$	0.0
	SiBSi ($D_{\infty h}$) $^2\Pi$	18.4
SiN_2	SiNN ($C_{\infty v}$) $^3\Sigma$	0.0
	NSiN ($D_{\infty h}$) $^3\Sigma$	80.9
Si_2N	SiNSi ($D_{\infty h}$) $^2\Pi$	0.0
	SiNSi (C_{2v}) $^2A_1$	5.7
Si_2P	SiPSi (C_{2v}) $^2A_1$	0.0
	SiPSi (C_s) $^2A''$	35.3
	SiSiP ($C_{\infty v}$) $^2\Pi$	44.0

Table 6.9 Atomic enthalpies of formation at 298 K.

Element	$\Delta_f H^o_{298}$ (kcal mol^{-1})
H	50.62
B	136.3
C	169.73
N	111.49
Al	80.8
P	108.2

CHAPTER 7

CONCLUDING REMARKS AND FUTURE OUTLOOK

In this dissertation, studies concerning the development and applications of the single reference ab initio composite method, the correlation consistent composite approach (ccCA) and the multi-reference correlation consistent composite approach (MR-ccCA) have been presented. It has been shown that the ccCA method for lighter main group compounds, its multi-reference equivalent (MR-ccCA method), and the single reference variant for heavier main group and transition metal compounds, the relativistic pseudopotential ccCA (rp-ccCA) method, can be used as an effective predictive tool due to their demonstrated quantitative accuracies. The hybrid of rp-ccCA and density functional theory within ONIOM framework (rp-ccCA-ONIOM) has also been shown to have comparable accuracy to the CCSD(T)/CBS method at a fraction of the computational cost for applications to larger systems.

In the comparative study of the performances of the ccCA, G3, and G3(MP2) composite methods in the accurate prediction of the enthalpies of formation for forty energetic nitrogen-containing species, the ccCA method resulted in the lowest mean absolute deviation and was subsequently utilized to predict the property for five endothermic tetrazine-based compounds with potential applications as insensitive high explosives. The efficient rp-ccCA-ONIOM method was thereafter used to predict the oxidative addition of the β-O-4 substructure of lignin to nickel, copper, palladium and platinum atoms. The reaction involving platinum atom was predicted to be more favorable due to its high endothermicity and low activation barrier.

The last two studies attest to the capability of the MR-ccCA method in the quantitative prediction of chemical processes that may require multi-configurational wavefunctions in their

reference states. The thermochemical and spectroscopic properties of unsaturated compounds, small diradicals and silicon-containing species were investigated and compared to available well-established experimental values. MR-ccCA was shown to be chemically accurate and versatile in the prediction of energetic properties for systems with and without significant contributions from non-dynamic correlation effects.

Like any scientific undertaking, the research described in this dissertation has generated myriads of questions ranging from applications to methodology. Apparently, there remains much to do to improve the performance and applicability of a computational method like MR-ccCA. One of the most important questions about the current formulation of MR-ccCA is the high costs associated with its usage for large molecular systems. A possible approach to lowering the costs involves the combination of MR-ccCA with DFT method in QM/QM manner, like the rp-ccCA-ONIOM method described above, for proper treatment of localized strong correlation in a large system. A difference course is to utilize a Cholesky decomposition of the two-electron integrals in the CASSCF wavefunction to facilitate the use of larger active space than presently obtainable. Other approaches to explore include the use of restricted active space SCF reference wavefunction and complete active space-DFT method.

In conclusion, a leading theme of this investigation has been the combination of quantum mechanical methodologies in such way that their cooperative strengths could be used to accurately predict chemical properties. Cognizance of possible accumulation of the weaknesses of the constituent methods has been taken by performing extensive validation and testing against reliable, well-established experimental observations. The ccCA series of

methods, most particularly the MR-ccCA, have thus been demonstrated to be very promising at quantitative prediction of energetic properties of chemical systems.

REFERENCES

(1) Andersson, K.; Malmqvist, P. A.; Roos, B. O.; Sadlej, A. J.; Wolinski, K. *J. Phys. Chem.* **1990**, *94*, 5483.

(2) Andersson, K.; Malmqvist, P. A.; Roos, B. O. *J. Chem. Phys.* **1992**, *96*, 1218.

(3) Langhoff, S. R.; Davidson, E. R. *Int. J. Quantum Chem.* **1974**, *8*, 61.

(4) Gdanitz, R. J.; Ahlrichs, R. *Chem. Phys. Lett.* **1988**, *143*, 413.

(5) Schrödinger, E. *Ann. Phys.* **1926**, *384*, 361.

(6) Schrödinger, E. *Ann. Phys.* **1926**, *384*, 489.

(7) Schrödinger, E. *Ann. Phys.* **1926**, *385*, 437.

(8) Schrödinger, E. *Ann. Phys.* **1926**, *386*, 109.

(9) Born, M.; Oppenheimer, R. *Ann. Phys.* **1927**, *389*, 457.

(10) Butler, L. J. *Annu. Rev. Phys. Chem.* **1998**, *49*, 125.

(11) Kutzelnigg, W. *Int. J. Quantum Chem.* **1994**, *51*, 447.

(12) Hartree, D. R. *Proc. Camb. Phil. Soc.* **1928**, *24*, 89.

(13) Hartree, D. R. *Proc. Camb. Phil. Soc.* **1928**, *24*, 111.

(14) Hartree, D. R. *Proc. Camb. Phil. Soc.* **1928**, *24*, 426.

(15) Pauli, W. *Z. Phys.* **1925**, *31*, 765.

(16) Pauli, W. "Exclusion principle and quantum mechanics." In *(Nobel Prize Lecture)* Geneva, Switzerland, **1945**.

(17) Slater, J. C. *Phys. Rev.* **1929**, *34*, 1293.

(18) Szabo, A.; Ostlund, N. S. *Modern Quantum Chemistry: Introduction to Advanced Electronic Structure Theory*; McGraw-Hill, Inc.: New York, NY, **1989**.

(19) Jensen, F. *Introduction to Computational Chemistry*; John Wiley & Sons Ltd.: Chichester, West Sussex, **2007**; Vol. 2nd Edition.

(20) Fock, V. *Z. Phys. A* **1930**, *61*, 126.

(21) Roothaan, C. C. J. *Rev. Mod. Phys.* **1951**, *23*, 69.

(22) Hall, G. G. *Proc. R. Soc. A* **1951**, *208*, 328.

(23) Koopmans, T. A. *Physica* **1933**, *1*, 104.

(24) Johnson, B. G.; Gill, P. M. W.; Pople, J. A. *J. Chem. Phys.* **1992**, *97*, 7846.

(25) Mintz, B.; Williams, G. T.; Howard, L.; Wilson, A. K. *J. Chem. Phys.* **2009**, *130*, 234104.

(26) Fink, R.; Staemmler, V. *Theor. Chim. Acta* **1993**, *87*, 129.

(27) Bartlett, R. J. *Annu. Rev. Phys. Chem.* **1981**, *32*, 359.

(28) Møller, C.; Plesset, M. S. *Phys. Rev.* **1934**, *46*, 618.

(29) Paldus, J.; Li, X. "A Critical Assessment of Coupled Cluster Method in Quantum Chemistry." In *Advances in Chemical Physics*; Prigogine, I., Rice, S., Eds.; John Wiley and Sons, Inc., **1999**; Vol. 110; pp 1.

(30) Paldus, J. "Coupled Cluster Theory." In *Methods in Computational Molecular Physics*; Wilson, S., Diercksen, H. F., Eds.; Plenum Press: New York, NY, **1992**.

(31) Barlett, R. J.; Sekino, H.; Purvis III, G. D. *Chem. Phys. Lett.* **1983**, *98*, 66.

(32) Raghavachari, K.; Trucks, G. W.; Pople, J. A.; Head-Gordon, M. *Chem. Phys. Lett.* **1989**, *157*, 479.

(33) Gustavo, E. S.; Timothy, J. L. *J. Chem. Phys.* **1990**, *93*, 5851.

(34) Levine, I. N. *Quantum Chemistry*; Prentice Hall: Upper Saddle River, New Jersey, **2000**; Vol. 5th Edition.

(35) Slater, J. C. *Phys. Rev.* **1930**, *36*, 57.

(36) Boys, S. F. *Proc. R. Soc. A* **1950**, *200*, 542.

(37) Dunning, T. H., Jr., *J. Chem. Phys.* **1989**, *90*, 1007.

(38) Almlöf, J.; Taylor, P. R. *J. Chem. Phys.* **1987**, *86*, 4070.

(39) Almlöf, J.; Taylor, P. R. *J. Chem. Phys.* **1990**, *92*, 551.

(40) Dunning, T. H., Jr., *J. Phys. Chem. A* **2000**, *104*, 9062.

(41) Woon, D. E.; Dunning, T. H., Jr., *J. Chem. Phys.* **1995**, *103*, 4572.

(42) de Jong, W. A.; Harrison, R. J.; Dixon, D. A. *J. Chem. Phys.* **2001**, 114, 48.

(43) Kutzelnigg, W.; Morgan III, J. D., *J. Chem. Phys.* **1992**, *96*, 4484.

(44) Cheung, L. M.; Sundberg, K. R.; Ruedenberg, K. *J. Am. Chem. Soc.* **1978**, *100*, 8024.

(45) Ruedenberg, K.; Cheung L. M.; Elbeig S. T. *Int. J. Quantum Chem.* **1979**, *16*, 1069.

(46) Ruedenberg, K.; Schmidt, M. W.; Gilbert, M. M.; Elbert, S. T. *Chem. Phys.* **1982**, *71*, 41.

(47) Ruedenberg, K.; Schmidt, M. W.; Gilbert, M. M. *Chem. Phys.* **1982**, *71*, 51.

(48) Feller, D. F.; Schmidt, M. W.; Ruedenberg, K. *J. Am. Chem. Soc.* **1982**, *104*, 960.

(49) Ruedenberg, K.; Schmidt, M. W.; Gilbert, M. M.; Elbert, S. T. *Chem. Phys.* **1982**, *71*, 65.

(50) Roos, B. O. The Complete Active Space Self-Consistent Field Method and its Applications in Electronic Structure Calculations. In *Advances in Chemical Physics*; Lawley, K. P., Ed., 2007; pp 399.

(51) Schmidt, M. W.; Gordon, M. S. *Annu. Rev. Phys. Chem.* **1998**, *49*, 233.

(52) Pauncz, R. *The Symmetric Group in Quantum Chemistry. Boca Raton, FL; CRC* **1995**.

(53) Tait, T.; Edward, G. H.; Sherrill, C. D. *J. Chem. Phys.* **2008**, *128*, 124111.

(54) Kowalski, K. *J. Chem. Phys.* **2005**, *123*, 014102.

(55) Klein, R. A.; Zottola, M. A. *Chem. Phys. Lett.* **2006**, *419*, 254.

(56) Szalay, P. G.; Vazquez J.; Simmons C.; Stanton, J. F. *J. Chem. Phys.* **2004**, *121*, 7624.

(57) Bruna, P. J.; Peyerimhoff, S. D.; Buenker, R. J. *Chem. Phys. Lett.* **1980**, *72*, 278.

(58) Szalay, P. G.; Bartlett, R. J. *Chem. Phys. Lett.* **1993**, *214*, 481.

(59) Hohenberg, P.; Kohn, W. *Phys. Rev.* **1964**, *136*, B864.

(60) Kohn, W.; Sham, L. J. *Phys. Rev.* **1965**, *140*, A1133.

(61) Becke, A. D. *Phys. Rev. A* **1988**, *38*, 3098.

(62) Becke, A. D. *J. Chem. Phys.* **1993**, *98*, 5648.

(63) Lee, C.; Yang, W.; Parr, R. G. *Phys. Rev. B* **1988**, *37*, 785.

(64) Perdew, J. P.; Burke, K.; Ernzerhof, M. *Phys. Rev. Lett.* **1996**, *77*, 3865.

(65) Zhao, Y.; Truhlar, D. *Theor. Chim. Acta* **2008**, *120*, 215.

(66) Grimme, S. *J. Chem. Phys.* **2006**, *124*, 034108.

(67) Department of the Army Technical Manual, *Military Explosives*; Department of Army, (Ed.); Headquarters, Department of the Army: Washington D. C, **1990**.

(68) Military Explosives In Department of Army (Ed.) Technical Manual*, Military Explosives*; Washington, D.C., **1984**; Vol. TM 9-1300-214; pp 2.

(69) Agrawal, R. D. *Organic Chemistry of Explosives*; John Wiley & Sons Ltd: Chichester, **2007**.

(70) David , E. C.; Michael , A. H.; Darren , L. N. *Propellants, Explosives, Pyrotechnics* **2004**, *29*, 209.

(71) LoPresti, V. *Los Alamos Research Quarterly* **2003**.

(72) Pagoria, P. F.; Lee, G. S.; Mitchell, A. R.; Schmidt, R. D. *Thermochim. Acta* **2002**, *384*, 187.

(73) Muthurajan, H.; Sivabalan, R.; Talawar, M. B.; Anniyappan, M.; Venugopalan, S. *J. Hazard. Mater.* **2006**, *133*, 30.

(74) Byrd, E. F.; Rice, B. M. *J. Phys. Chem. A* **2006**, *110*, 1005.

(75) Martin, J. M. L.; Taylor, P. R. *J. Chem. Phys.* **1997**, *106*, 8620.

(76) Boese, A. D.; Oren, M.; Atasoylu, O.; Martin, J. M. L.; Kallay, M.; Gauss, J. *J. Chem. Phys.* **2004**, *120*, 4129.

(77) Karton, A.; Rabinovich, E.; Martin, J. M. L.; Ruscic, B. *J. Chem. Phys.* **2006**, *125*, 144108.

(78) Martin, J. M. L.; Oliveira, de G. *J. Chem. Phys.* **1999**, *111*, 1843.

(79) Parthiban, S.; Martin, J. M. L. *J. Chem. Phys.* **2001**, *114*, 6014.

(80) Bomble, Y. J.; Vazquez, J.; Kallay, M.; Michauk, C.; Szalay, P. G.; Csaszar, A. G.; Gauss, J.; Stanton, J. F. *J. Chem. Phys.* **2006**, *125*, 064108.

(81) Harding, M. E.; Vazquez, J.; Ruscic, B.; Wilson, A. K.; Gauss, J.; Stanton, J. F. *J. Chem. Phys.* **2008**, *128*, 15.

(82) Curtiss, L. A.; Raghavachari, K.; Redfern, P. C.; Pople, J. A. *J. Chem. Phys.* **1997**, *106*, 1063.

(83) Curtiss, L. A.; Raghavachari, K.; Redfern, P. C.; Pople, J. A. *J. Chem. Phys.* **2000**, *112*, 7374.

(84) Curtiss, L. A.; Raghavachari, K.; Trucks, G. W.; Pople, J. A. *J. Chem. Phys.* **1991**, *94*, 7221.

(85) Curtiss, L. A.; Redfern, P. C.; Raghavachari, K. *J. Chem. Phys.* **2005**, *123*, 124107.

(86) Curtiss, L. A.; Redfern, P. C.; Raghavachari, K.; Rassolov, V.; Pople, J. A. *J. Chem. Phys.* **1999**, *110*, 4703.

(87) Pople, J. A.; Head-Gordon, M.; Fox, D. J.; Raghavachari, K.; Curtiss, L. A. *J. Chem. Phys.* **1989**, *90*, 5622.

(88) Raghavachari, K.; Curtiss, L. A.; Clifford, E. D.; Gernot, F.; Kwang, S. K.; Gustavo, E. S. G2, G3 and Associated Quantum Chemical Models for Accurate Theoretical Thermochemistry. In *Theory and Applications of Computational Chemistry*; Elsevier: Amsterdam, 2005; pp 785.

(89) DeYonker, N. J.; Cundari, T. R.; Wilson, A. K. *J. Chem. Phys.* **2006**, *124*, 114104.

(90) DeYonker, N. J.; Grimes, T.; Yockel, S.; Dinescu, A.; Mintz, B.; Cundari, T. R.; Wilson, A. K. *J. Chem. Phys.* **2006**, *125*, 104111.

(91) DeYonker, N. J.; Williams, T. G.; Imel, A. E.; Cundari, T. R.; Wilson, A. K. *J. Chem. Phys.* **2009**, *131*, 024106.

(92) DeYonker, N. J.; Wilson, B. R.; Pierpont, A. W.; Cundari, T. R.; Wilson, A. K. *Mol. Phys.* **2009**, *107*, 1107.

(93) DeYonker, N. J.; Ho, D. S.; Wilson, A. K.; Cundari, T. R. *J. Phys. Chem. A* **2007**, *111*, 10776.

(94) Deyonker, N. J.; Peterson, K. A.; Steyl, G.; Wilson, A. K.; Cundari, T. R. *J. Phys. Chem. A* **2007**, *111*, 11269.

(95) Wilson, A. K.; van Mourik, T.; Dunning, T. H., Jr., *J. Mol. Struct. (THEOCHEM)* **1996**, *388*, 339.

(96) Peterson, K. A.; Dunning, T. H., Jr., *J. Chem. Phys.* **2002**, *117*, 10548.

(97) Kiselev, V. G.; Gritsan, N. P. *J. Phys. Chem. A* **2008**, *112*, 4458.

(98) Curtiss, L. A.; Redfern, P. C.; Raghavachari, K.; Pople, J. A. *Chem. Phys. Lett.* **1999**, *313*, 600.

(99) Mebel, A. M.; Morokuma, K.; Lin, M. C. *J. Chem. Phys.* **1995**, *103*, 7414.

(100) Lee, K. Y.; Storm, C. B.; Hiskey, M. A.; Coburn, M. D. *J. Energ. Mat.* **1991**, *9*, 415.

(101) Zhao, Y.; Truhlar, D. G. *J. Phys. Chem. A* **2004**, *108*, 6908.

(102) Miroshnichenko E. A.; Kon'kova T. S.; Inozemtsev Y. O.; Vorob'eva V. P.; Matyushin Y. N.; Shevelev, S. A. *Russ. Chem. Bull.* **2009**, *58*, 772.

(103) Koppes, W. M.; Sitzmann, M. E. Triazolyl-tetrazinyl-aminotriazine Compounds Useful in Pyrotechnic Compositions and Process Thereof, United States Patent 6602366, **2003**; pp 9.

(104) Chavez, D. E., Michael A.; Huynh, M. H.; Naud, D. L.; Son, S. F.; Tappan, B. C. *J.Pyrotech.* **2006**, *23*, 70.

(105) Teselkin, V. *Combust. Explo. Shock Waves* **2009**, *45*, 632.

(106) Pierre, A.; Fabien, M.; Gilles, C.; Marie-Claude, V.; Sophie, B.; Rachel, M.-R. *Chem-Eur. J.* **2005**, *11*, 5667.

(107) Saracoglu, N. *Tetrahedron* **2007**, *63*, 4199.

(108) Soloducho, J.; Doskocz, J.; Cabaj, J.; Roszak, S. *Tetrahedron* **2003**, *59*, 4761.

(109) Churakov, A. M.; Tartakovsky, V. A. *Chem. Rev.* **2004**, *104*, 2601.

(110) Kiselev, V.; Gritsan, N.; Zarko, V.; Kalmykov, P.; Shandakov, V. *Combust. Explo. Shock Waves* **2007**, *43*, 562.

(111) Christe, K. O. H., R. ; Wagner, R. I. ; Jones, CJ. *Synthesis of New High-Oxygen Carriers and Ditetrazinetetroxide (DTTO)*, California Univ. Los Angeles Dept. of Chem. and Biochem. **2009**.

(112) Tartakovsky, V. A.; Filatov, I. E.; Churakov, A. M.; Ioffe, S. L.; Strelenko, Y. A.; Kuz'min, V. S.; Rusinov, G. L.; Pashkevich, K. I. *Russ. Chem. Bull.* **2004**, *53*, 2577.

(113) Smirnov, O. Y.; Churakov, A. M.; Strelenko, Y. A.; Ioffe, S. L.; Tartakovsky, V. A. *Russ. Chem. Bull.* **2002**, *51*, 1841.

(114) Feller, D. *J. Chem. Phys.* **1992**, *96*, 6104.

(115) Halkier, A.; Helgaker, T.; Jørgensen, P.; Klopper, W.; Olsen, J. *Chem. Phys. Lett.* **1999**, *302*, 437.

(116) Peterson, K. A.; Woon, D. E.; Dunning, T. H., Jr, *J. Chem. Phys.* **1994**, *100*, 7410.

(117) Helgaker, T.; Klopper, W.; Koch, H.; Noga, J. *J. Chem. Phy.* **1997**, *106*, 9639.

(118) Frisch, M. J.; Trucks, G. W.; Schlegel, H. B.; Scuseria, G. E.; Robb, M. A.; Cheeseman, J. R.; Montgomery, J. A., Jr.; Vreven, T.; Kudin, K. N.; Burant, J. C.; Millam, J. M.; Iyengar, S. S.; Tomasi, J.; Barone, V.; Mennucci, B.; Cossi, M.; Scalmani, G.; Rega, N.; Petersson, G. A.; Nakatsuji, H.; Hada, M.; Ehara, M.; Toyota, K.; Fukuda, R.; Hasegawa, J.; Ishida, M.; Nakajima, T.; Honda, Y.; Kitao, O.; Nakai, H.; Klene, M.; Li, X.; Knox, J. E.; Hratchian, H. P.; Cross, J. B.; Bakken, V.; Adamo, C.; Jaramillo, J.; Gomperts, R.; Stratmann, R. E.; Yazyev, O.; Austin, A. J.; Cammi, R.; Pomelli, C.; Ochterski, J. W.; Ayala, P. Y.; Morokuma, K.; Voth, G. A.; Salvador, P.; Dannenberg, J. J.; Zakrzewski, V. G.; Dapprich, S.; Daniels, A. D.; Strain, M. C.; Farkas, O.; Malick, D. K.; Rabuck, A. D.; Raghavachari, K.; Foresman, J. B.; Ortiz, J. V.; Cui, Q.; Baboul, A. G.; Clifford, S.; Cioslowski, J.; Stefanov, B. B.; Liu, G.; Liashenko, A.; Piskorz, P.; Komaromi, I.; Martin, R. L.; Fox, D. J.; Keith, T.; Al-Laham, M. A.; Peng, C. Y.; Nanayakkara, A.; Challacombe, M.; Gill, P. M. W.; Johnson, B.; Chen, W.; Wong, M. W.; Gonzalez, C.; Pople, J. A. **2004**.

(119) Tasi, G.; Izsák, R.; Matisz, G.; Császár, A. G.; Kállay, M.; Ruscic, B.; Stanton, J. F. *ChemPhysChem* **2006**, *7*, 1664.

(120) Curtiss, L. A.; Raghavachari, K.; Deutsch, P. W.; Pople, J. A. *J. Chem. Phys.* **1991**, *95*, 2433.

(121) Zakzeski, J.; Bruijnincx, P. C. A.; Jongerius, A. L.; Weckhuysen, B. M. *Chem. Rev.* **2010**, *110*, 3552.

(122) Argyropoulos, D. S.; Menachem, S. B. *Adv. Biochem. Eng. Biot.* **1997**, *57*, 127.

(123) Hamelinck, C. N.; Hooijdonk, G. v.; Faaij, A. P. C. *Biomass and Bioenerg.* **2005**, *28*, 384.

(124) Kirk, T. K.; Tien, M.; Kersten, J. P.; Mozuch, D. M.; Kalyanaraman, B. *Biochem. J.* **1986**, *236*, 279.

(125) Elder, T. *Holzforschung* **2010**, *64*, 435.

(126) Beste, A.; Buchanan, A. C. *J. Org. Chem.* **2011**, *76*, 2195.

(127) Britt, P. F.; Buchanan, A. C.; Cooney, M. J.; Martineau, D. R. *J. Org. Chem.* **2000**, *65*, 1376.

(128) Britt, P. F.; Buchanan, A. C.; Malcolm, E. A. *Energy & Fuels* **2000**, *14*, 1314.

(129) Drage, T. C.; Vane, C. H.; Abbott, G. D. *Org. Geochem.* **2002**, *33*, 1523.

(130) Beste, A.; Buchanan, A. C. *J. Org. Chem.* **2009**, *74*, 2837.

(131) Wong, D. *Appl. Biochem. Biotech.* **2009**, *157*, 174.

(132) Tien, M.; Kirk, T. K. *P. Natl. Acad. Sci.* **1984**, *81*, 2280.

(133) Li, J.; Yuan, H.; Yang, J. *Front. Bio. China* **2009**, *4*, 29.

(134) Vicuna, R.; Gonzalez, B.; Mozuch, M. D.; Kirk, T. K. *Appl. Environ. Microb.* **1987**, *53*, 2605.

(135) Wan, Y.; Chen, P.; Zhang, B.; Yang, C.; Liu, Y.; Lin, X.; Ruan, R. *J. Anal. Appl. Pyrol.* **2009**, *86*, 161.

(136) Balat, M.; Balat, H.; Öz, C. *Prog. Energ. Combust. Sci.* **2008**, *34*, 551.

(137) Swiegers, G. F. *Heterogeneous, Homogeneous, and Enzymatic Catalysis. A Shared Terminology and Conceptual Platform. The Alternative of Time-Dependence in Catalysis*; John Wiley & Sons, Inc., **2008**.

(138) Lin, Y.-C.; Huber, G. W. *Energ. Environ. Sci.* **2009**, *2*, 68.

(139) Carroll, J. J.; Haug, K. L.; Weisshaar, J. C.; Blomberg, M. R. A.; Siegbahn, P. E. M.; Svensson, M. *J. Phys. Chem.* **1995**, *99*, 13955.

(140) Huber, G. W.; Iborra, S.; Corma, A. *Chem. Rev.* **2006**, *106*, 4044.

(141) Schroden, J. J.; Davis, H. F. *Reactions of Neutral Transition Metal Atoms with Small Molecules in the Gas Phase, Eds.; WILEY-VCH Verlag,* **2006**, Vol. *37*, pp. 215.

(142) Williams, T. G.; DeYonker, N. J.; Ho, B. S.; Wilson, A. K. *Chem. Phys. Lett.* **2011**, *504*, 88.

(143) Jiang, W.; Rogers, J.; Wilson, A. K. *J. Chem. Phys.* **2011**, *134*, 034101.

(144) J. A. Montgomery, Jr.; Frisch, M. J.; Ochterski, J. W.; Petersson, G. A. *J. Chem. Phys.* **1999**, *110*, 2822.

(145) Piecuch, P.; Maruani, J.; Delgado-Barrio, G.; Wilson, S.; Wilson, A. K.; DeYonker, N. J.; Cundari, T. R. The Correlation Consistent Composite Approach (ccCA): Efficient and Pan-Periodic Kinetics and Thermodynamics. In *Advances in the Theory of Atomic and Molecular Systems*; Springer Netherlands, 2009; Vol. 19; pp 197.

(146) Curtiss, L. A.; Raghavachari, K.; Redfern, P. C.; Rassolov, V.; Pople, J. A. *J. Chem. Phys.* **1998**, *109*, 7764.

(147) Ochterski, J. W.; Petersson, G. A.; Montgomery, J. A., Jr. *J. Chem. Phys.* **1996**, *104*, 2598.

(148) Boese, A. D.; Oren, M.; Atasoylu, O.; Martin, J. M. L.; Kallay, M.; Gauss, J. *J. Chem. Phys.* **2004**, *120*, 4129.

(149) Oyedepo, G. A.; Wilson, A. K. *J. Phys. Chem. A* **2010**, *114* 8806.

(150) Majkut, M.; Wilson, A. K. *J. Phys. Chem. A* **Submitted**.

(151) Jorgensen, K. R.; Oyedepo, G. A.; Wilson, A. K. *J. Hazard. Mater.* **2011**, *186*, 583.

(152) Mintz, B.; Williams, T. G.; Howard, L.; Wilson, A. K. *J. Chem. Phys.* **2009**, *130*, 234104.

(153) Tajti, A.; Szalay, P. G.; Csaszar, A. G.; Kallay, M.; Gauss, J.; Valeev, E. F.; Flowers, B. A.; Vazquez, J.; Stanton, J. F. *J. Chem. Phys.* **2004**, *121*, 11599.

(154) Zhao, Y.; González-García, N.; Truhlar, D. G. *J. Phys. Chem. A* **2005**, *109*, 2012.

(155) Sousa, S. F.; Fernandes, P. A.; Ramos, M. J. *J. Phys. Chem. A* **2007**, *111*, 10439.

(156) Wu, J.; Ying Zhang, I.; Xu, X. *ChemPhysChem* **2010**, *11*, 2561.

(157) DeYonker, N. J.; Mintz, B.; Cundari, T. R.; Wilson, A. K. *J. Chem. Theory Comput.* **2008**, *4*, 328.

(158) Gao, Y.; DeYonker, N. J.; Garrett, E. C.; Wilson, A. K.; Cundari, T. R.; Marshall, P. *J. Phys. Chem. A* **2009**, *113*, 6955.

(159) Grimes, T. V.; Wilson, A. K.; DeYonker, N. J.; Cundari, T. R. *J. Chem. Phys.* **2007**, *127*, 154117.

(160) Ho, D. S.; DeYonker, N. J.; Wilson, A. K.; Cundari, T. R. *J. Phys. Chem. A* **2006**, *110*, 9767.

(161) Prascher, B. P.; Lucente-Schultz, R. M.; Wilson, A. K. *Chem. Phys.* **2009**, *359*, 1.

(162) Das, S. R.; Williams, T. G.; Drummond, M. L.; Wilson, A. K. *J. Phys. Chem. A* **2010**, *114*, 9394.

(163) Svensson, M.; Humbel, S.; Froese, R. D. J.; Matsubara, T.; Sieber, S.; Morokuma, K. *J. Phys. Chem.* **1996**, *100*, 19357.

(164) Figgen, D.; Peterson, K. A.; Dolg, M.; Stoll, H. *J. Chem. Phys.* **2009**, *130*, 164108.

(165) Dolg, M.; Wedig, U.; Stoll, H.; Preuss, H. *J. Chem. Phys.* **1987**, *86*, 866.

(166) Andrae, D.; Häußermann, U.; Dolg, M.; Stoll, H.; Preuß, H. *Theor. Chim. Acta* **1990**, *77*, 123.

(167) Peterson, K. A.; Figgen, D.; Dolg, M.; Stoll, H. *J. Chem. Phys.* **2007**, *126*, 124101.

(168) Peterson, K. A.; Puzzarini, C. *Theor. Chim. Acta* **2005**, *114*, 283.

(169) Siegbahn, P. E. M. Electronic Structure Calculations for Molecules Containing Transition Metals. In *Advances in Chemical Physics*; John Wiley & Sons, Inc., 2007; pp 333.

(170) Kasper, P. J.; Björn, O. R.; Ulf, R. *J. Chem. Phys.* **2007**, *126*, 014103.

(171) Dennington, R.; Keith, T.; Millam, J. GaussView Version 5; Semichem Inc., Shawnee Mission KS 2009.

(172) Gaussian 09, R. A., M. J. Frisch, G. W. Trucks, H. B. Schlegel, G. E. Scuseria, M. A. Robb, J. R. Cheeseman, G. Scalmani, V. Barone, B. Mennucci, G. A. Petersson, H. Nakatsuji, M. Caricato, X. Li, H. P. Hratchian, A. F. Izmaylov, J. Bloino, G. Zheng, J. L. Sonnenberg, M. Hada, M. Ehara, K. Toyota, R. Fukuda, J. Hasegawa, M. Ishida, T. Nakajima, Y. Honda, O. Kitao, H. Nakai, T. Vreven, J. A. Montgomery, Jr., J. E. Peralta, F. Ogliaro, M. Bearpark, J. J. Heyd, E. Brothers, K. N. Kudin, V. N. Staroverov, R. Kobayashi, J. Normand, K. Raghavachari, A. Rendell, J. C. Burant, S. S. Iyengar, J. Tomasi, M. Cossi, N. Rega, J. M. Millam, M. Klene, J. E. Knox, J. B. Cross, V. Bakken, C. Adamo, J. Jaramillo, R. Gomperts, R. E. Stratmann, O. Yazyev, A. J. Austin, R. Cammi, C. Pomelli, J. W. Ochterski, R. L. Martin, K. Morokuma, V. G. Zakrzewski, G. A. Voth, P. Salvador, J. J. Dannenberg, S. Dapprich, A. D. Daniels, O. Farkas, J. B. Foresman, J. V. Ortiz, J. Cioslowski, and D. J. Fox, Gaussian, Inc., Wallingford CT, 2009.

(173) Werner, H. J. K., P. J.; Lindh, R.; Manby, F. R.; Schtz, M.; Celani, P.; Korona, T.; Rauhut, G.; Amos, R. D.; Bernhardsson, A.; Berning, A.; Cooper, D. L.; Deegan, J. O.; Dobbyn, A. J.; Eckert, F.; Hampel, C.; Hetzer, G.; Lloyd, A. W.; McNicholas, S. J.; Meyer, W.; Mura, M. E.; Nicklass, A.; Palmieri, P.; Pitzer, R.; Schumann, U.; Stoll, H.; Stone, A. J.; Tarroni, R.; Thorsteinsson, T. See http://www.molpro.net. MOLPRO Software Package.

(174) Ralchenko, Y.; Kramida, A. E.; Reader, J., and NIST ASD Team (2011). *NIST Atomic Spectra Database (ver. 4.1.0), [Online]. Available: http://physics.nist.gov/asd3 [2011, June 9]. National Institute of Standards and Technology, Gaithersburg, MD.* **2011**.

(175) Goerigk, L.; Grimme, S. *J. Chem. Theory Comput.* **2011**, *7*, 291.

(176) Zhao, Y.; Truhlar, D. G. *Accounts of Chem. Res.* **2008**, *41*, 157.

(177) Carroll, J. J.; Weisshaar, J. C.; Siegbahn, P. E. M.; Wittborn, C. A. M.; Blomberg, M. R. A. *J. Phys. Chem.* **1995**, *99*, 14388.

(178) Bondi, A. *J. Phys. Chem.* **1964**, *68*, 441.

(179) Siegbahn, P. E. M. *Faraday Symp. Chem. Soc.* **1984**, *19*, 97.

(180) Sherrill, C. D. *Annu. Rep. Comput. Chem., Vol. 1, edited by D. Spellmeyer (Elsevier, Amsterdam, 2005)* **2005**, 45.

(181) Shavitt, I. *Modern Theoretical Chemistry, edited by H. F. Schaefer (Plenum, New York, 1977), Vol. 3, pp. 189-275.* **1977**.

(182) Kim, K.; Jordan, K. D. *J. Phys. Chem.* **1994**, *98*, 10089.

(183) Stephens, P. J.; Devlin, F. J.; Chabalowski, C. F.; Frisch, M. J. *J. Phys. Chem.* **1994**, *98*, 11623.

(184) Curtiss, L. A.; Raghavachari, K.; Pople, J. A. *J. Chem. Phys.* **1993**, *98*, 1293.

(185) Curtiss, L. A.; Carpenter, J. E.; Raghavachari, K.; Pople, J. A. *J. Chem. Phys.* **1992**, *96*, 9030.

(186) Curtiss, L. A.; Raghavachari, K. *Theor. Chim. Acta* **2002**, *108*, 61.

(187) Curtiss, L. A.; Redfern, P. C.; Raghavachari, K.; Rassolov, V.; Pople, J. A. *J. Chem. Phys.* **1999**, *110*, 4703.

(188) Curtiss, L. A.; Redfern, P. C.; Raghavachari, K. *J. Chem. Phys.* **2007**, *126*, 084108.

(189) J. A. Montgomery, Jr.; Frisch, M. J.; Ochterski, J. W.; Petersson, G. A. *J. Chem. Phys.* **2000**, *112*, 6532.

(190) Karton, A.; Rabinovich, E.; Martin, J. M. L.; Ruscic, B. *J. Chem. Phys.* **2006**, *125*, 144108.

(191) Bomble, Y. J.; Vazquez, J.; Kallay, M.; Michauk, C.; Szalay, P. G.; Csaszar, A. G.; Gauss, J.; Stanton, J. F. *J. Chem. Phys.* **2006**, *125*, 064108.

(192) Harding, M. E.; Vazquez, J.; Ruscic, B.; Wilson, A. K.; Gauss, J.; Stanton, J. F. *J. Chem. Phys.* **2008**, *128*, 114111.

(193) DeYonker, N. J.; Cundari, T. R.; Wilson, A. K.; Sood, C. A.; Magers, D. H. *Theochem* **2006**, *775*, 77.

(194) Prascher, B. P.; Lai, J. D.; Wilson, A. K. *J. Chem. Phys.* **2009**, *131*, 044130.

(195) Williams, T. G.; Wilson, A. K. *J. Sulfur Chem.* **2008**, *29*, 353.

(196) Sølling, T. I.; Smith, D. M.; Radom, L.; Freitag, M. A.; Gordon, M. S. *J. Chem. Phys.* **2001**, *115*, 8758.

(197) Detlef, S. *Angew. Chem. Int. Edit.* **2002**, *41*, 1071.

(198) Mintz, B.; Chan, B.; Sullivan, M. B.; Buesgen, T.; Scott, A. P.; Kass, S. R.; Radom, L.; Wilson, A. K. *J. Phys. Chem. A* **2009**, *113*, 9501.

(199) Balkova, A.; Barlett, J. R. *J. Chem. Phys.* **1994**, *101*, 8972.

(200) Li, X.; Paldus, J. *J. Chem. Phys.* **2006**, *124*, 174101/1.

(201) Li, X.; Paldus, J. *J. Chem. Phys.* **2006**, *125*, 164107/1.

(202) Li, X.; Paldus, J. *J. Chem. Phys.* **2008**, *128*, 144119/1.

(203) Sancho-Garcia, J. C.; Pittner, J.; Carsky, P.; Hubac, I. *J. Chem. Phys.* **2000**, *112*, 8785.

(204) Evangelista, F. A.; Simmonett, A. C.; Allen, W. D.; Schaefer III, H. F.; Gauss, J. *J. Chem. Phys.* **2008**, *128*, 124104.

(205) Szalay, P. G. *Chem. Phys.* **2008**, *349*, 121.

(206) Hubac, I.; Pittner, J.; Carsky, P. *J. Chem. Phys.* **2000**, *112*, 8779.

(207) Sears, J. S.; Sherrill, C. D.; Krylov, A. I. *J. Chem. Phys.* **2003**, *118*, 9084.

(208) Schwartz, C. *Phys. Rev.* **1962**, *126*, 1015.

(209) Halkier, A.; Helgaker, T.; Jørgensen, P.; Klopper, W.; Koch, H.; Olsen, J.; Wilson, A. K. *Chem. Phys. Lett.* **1998**, *286*, 243.

(210) Helgaker, T.; Klopper, W.; Koch, H.; Noga, J. *J. Chem. Phys.* **1997**, *106*, 9639.

(211) Kutzelnigg, W. *Theor. Chim. Acta* **1985**, *68*, 445.

(212) Williams, T. G.; DeYonker, N. J.; Wilson, A. K. *J. Chem. Phys.* **2008**, *128*, 044101.

(213) Hess, B. A. *Phys. Rev. A* **1986**, *33*, 3742.

(214) Hess, B. A. *Phys. Rev. A* **1985**, *32*, 756.

(215) Douglas, M.; Kroll, N. M. *Ann. Phys.* **1974**, *82*, 89.

(216) Davidson, E. R.; Borden, W. T. *J. Phys. Chem.* **1983**, *87*, 4783.

(217) Crawford, T. D.; Elfi, K.; John, F. S.; Dieter, C. *J. Chem. Phys.* **2001**, *114*, 10638.

(218) Bearpark, M. J.; Blancafort, L.; Robb, M. A. *Mol. Phys.* **2002**, *100*, 1735.

(219) Filatov, M.; Shaik, S. *Chem. Phys. Lett.* **2000**, *332*, 409.

(220) Andersson, K. *Theor. Chim. Acta* **1995**, *91*, 31.

(221) Slipchenko, L. V.; Krylov, A. I. *J. Chem. Phys.* **2002**, *117*, 4694.

(222) Schaefer, H. F., III. *Science* **1986**, *231*, 1100.

(223) Jensen, P.; Bunker, P. R. *J. Chem. Phys.* **1988**, *89*, 1327.

(224) Kalemos, A.; Dunning, T. H., Jr.; Mavridis, A.; Harrison, J. F. *Can. J. Chem.* **2004**, *82*, 684.

(225) Apeloig, Y.; Pauncz, R.; Karni, M.; West, R.; Steiner, W.; Chapman, D. *Organometallics* **2003**, *22*, 3250.

(226) Kasdan, A.; Herbst, E.; Lineberger, W. C. *J. Chem. Physics* **1975**, *62*, 541.

(227) Baldridge, K. K.; Boatz, J. A.; Koseki, S.; Gordon, M. S. *Annu. Rev. Phys. Chem.* **1987**, *38*, 211.

(228) Berkowitz, J.; Greene, J. P.; Cho, H.; Ruscic, B. *J. Chem. Phys.* **1987**, *86*, 1235.

(229) Balasubramanian, K.; McLean, A. D. *J. Chem. Phys.* **1986**, *85*, 5117.

(230) Wood, G. P. F.; Radom, L.; Petersson, G. A.; Barnes, E. C.; Frisch, M. J.; Montgomery, J. A., Jr. *J. Chem. Phys.* **2006**, *125*, 094106.

(231) Gordon, M. S.; Francisco, J. S.; Schlegel, H. B. *Adv. Silicon Chem.* **1993**, *2*, 137.

(232) Erwin, J. W.; Ring, M. A.; O'Neal, H. E. *Int. J. Chem. Kinet.* **1985**, *17*, 1067.

(233) Jasinski, J. M.; Chu, J. O. *J. Chem. Phys.* **1988**, *88*, 1678.

(234) Roenigk, K. F.; Jensen, K. F.; Carr, R. W. *J. Phys. Chem.* **1987**, *91*, 5732.

(235) Lee, T. J.; Taylor, P. R. *Int. J. Quantum Chem.* **1989**, *36*, 199.

(236) Lee, T. J.; Rice, J. E.; Scuseria, G. E.; Schaefer, H. F., III. *Theor. Chim. Acta* **1989**, *75*, 81.

(237) Korth, M.; Grimme, S. *J. Chem. Theory Comput.* **2009**, *5*, 993.

(238) Bofill, J. M.; Pulay, P. *J. Chem. Phys.* **1989**, *90*, 3637.

(239) Pulay, P.; Hamilton, T. P. *J. Chem. Phys.* **1988**, *88*, 4926.

(240) Richard, G. A. B.; Péter, P. *Int. J. Quantum Chem.* **1993**, *45*, 133.

(241) Huber, K. P.; Herzberg, G. *Molecular Spectra and Molecular Structure IV. Constants of Diatomic Molecules*; Van Nostrand: Reinhold: New York, 1979.

(242) Setzer, K. D.; Fink, E. H.; Ramsay, D. A. *J. Mol. Spectrosc.* **1999**, *198*, 163.

(243) Peterson, K. A.; Lyons, J. R.; Francisco, J. S. *J. Chem. Phys.* **2006**, *125*, 084314.

(244) Chase, M.W. J. *NIST-JANAF Thermochemical Tables, 4th ed. J. Phys. Chem. Ref. Data, Mono. Vol. 9* **1998**.

(245) Schwartz, R. L.; Davico, G. E.; Ramond, T. M.; Lineberger, W. C. *J. Phys. Chem. A* **1999**, *103*, 8213.

(246) Barden, C. J.; Schaefer III, H. F. *J. Chem. Phys.* **2000**, *112*, 6515.

(247) Shen, J.; Fang, T.; Li, S. *Science in China Series B: Chemistry* **2008**, *51*, 1197.

(248) Schwartz, M.; Marshall, P. *J. Phys. Chem. A* **1999**, *103*, 7900.

(249) Demaison, J.; Margules, L.; Martin, J. M. L.; Boggs, J. E. *Phys. Chem. Chem. Phys.* **2002**, *4*, 3282.

(250) Tao, C.; Mukarakate, C.; Judge, R. H.; Reid, S. A. *J. Chem. Phys.* **2008**, *128*, 171101.

(251) Gilles, M. K.; Ervin, K. M.; Ho, J.; Lineberger, W. C. *J. Phys. Chem.* **1992**, *96*, 1130.

(252) Zhou, S.; Zhan, M.; Qiu, Y.; Liu, S.; Shi, J.; Li, F.; Yao, J. *Chem. Phys. Lett.* **1985**, *121*, 395.

(253) Shin, S. K.; Goddard, W. A.; Beauchamp, J. L. *J. Phys. Chem.* **1990**, *94*, 6963.

(254) Poutsma, J. C.; Paulino, J. A.; Squires, R. R. *J. Phys. Chem. A* **1997**, *101*, 5327.

(255) Matus, M. H.; Nguyen, M. T.; Dixon, D. A. *J. Phys. Chem. A* **2006**, *110*, 8864.

(256) Bruna, P. J.; Hachey, M. R. J.; Grein, F. *J. Phys. Chem.* **1995**, *99*, 16576.

(257) Lee, T. J. *Chem. Phys. Lett.* **1990**, *169*, 529.

(258) Flemmig, B.; Wolczanski, P. T.; Hoffmann, R. *J. Am. Chem. Soc.* **2005**, *127*, 1278.

(259) Hobza, P.; Spirko, V.; Selzle, H. L.; Schlag, W. *J. Phys. Chem. A* **1998**, *102*, 2501.

(260) Qu, Z. W.; Zhu, H.; Grebenshchikov, S. Y.; Schinke, R. *J. Chem. Phys.* **2005**, *123*, 074305.

(261) Tsuneda, T.; Nakano, H.; Hirao, K. *J. Chem. Phys.* **1995**, *103*, 6520.

(262) Siebert, R.; Fleurat-Lessard, P.; Schinke, R.; Bittererova, M.; Farantos, S. C. *J. Chem. Phys.* **2002**, *116*, 9749.

(263) Qu, Z.-W.; Zhu, H.; Schinke, R. *Chem. Phys. Lett.* **2003**, *377*, 359.

(264) Grebenshchikov, S. Y.; Qu, Z. W.; Zhu, H.; Schinke, R. *Phys. Chem. Chem. Phys.* **2007**, *9*, 2044.

(265) Ahmed, M.; Peterka, D. S.; Suits, A. G. *J. Chem. Phys.* **1999**, *110*, 4248.

(266) Nguyen, M. T.; Matus, M. H.; Lester, W. A.; Dixon, D. A. *J. Phys. Chem. A* **2008**, *112*, 2082.

(267) Sherrill, C. D.; Byrd, E. F. C.; Head-Gordon, M. *J. Chem. Phys.* **2000**, *113*, 1447.

(268) Lundberg, J. K.; Field, R. W.; Sherrill, C. D.; Seidl, E. T.; Xie, Y.; Schaefer III, H. F. *J. Chem. Phys.* **1993**, *98*, 8384.

(269) Voter, A. F.; Goodgame, M. M.; Goddard, W. A. *Chem. Phys.* **1985**, *98*, 7.

(270) Buenker, R. J.; Peyerimhoff, S. D. *Chem. Phys.* **1976**, *9*, 75.

(271) Brooks, B. R.; Schaefer, H. F. *J. Am. Chem. Soc.* **1979**, *101*, 307.

(272) Kollmar, H.; Staemmler, V. *Theor. Chim. Acta* **1978**, *48*, 223.

(273) Yamaguchi, Y.; Osamura, Y.; Schaefer, H. F. *J. Am. Chem. Soc.* **1983**, *105*, 7506.

(274) Schmidt, M. W.; Truong, P. N.; Gordon, M. S. *J. Am. Chem. Soc.* **1987**, *109*, 5217.

(275) Borden, W. T. *J. Am. Chem. Soc.* **1975**, *97*, 5968.

(276) Douglas, J. E.; Rabinovitch, B. S.; Looney, F. S. *J. Chem. Phys.* **1955**, *23*, 315.

(277) Akramine, O. E.; Kollias, A. C.; W. A. Lester, Jr. *J. Chem. Phys.* **2003**, *119*, 1483.

(278) Krylov, A. I. *Accounts Chem. Res.* **2006**, *39*, 83.

(279) Dolgonos, G. *Chem. Phys. Lett.* **2008**, *466*, 11.

(280) Andrews, L.; Wang, X. *J. Phys. Chem. A* **2002**, *106*, 7696.

(281) Curtiss, L. A.; Raghavachari, K.; Deutsch, P. W.; Pople, J. A. *J. Chem. Phys.* **1991**, *95*, 2433.

(282) Olbrich, G.; Potzinger, P.; Reimann, B.; Walsh, R. *Organometallics* **1984**, *3*, 1267.
(283) Sax, A. F.; Kalcher, J. *J. Phys. Chem.* **1991**, *95*, 1768.

(284) Katzer, G.; Ernst, M. C.; Sax, A. F.; Kalcher, J. *J. Phys. Chem. A* **1997**, *101*, 3942.

(285) Ruscic, B.; Berkowitz, J. *J. Chem. Phys.* **1991**, *95*, 2416.

(286) Lee, E. P. F.; Dyke, J. M.; Wright, T. G. *Chem. Phys. Lett.* **2000**, *326*, 143.

(287) Sari, L.; McCarthy, M. C.; Schaefer III, H. F.; Thaddeus, P. *J. Am. Chem. Soc.* **2003**, *125*, 11409.

(288) Batey, J.; Tierney, E. *J. Appl. Phys.* **1986**, *60*, 3136.

(289) McCarthy, M. C.; Gottlieb, C. A.; Thaddeus, P. *Mol. Phys.* **2003**, *101*, 697.

(290) Segal, A. S.; Vorob'ev, A. N.; Karpov, S. Y.; Mokhov, E. N.; Ramm, M. G.; Ramm, M. S.; Roenkov, A. D.; Vodakov, Y. A.; Makarov, Y. N. *J. Crystal Growth* **2000**, *208*, 431.

(291) Wong, H.-W.; Alva Nieto, J. C.; Swihart, M. T.; Broadbelt, L. J. *J. Phys. Chem. A* **2004**, *108*, 874.

(292) Heckingbottom, R.; Davies, G. J.; Prior, K. A. *Surf. Sci.* **1983**, *132*, 375.

(293) Spiniello, M.; White, J. M. *Organometallics* **2008**, *27*, 994.

(294) Turley, J. W.; Boer, F. P. *J. Am. Chem. Soc.* **1969**, *91*, 4129.

(295) Hajdasz, D. J.; Squires, R. R. *J. Am. Chem. Soc.* **1986**, *108*, 3139.

(296) Kinrade, S. D.; Gillson, A.-M. E.; Knight, C. T. G. *J. Chem. Soc. Dalton Trans.* **2002**, 307.

(297) Samsonov, G. V. *Powder Metall. Metal Ceramics* **1967**, *6*, 825.

(298) Green, S. *Astrophys. J.* **1983**, *226*, 895.

(299) Karton, A.; Martin, J. M. L. *J. Phys. Chem. A* **2007**, *111*, 5936.

(300) Spielfiedel, A.; Carter, S.; Feautrier, N.; Chambaud, G.; Rosmus, P. *J. Phys. Chem.* **1996**, *100*, 10055.

(301) Miki, T.; Morita, K.; Sano, N. *Metall. Mater. Trans. B* **1996**, *27*, 937.

(302) Viswanathan, R.; Schmude Jr, R. W.; Gingerich, K. A. *J. Chem. Thermodyn.* **1995**, *27*, 763.

(303) Viswanathan, R.; Schmude Jr, R. W.; Gingerich, K. A. *J. Chem. Thermodyn.* **1995**, *27*, 1303.

(304) Schmude, R. W.; Ran, Q.; Gingerich, K. A.; Kingcade, J. E. *J. Chem. Phys.* **1995**, *102*, 2574.

(305) Berkowitz, J.; Greene, J. P.; Cho, H.; Ruscic, B. *J. Chem. Phys.* **1987**, *86*, 1235.

(306) Gauss, J.; Cremer, D.; Stanton, J. F. *J. Phys. Chem. A* **2000**, *104*, 1319.

(307) Al-Saadi, A. A.; Meinander, N.; Laane, J. *J. Mol. Spectrosc.* **2007**, *242*, 17.

(308) Tekarli, S. M.; Williams, T. G.; Cundari, T. R. *J. Chem. Theory Comput.* **2009**, *5*, 2959.

(309) Lee, T. J. *Chem. Phys. Lett.* **2003**, *372*, 362.

(310) Woon, D. E.; Dunning, T. H. *J. Chem. Phys.* **1993**, *98*, 1358.

(311) Martin, J. M. L. *J. Chem. Phys.* **1998**, *108*, 2791.

(312) Dunning, T. H., Jr.,; Peterson, K. A.; Wilson, A. K. *J. Chem. Phys.* **2001**, *114*, 9244.

(313) Kutzelnigg, W.; Morgan, J. D. *J. Chem. Phys.* **1992**, *96*, 4484.

(314) Hess, B. A. *Phys. Rev. A* **1985**, *32*, 756.

(315) Hess, B. A. *Phys. Rev. A* **1986**, *33*, 3742.

(316) Douglas, M.; Kroll, N. M. *Ann. Phys.* **1974**, *82*, 89.

(317) C. E. Moore. *Atomic Energy Levels, Natl. Bur. Stand. Ref. Data Ser., Natl. Bur. Stand. (U.S.) Circ. No. 35 (U.S. Department of Commerce, Washington D.C., 1971)*.

(318) Carlson, T. A.; Duric, N.; Erman, P.; Larsson, M. *J. Phys. B* **1978**, *11*, 3667.

(319) Larsson, M. *J. Chem. Phys.* **1987**, *86*, 5018.

(320) Kalemos, A.; Mavridis, A.; Metropoulos, A. *J. Chem. Phys.* **2002**, *116*, 6529.

(321) Park, C. *J. Quant. Spectrosc. Ra.* **1979**, *21*, 373.

(322) Kasdan, A.; Herbst, E.; Lineberger, W. C. *Chem. Phys. Lett.* **1975**, *31*, 78.

(323) Peterson, K. A.; Shepler, B. C.; Singleton, J. M. *Mol. Phys.* **2007**, *105*, 1139.

(324) Hsu, Y.-C.; Chen, F.-T.; Chou, L.-C.; Shiu, Y.-J. *J. Chem. Phys.* **1996**, *105*, 9153.

(325) Parthiban, S.; Martin, J. M. L. *J. Chem. Phys.* **2001**, *114*, 6014.

(326) Kollias, A. C.; Domin, D.; Hill, G.; Frenklach, M.; Golden, D. M.; Lester, W. A. *Int. J. Chem. Kinet.* **2005**, *37*, 583.

(327) Golovin, A. V.; Takhistov, V. V. *J. Mol. Struct.* **2004**, *701*, 57.

(328) Dolgonos, G. *Chem. Phys. Lett.* **2008**, *454*, 190.

(329) Sillars, D.; Bennett, C. J.; Osamura, Y.; Kaiser, R. I. *Chem. Phys. Lett.* **2004**, *392*, 541.

(330) Curtiss, L. A.; Redfern, P. C.; Raghavachari, K.; Pople, J. A. *J. Chem. Phys.* **1998**, *109*, 42.

(331) Dixon, D. A.; Feller, D.; Peterson, K. A.; Gole, J. L. *J. Phys. Chem. A* **2000**, *104*, 2326.

(332) Grossman, J. C. *J. Chem. Phys.* **2002**, *117*, 1434.

(333) Kitsopoulos, T. N.; Chick, C. J.; Zhao, Y.; Neumark, D. M. *J. Chem. Phys.* **1991**, *95*, 1441.

(334) Sefyani, F. L.; Schamps, J. *Astrophys. J.* **1994**, *434*, 816.

(335) Karton, A.; Tarnopolsky, A.; M.L. Martin, J. *Mol. Phys.* **2009**, *107*, 977.

(336) Bauschlicher, J. C. W.; Langhoff, S. R. *J. Chem. Phys.* **1987**, *87*, 2919.

(337) McCarthy, M. C.; Thaddeus, P. *Phys. Rev. Lett.* **2003**, *90*, 213003.

(338) Raghavachari, K. *J. Chem. Phys.* **1985**, *83*, 3520.

(339) Schmude, J. R. W.; Ran, Q.; Gingerich, K. A.; Kingcade, J. J. E. *J. Chem. Phys.* **1995**, *102*, 2574.

(340) Weltner, W.; Van Zee, R. J. *Chem. Rev.* **1989**, *89*, 1713.

(341) Viswanathan, R.; Schmude, R. W.; Gingerich, K. A. *J. Phys. Chem.* **1996**, *100*, 10784.

(342) Ornellas, F. R.; Iwata, S. *J. Chem. Phys.* **1997**, *107*, 6782.

(343) Melius, C. F.; Ho, P. *J. Phys. Chem.* **1991**, *95*, 1410.

(344) Cai, Z. L.; Martin, J. M. L.; François, J. P. *J. Mol. Spectrosc.* **1998**, *188*, 27.

(345) Bruna, P. J.; Dohmann, H.; Peyerimhoff, S. D. *Can. J. Phys.* **1984**, *62*, 1508.

(346) Ornellas, F. R.; Iwata, S. *Chem. Phys.* **1998**, *232*, 95.

(347) Davy, R.; Skoumbourdis, E.; Dinsmore, D. *Mol. Phys.* **2005**, *103*, 611.

(348) Deutsch, P. W.; Curtiss, L. A. *Chem. Phys. Lett.* **1994**, *226*, 387.

(349) Nielsen, I. M. B.; Allen, W. D.; Csaszar, A. G.; Schaefer III, H. F. *J. Chem. Phys.* **1997**, *107*, 1195.

(350) Subramanian, V.; Venkatesh, K.; Sivanesan, D.; Ramasami, T. *J. Chem. Sci.* **1998**, *110*, 127.

(351) Sabin, J. R.; Oddershede, J.; Diercksen, G. H. F.; Gruner, N. E. *J. Chem. Phys.* **1986**, *84*, 354.

(352) Rittby, C. M. L. *J. Chem. Phys.* **1991**, *95*, 5609.

(353) Presilla-Marquez, J. D.; Graham, W. R. M. *J. Chem. Phys.* **1991**, *95*, 5612.

(354) Kafafi, Z. H.; Hauge, R. H.; Fredin, L.; Margrave, J. L. *J. Phys. Chem.* **1983**, *87*, 797.

(355) Neese, F. *J. Chem. Phys.* **2003**, *119*, 9428.

(356) Bartlett, R. J.; Purvis, G. D. *Int. J. Quantum Chem.* **1978**, *14*, 561.

(357) Ignatyev, I. S.; Schaefer, H. F. *J. Phys. Chem.* **1992**, *96*, 7632.

(358) Lembke, R. R.; Ferrante, R. F.; Weltner, W. *J. Am. Chem. Soc.* **1977**, *99*, 416.

(359) Amicangelo, J. C.; Dine, C. T.; Irwin, D. G.; Lee, C. J.; Romano, N. C.; Saxton, N. L. *J. Phys. Chem. A* **2008**, *112*, 3020.

(360) Ornellas, F. R.; Ueno, L. T.; Iwata, S. *J. Chem. Phys.* **1997**, *106*, 151.

(361) Maier, G.; Reisenauer, H. P.; Glatthaar, J. *Organometallics* **2000**, *19*, 4775.

(362) K. F. Zmbov; Margrave, J. L. *J. Am. Chem. Soc.* **1967**, 2492.

(363) Gizenko, N. V.; Emlin, B. I.; Kilesso, S. N.; Gasik, M. I.; Zav'yalov, A. L. *Izvestiya Akademii Nauk SSSR, Metally* **1983**, 33.

(364) Davy, R. D.; Schaefer III, H. F. *Chem. Phys. Lett.* **1996**, *255*, 171.

(365) Elorza, J. M.; Ugalde, J. M. *Can. J. Chem.* **1996**, *74*, 2476.

(366) Pietschnig, R.; Orthaber, A. *Eur. J. Inorg. Chem.* **2006**, *2006*, 4570.

(367) NIST Chemistry WebBook*, NIST Standard Reference Database Number 69*; Linstrom, P. J.; Mallard, W. G.; Eds.; National Institute of Standards and Technology, Gaithersburg, MD, June **2009**; 20899 (http://webbook.nist.gov/chemistry/).

(368) Ruscic, B.; Pinzon, R. E. ; Morton, M. L. ; Srinivasan, N. K. ; Su, M-C; Sutherland, J. W.; Michael, J. V.; *J. Phys. Chem. A* 110 (**2006**) 6592.

(369) Davis, L. P. ; Storch, D. ; Guidry, R. M. *J. Energ. Mater.* 5 (**1987**) 89.

(370) Matyushin, Y. N.; V'Yunova, I. B.; Pepekin, V. I. ; Apin, A. Y. ; *Izvestiya Akademii Nauk SSSR, Seriya Khimicheskaya* 11 (**1971**) 2443.

(371) Cox, J. D. ; Pilcher, G. *Thermochemistry of organic and organometallic compounds*, Academic Press London, **1970**.

(372) Holcomb, D. E.; Dorsey, C. L. *J. Ind. Eng. Chem.* 41 (**1949**) 2788.

(373) Verevkin, S. P. *Thermochim. Acta* 307 (**1997**) 17.

(374) Pedley, J. B. ; Naylor, R. D. ; Kirby, S. P. *Thermochemical data of organic compounds*, 2nd Edition, Chapman and Hall, London, New York, **1986**.

(375) Pepekin, V. I.; Matyushin, Y. N.; Lebedev, Y. A. *Russian Chem. Bull.* 23 (**1974**) 1707.

(376) Nitta, I. ; Seki, S. ; Momotani, M.; Sato, K. *J. Chem. Soc. Jpn.* 71 (**1950**) 378.

(377) Lias, S. G.; Bartnmess, J. E.; Liebman, J. F.; Holmes, J. L.; Levin, R. D.; Mallard, W. G. *J. Phys. Chem. Ref. Data* 17 (**1988**) 1.

(378) Miroshnichenko, E. A. ; Vorob'eva, V. P.; *Russ. J. Phys. Chem. (Engl. Transl.)* 73 (**1999**) 349.

(379) Lenchitz, C.; Velicky, R.W.; Silvestro, G.; Schlosberg, L.P. *J. Chem. Thermodyn.* 3 (**1971**) 689.

(380) Kalcher, J; Sax, A. F. *J. Mol. Struct.* 313, **1994**, 41.

(381) dos Santos, L. G.; Ornellas, F. R. *Chem. Phys.* 295, **2003**, 195.